Bilayer Composite Hydrogels for Corneal Prostheses

by

Edward Peña Perez

Submitted to the Department of Chemical Engineering in
partial fulfillment of the requirements for the degree of

Doctor of Philosophy

at the

MASSACHUSETTS INSTITUTE OF TECHNOLOGY

January 30, 1995

Author .....
Chemical Engineering
January 30, 1995

Certified by .....
Professor Edward W. Merrill
Carbon P. Dubbs Professor of Chemical Engineering
Thesis Co-Supervisor

Certified by .....
Professor Linda G. Cima
Karl van Tassel Assisstant Professor of Chemical Engineering
Thesis Co-Supervisor

Accepted by .....
Professor Robert E. Cohen
Chairman, Committee for Graduate Students

Bilayer Composite Hydrogels for Corneal Prostheses

by

Edward Peña Perez

Submitted to the Department of Chemical Engineering on January 30, 1995, in partial fulfillment of the requirements for the degree of Doctorate of Philosophy

Abstract

This document describes the synthesis and analysis of a two layer composite material composed of a thin layer of corneal tissue and a synthetic polyethylene oxide (PEO) hydrogel. The material was designed to provide a suitable substrate for epithelial cell growth while maintaining the desirable characteristics of hydrogels, i.e. clarity, flexibility, and permeability to water soluble nutrients. The hydrogels were synthesized via electron irradiation induced cross-linking of an aqueous solution of PEO onto a thin layer of collagenous tissue substrate: corneal stroma.

Light microscopic studies indicated that the interface between the tissue and PEO hydrogel appeared to be well adherent with no discernible gaps in the interface. Surface analytical techniques were used to identify peptides covalently grafted to the hydrogels at the hydrogel/collagen interface after bulk proteinaceous material was removed. Electron Spectroscopy for Chemical Analysis (ESCA) survey scans identified the presence of nitrogen on exposed hydrogel-collagen interfaces and amino acid labelling of these hydrogels confirmed the presence of nitrogen in amine form. Infrared Multiple Internal Reflectance (IR-MIR) studies identified increased absorption for the hydrogel collagen interfaces at *1640* cm^{-1} and *1540* cm^{-1} which is indicative of bound peptides. Quantitative assessments of collagen-hydrogel grafting were obtained using fluorescent labelling of immobilized collagen. PEO molecular weight and concentration were found to have no effect on grafting. Collagen grafting to PEO was found to be linear with respect to the electron beam dose given to the sample. In addition, collagen grafting to PEO star molecules was about half of that found for linear PEO, at a given radiation dose and PEO concentration.

Clear bubble-free poly(ethylene oxide) hydrogels were made by sequential bolus dose electron beam irradiation. These hydrogels were swollen to equilibrium in water with the resulting volume fraction polymer that ranged from *0.016* to *0.064* (*2-8 wt/vol%*). Time lag analysis was used to determine the diffusion coefficient of these materials. A mass balance analysis was used to determine the partition coefficient separately. Glucose partition coefficients in poly(ethylene oxide) hydrogels (K_p=*1.6-1.9*) showed a positive correlation with the volume fraction polymer in the gel. Glucose diffusivity (D)varied from *4.2 x* 10^{-6} cm^2/sec to *1.8 x* 10^{-6} cm^2/sec and showed a negative correlation with volume fraction polymer in the gel. These results indicated that glucose was interacting with the poly(ethylene oxide) network. In addition to the simple obstructional effect from the polymer in the swollen hydrogel membrane, the sorption and desorption of glucose onto poly(ethylene oxide) introduced an additional barrier to diffusion. Nevertheless, the apparent diffusivities ($D \cdot K_p$) for glucose in PEO hydrogels ranged from *6.7 x* 10^{-6} cm^2/sec to *6.5 x* 10^{-6} cm^2/sec which is very close to that of glucose diffusion in water.

Biocompatibility studies were performed in a system that was specifically constructed to reproduce the physiological environment and to allow *in situ* observation of epithelial wound healing. These studies evaluated the early phase and late phase corneal epithelial healing. Early phase wound healing was evaluated by quantifying the movement of corneal epithelial cells over the composite hydrogel surface. Migration in diffusion limited composite hydrogels was initially slowed but resolved to a rate similar to that of the control specimen. Late phase healing was evaluated in terms of epithelium morphology and deposition of the basement membrane component laminin. Confluent epithelial cells grown on composite hydrogels maintained a rounded-polygonal appearance characteristic of normal epithelium. Light microscopy showed multilayered epithelia developed in culture after one week. Immunohistochemistry showed development of a continuous basal layer of laminin appearing at one week and remaining intact up to two months.

A theoretical model of epithelial healing over a permeable keratoprosthesis was formulated. This model was based on the diffusion of a soluble mediator through the hydrogel that influences the migration/healing rate of the cells covering the wound. In this model, device performance is described in terms of geometry, solute diffusivity, and healing rate. Analysis of in vitro epithelial wound healing data indicated that the soluble mediator diffusivity is on the order of $5.5 \times 10^{-8} cm^2/sec$. Design criteria are proposed for a refractive prosthetic cornea based on corneal epithelial wound healing and long term nutrient homeostasis.

Edward W. Merrill, Ph.D.
Carbon P.Dubbs
Professor of Chemical Engineering

Linda G. Cima, Ph.D.
Karl van Tassel
Asst. Professor of Chemical Engineering

Acknowledgments

It has been an extremely gratifying experience to work with my co-advisors Professor Edward Merrill and Professor Linda Cima. Their expertise, their encouragement, and their belief in me has allowed me to learn and to mature as an applied scientist during the course of this study. The project would not have arisen or developed if Dr. David Miller was not a vital advisor in my thesis work. His creativity and the applicability of his ideas to the real world kept my work firmly grounded in reality. His friendship and the friendship of Professor Merrill and Professor Cima is something I will always treasure.

There are a great many people who have aided me in one way or another during this project. Kenneth Wright at the MIT High Voltage Research Laboratory always found time to process my samples and work with cumbersome "new" techniques. I have had the pleasure to work with talented undergraduates such as Amy S. Chang and Maya Trotz, whose work helped to advance this study. Julian Guerra de la Torre was first of all a friend. Still as a great mechanical engineer, Julian could always machine perfect pieces of equipment for my project. There are also several Harvard Medical School students who have all made significant contributions to the biological studies. Donald Park worked with me to develop techniques of tissue harvest at the Beth Israel Hospital. Brian Stidham helped me to establish methods of organ culture. Seth Weinreb was critical in performing the immunohistochemistry on various samples.

MIT has also given me the opportunity to meet and associate with many colleagues and friends. Of course, the people in the lab are a big part of my MIT experience. Stephanie Sung, Deb Savage, Tim Donahue, Ambuj Sagar, Susan Sophia, and Premnath Venugopalan were all part of the Merrill lab experience. Stephanie Lopina, Mark Powers, Ann Park, Phillip Kuhl, Eric Hancock and Sue Hobbs provided the other half of my MIT life, the Cima lab experience. To those many more I have not mentioned directly, my appreciation goes out to you.

Most of my financial support was provided by an Individual Pre-doctoral National Research Service Award which I obtained competitively from NIH. I am greatly appreciative to Polymer Technology, Inc. for sponsoring some portions of my work and for their eagerness and foresight in developing this technology. I am also very thankful to Professor Merrill for the financial support and supplementation he provided over the years.

The most important acknowledgment has to go out to my family. My family has been with me from the first...and they were there with me at the last. There is no way to express my indebtedness and love for my family. They helped me even though they were a thousand miles away. Over the years, during good times and bad times, there was nothing more inspiring than looking into your faces in photographs on my wall. Thank you Mother, Father, Rey and Daniel.

This work is dedicated
to my
Father and Mother

Reymundo Perez and Anita Peña Perez

Table of Contents

List of Figures

List of Tables

Chapter 1

Introduction

1.1 Background

Our ability to see is made possible through a complex system of neural networks, biochemistry and specialized anatomical structures. The transmission of clear and focused images from our surroundings into the neural processing of the brain is a single but indispensable part of sight. The eye's clear cornea is the anatomical intermediary between the outer environment and internal visual processing. The irreversible loss of corneal tissue clarity prompts the replacement of a patient's cornea.[1,2,3] In spite of the success of corneal transplants, there is still a need for a viable prosthetic alternative for intractable pathology such as caustic burns or repeated rejection of corneal transplants.[3,4,5] In addition, the complications due to aquired immune deficiency syndrome (AIDS) and other tissue-borne diseases have led to increased scrutiny and mistrust of donor tissue. Another major application of prosthetics in corneal surgery is the rising interest in refractive surgery.[6] Refractive surgery changes the focusing power of the cornea. By adjusting the magnification of the cornea, images can properly be focused on the retina thereby circumventing the need for glasses.

Figure 1.1 shows a schematic representation of the eye. The major anatomic divisions of the eye are the sclera, uveal tract, retina, vitreous, lens, anterior chamber, and the cornea. The clear cornea and gray-white opaque sclera are fused together and completely enclose the other portions of the eye. Under the influence of intra-ocular pressure, the cornea and sclera form a semi-rigid spherical organ.

The cornea occupies the anterior pole of what is referred to as the globe. In adults the cornea measures 12mm in the horizontal meredian and 11 mm in the vertical meridian. The central one-third of the cornea is nearly spherical and measures 4 mm in diameter. The cornea is also thinner (0.5mm) in the center than in the periphery (1.0mm). Histologically the cornea is composed of 5 layers: epithelium, Bowman's membrane, stroma, Descemet's membrane, and endothelium. The most metabolically active layers are the limiting layers, endothelium and epithelium which are primarily cellular layers. The epithelium serves to maintain the tear film and provide an anatomic barrier to infectious agents. In contrast to the limiting layers, the stroma is only 3-5% cellular. Thus the bulk of the cornea is collagen I (70% of dry weight) with the balance being glycosaminoglycans and cellular elements. The cornea is 77% water under normal physiologic conditions.[1,2] The cornea is essentially a highly specialized form of connective tissue: a natural collagenous hydrogel.

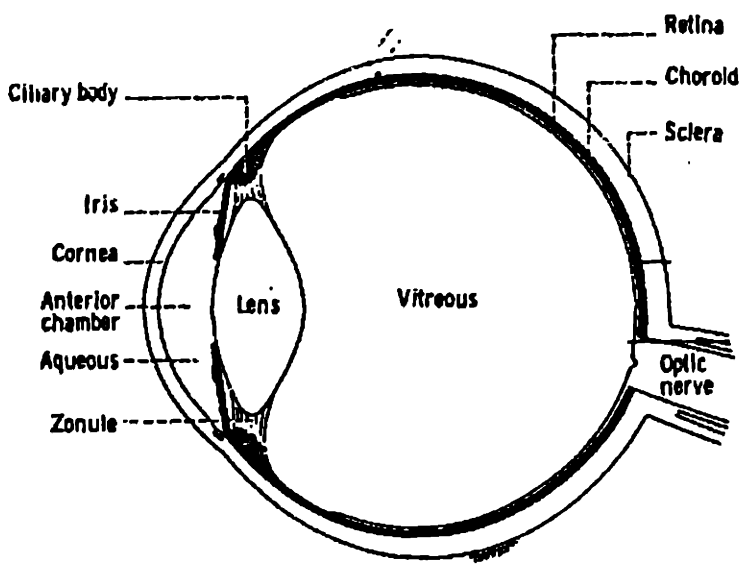

Figure 1.1: Anatomy of the Eye

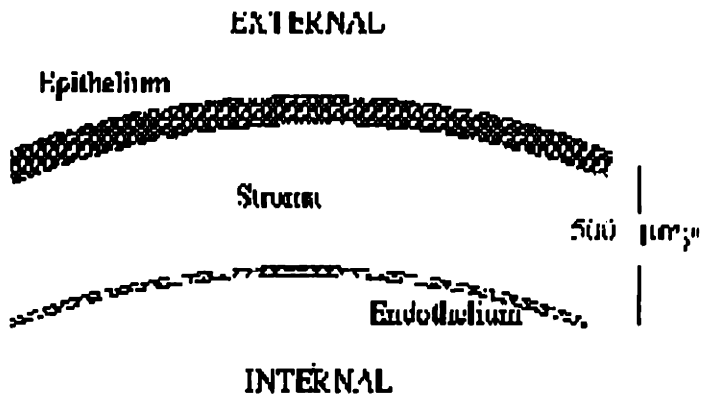

Figure 1.2: Corneal Micro-anatomy

Use of synthetic materials in corneal surgery has existed, at least theoretically, since 1771 when Pellier de Quengsy conceived of implanting transparent material in the scarred cornea. In the late 1800's, glass buttons were implanted into the cornea to increase the clarity of scarred corneas. Modern devices have been designed as optically clear poly (methyl methacrylate) cylinders that penetrate the cornea and are anchored by a collar.[4] A schematic of these devices is shown below. These prostheses are short lived due to the progressive necrosis and stromal melting of the cornea close to the cylinder. The impermeability and rigidity of these devices are believed to eventually cause the failure of the device.[5] There is no complete barrier (epithelium) covering the implant, thus the edges of the implant serve as a site for infection.

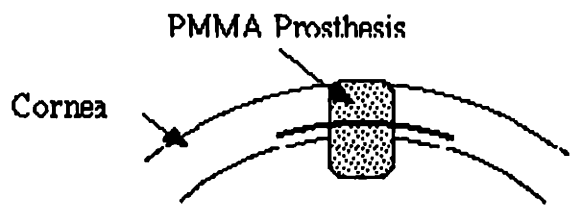

Figure 1.3: Poly(methyl methacylate) Corneal Prosthesis

Hydrogels were originally conceived only as *intra*-stromal implants.[7] The clinical application of these *intra*-corneal hydrogels was to affect the shape of the cornea for refractive surgery(see Figure 4). Initially three different hydrogel materials were used in corneal surgery. These substances were poly(2-hydroxyethyl methacrylate) pHEMA, poly(glycerol methacrylate) pGMA, and polyelectrolyte materials.[8] The desired characteristics of these materials only included their bulk characteristics such as: solute permeability, chemical and mechanical stability, and optical clarity. Biologically, these materials only needed to be non-inflammatory.[9]

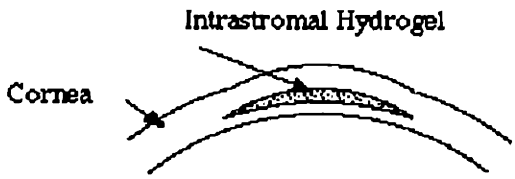

Figure 1.4: Intrastromal Hydrogel

High water content intrastromal implants were ineffective in altering the focusing power of the cornea. The implants failed because they only displaced the posterior surface of the cornea.* A change in the focusing (dioptric) power of the cornea was effective if curvature change was on the anterior surface (air/cornea interface).† This has forced research in refractive surgery to consider a prosthesis which was situated at the surface of the cornea. The placement of a refractive corneal prosthesis on the corneal surface must maintain the anatomical barrier function of the cornea. Maintaining a contiguous barrier

---

* High index of refraction materials can change the power of the cornea, but they are negligibly permeable to water and aqueous solutes.

† The magnification of a surface in diopters (D) is described by the equation: $D = \frac{n_1 - n_2}{r}$. Indices of refraction(n) of the media on either side of the surface are n_1 and n_2. The surface curvature (r) will only result in magnification at that interface if (n_1 - n_2) is non-zero. For the anterior surface: n_{cornea}-n_{air} = 0.336. For the posterior surface: n_{cornea}-$n_{aqueous} \simeq 0.0$

between environment and host was also an issue in a therapeutic corneal prosthesis. As such, further development of prostheses, for either refractive or therapeutic corneal surgery, centered on this problem.[3,6,10,11,12,13]

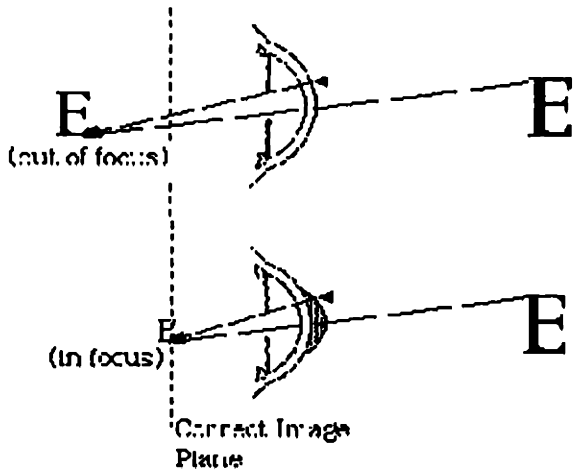

Figure 1.5: Corneal Curvature Changes in Surgical Refraction

The complete replacement of the cornea including one or both of the limiting layers (epithelium or endothelium) is still addressed with materials such as poly (methyl methacrylate)[5] or silicone membranes.[8] A prosthetic device that penetrates the epithelium of the cornea will always have a junction or fissure between prosthesis and the surrounding epithelium. Upon re-evaluation of the concept of a prosthetic cornea, the issue of biological activity (epithelial cell and tissue response) of the synthetic surface became a consideration.[14] The healing of epithelium over the implant is important in maintaining the barrier function of the cornea.[3] Normally, the epithelium is a labile cellular population which will grow back over an injured area of the cornea.[1,2,15] Thus, a prosthetic corneal surface must provide an environment that is conducive to stable epithelial cell growth.

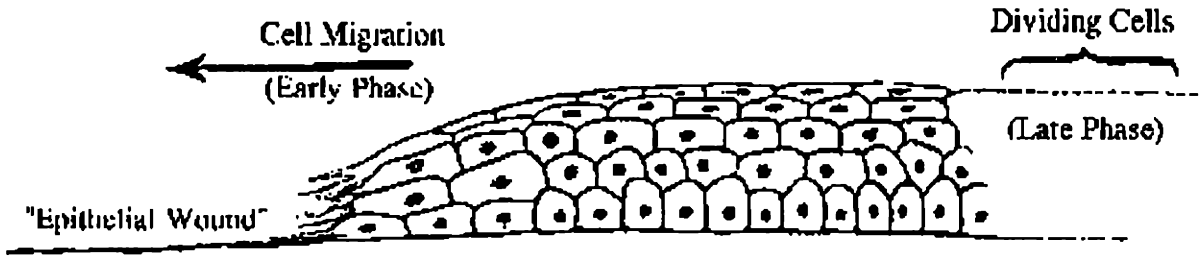

Figure 1.6: Growth of Epithelium over a Corneal Wound

1.2 Biomaterial Surface Modification

Analysis of the surface chemistry of synthetic material surfaces conducive to epithelialization has led to several very basic insights.[16,17,18,19] Factors such as negative charge, intermediate wettabilities, moderate hydroxylation, and low polymer chain rigidity are believed to be conducive to epithelialization. These factors are shown in Table 1.1. In spite of identification of these factors, investigators could not rule out the contribution of passive surface protein adsorption which aided in the adherence of cells.

Table 1.1: Factors Important in Cell Growth

Physical Property	Range
Wettability	45° -75° (contact angle)
Composition	High [OH] Low [COOH]
Chain Rigidity	Low Mobility

Protein or peptide attachment to surfaces is an attractive method of surface modification.[20] Proteins which are involved in the cell-substratum interactions have been shown to enhance the adherence of cells to synthetic surfaces. Efforts to specifically utilize these

proteins to enhance the adherence of corneal epithelial cells has been performed with PVA copolymer hydrogels.[3] Although the initial cell-hydrogel adherence is enhanced with these materials, prolonged attachment is not maintained. This result was probably due to the method of protein surface coating, which is based fundamentally on physical adsorption of proteins.[10]

Another approach to this problem attempts to synthesize a material whose intrinsic surface is one conducive to epithelial cell growth. Collagen possesses peptide regions known to be involved in cell-substrate adhesion.[21] The synthesis of these materials utilizes cross-linking methods to form hydrogels from the collagen types (I and IV).[6,11] Unfortunately, materials like this have been found to be susceptible to proteolysis. Other investigators have also synthesized collagen-HEMA copolymers to support epithelial cell growth.[22,23] These materials were found to be susceptible to proteolysis and brittle.

Table 1.2: Biomaterials Evaluated for Corneal Prostheses

Surface	Material	Modification
Intrinsic	Type I Crosslinked Collagen	Collagen
	Type IV Crosslinked Collagen	Collagen
	Collagen-HEMA copolymer	Collagen
Modified	Poly(vinyl alcohol) copolymer	Basement Membrane Proteins
	Poly(2-Hydroxyethyl methacrylate	Plasma Exposure
	P(HEMA)/P(EMA) copolymer	[OH] Variation

The current modalities[24] for using proteins/peptides as materials of hydrogel-fabrication or hydrogel-surface-modification are confounded by factors such as proteolytic digestion, poor protein adherence to the synthetic surface, and brittleness or fragility.[6] However, with these factors in consideration, utilizing cell-adhesion proteins immobilized

on a synthetic surface is attractive since proteins are ultimately involved in-vivo epithelialization. Table 1.2 shows materials reviewed for potential corneal prostheses.

1.3 The Composite Hydrogel

The term composite hydrogel is a descriptive one. Corneal stroma is a natural hydrogel composed primarily of collagen and water. This superficial and very thin layer of "hydrogel" is bonded to a support of synthetic hydrogel material. The aim of this configuration is to combine the attributes of both materials in a manner to address the requirements in the device's performance. Table 1.3 shows these device requirements and attributes of stroma or hydrogel.

Table 1.3: Functional Device Consideration

Functional Requirements	Device/Material Attributes
Stable Epithelial Cell Growth (Attachment/Migration) (Non-Toxic) (Resistant to Degradation)	Corneal Stroma
Tensile Strength	Corneal Stroma
Permanence	Corneal Stroma Synthetic Hydrogels
Clarity	Synthetic Hydrogels
Permeability to Aqueous Solutes	Corneal Stroma Synthetic Hydrogels

These studies were devoted to using native corneal tissue to synthesize a hydrogel surface conducive to epithelialization. Corneal tissue itself was chosen for several reasons. These reasons included the fact that corneal stroma has proven biocompatibility, is perme-

able to solutes, in resistant to non specific proteolysis, is composed of type I collagen and is clear. Over 70% of the cornea itself is fibrillar type I collagen.[2] Type I collagen possesses peptide regions known to be involved in cell-substrate adhesion.[25] Purified forms of type I collagen are commercially available as a substrate for cellular growth.[13] Still, purified forms of type I collagen suffer from susceptibility to non-specific proteolysis and renatured collagen materials are not optically clear. Fibrillar type I collagen in native corneal tissue form is not susceptible to non-specific proteolytic enzymes[6,26] and is optically clear. In addition to proteolytic resistance and optical clarity, fibrillar corneal collagen oriented in its normal tissue architecture can provide increased tensile strength[2,27] to the surface because of the orientation of the collagen fibers.

It is clear that using corneal tissue to impart favorable surface properties makes the development of corneal prosthesis an attainable goal. However, the current methods of attaching protein material onto hydrogels binds single protein molecules or small molecular aggregates onto surface sites resulting in a fragile superficial coating.[24,20] In some cases the bonding is only passive adsorption.[3,10] This approach did not attempt to preserve the higher organizational structure of collagen in corneal tissue. Collagen in corneal tissue is organized into a complex structure of fibrils oriented in parallel planes.[2] Collagen is not easily manipulated in processing techniques unless it is solubilized. However, in its soluble form, it no longer has the same architecture that it originally had in connective tissue.[28]

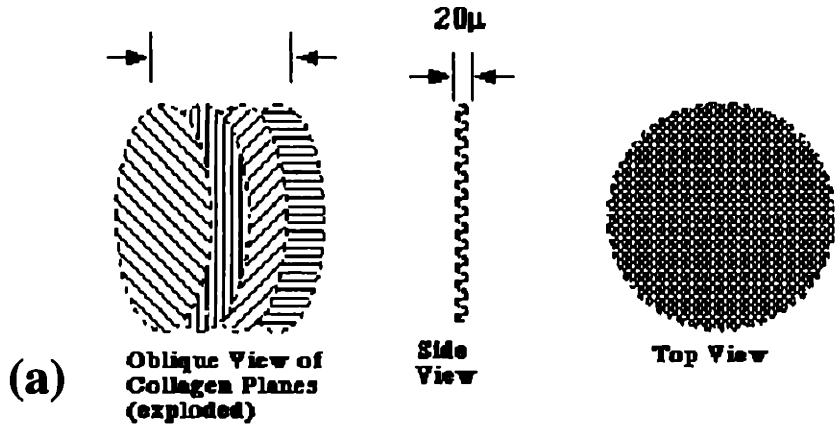

Figure 1.7: (a) Schematic of Corneal Collagen Lamellae
(b) SEM of Corneal Collagen Lamellae (oblique view)

One consideration in the use of corneal stroma is preservation of the natural architecture of corneal collagen fibrils. Currently, the reproduction of this complex collagen architecture is relegated to the biological environment of organogenesis during embryonic development.[1,4] The ultrastructural architecture of corneal tissue is not reproducible by

conventional synthetic means.[28] So, further device development and analysis was contingent upon determining a method to attach a tissue layer onto a hydrogel. The embodiment of a corneal prosthesis which uses stromal tissue as a bio-active surface, or more appropriately as an interface between organism and synthetic, is termed a bilayer composite hydrogel. The device embodiment is shown in Figure 1.11.

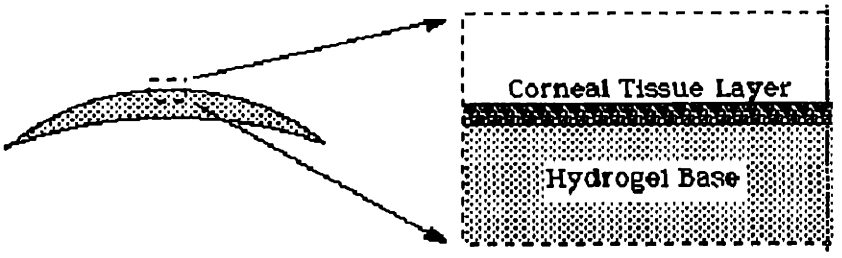

Figure 1.8: Bilayer Composite Hydrogel Onlay

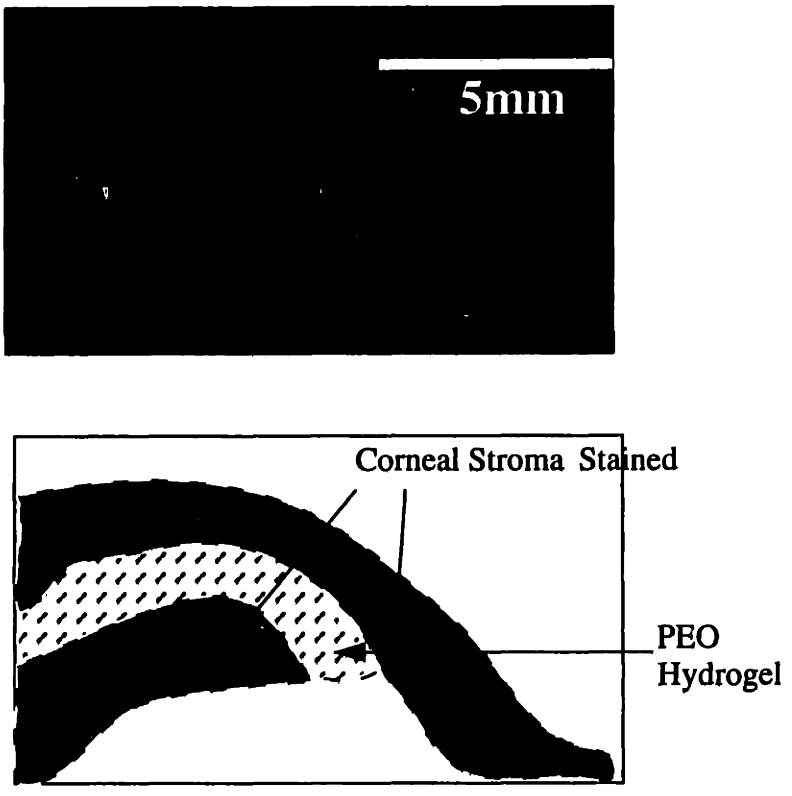

Figure 1.9: Methylene Blue Stained Composite Hydrogel

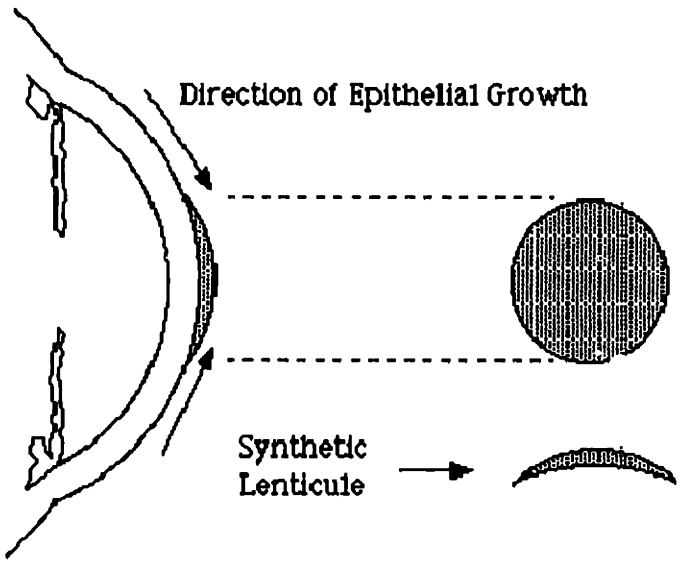

Figure 1.10: Anatomical Location of a Refractive Corneal Prosthesis

1.4 Scope of Research

This thesis deals with the synthesis and examination of a hydrogel whose ultimate use was for the construction of an artificial cornea. The design rationale was to construct a material possessing a surface environment conducive to epithelial cell growth in addition to possessing the proper optical, diffusive, and mechanical characteristics of the cornea. The research made use of electron-irradiation-induced (EII) cross-linking[29,30,31,32] to synthesize a hydrogel network and simultaneously attach the polymeric network to a collagenous[33,37] substrate. The body of the work presented in this document discusses several major areas: (1) the synthesis of a bilayer composite material composed of a thin layer of native corneal tissue adhered onto a mechanically stable hydrogel; (2) the analysis of the collagen immobilization via bonding between polymer molecules and fibrillar collagen matrix when aqueous poly(ethlyene oxide) was cross-linked via electron beam irradiation;

(3) the analysis of nutrient mass transport across PEO hydrogel materials; and (4) short term and long term biocompatibility studies on the composite hydrogels.

1.4.1 Composite Hydrogel Synthesis

Applying a thin layer of tissue to the surface of a hydrogel can be problematic because of difficulties in handling such fragile maleable material. An obvious consideration is to use an adhesive to bind one material to the other. However, the ability to perform such small manipulations with delicate materials (i.e. 20 micron thickness of cornea) is difficult. Problems such as uniform interfacial adherence, poor apposition, and the interfacial inclusion of adhesive can provide significant impediments to device construction. Additionally, the device must act as a single unit. The unification of corneal tissue to a hydrogel lens (the construction of a composite hydrogel) has been addressed in a straightforward manner in this investigation. Composite hydrogels are made by *synthesizing the hydrogel and grafting onto* the corneal tissue layer.

Synthesizing the hydrogel from a fluid state and simultaneously grafting the hydrogel onto the surface of the tissue layer assures perfect apposition of the two materials obviating the need for additional materials such as adhesives. Corneal tissue was sectioned into thin layers and applied onto the inner surface of a mold. Gelling fluid was placed into the tissue lined mold. When the hydrogel was removed, it was coated with a thin layer of tissue. This process was amenable to any hydrogel which could be synthesized under constant volume constraints.

In these studies, electron irradiation induced cross-linking of poly(ethylene oxide) [PEO] which was used to make composite hydrogels.[31,32,34,35] Electron irradiation of PEO was chosen because there were no potentially toxic leachable reagents necessary for cross-linking. Electron irradiation simultaneously cross-linked PEO and sterilized the material for surgical applications.[36] PEO hydrogels are FDA approved and are considered

to be the most biocompatible of synthetic materials. Lastly electron irradiation induced cross-linking can potentially stabilize[37,38,39,40] the interfacial union of the PEO hydrogel and tissue by cross-linking PEO molecules to collagen molecules in tissue.

With respect to synthesizing usable PEO hydrogels for these studies and device construction, investigation into refinements of the synthetic procedure was performed. There were some inherent drawbacks in using electron irradiation of aqueous solutions of PEO. These drawbacks included the creation of hydrogen bubble defects and significant swelling of formed hydrogels. Methods to circumvent these problems were developed and used to synthesize materials for evaluation of PEO mass transport properties and biocompatibility testing. In addition, a detailed evaluation of the PEO-collagen interface was performed. Collagen immobilization onto PEO hydrogels was detected using surface analytical techniques and quantified via fluorescence spectroscopy.

1.4.2 Diffusion of Solutes

Transport of nutrients, metabolites, and other solutes is an important physiological process in the cornea.[1,2] The adequate supply of nutrients is very important to the health of the primarily cellular and highly metabolic regions of the cornea.[7,41] In particular, the pathway of nutrient flow to the epithelium originates from the anterior chamber and travels across the cornea to the epithelium. There are no blood vessels to supply nutrients into the cornea because the cornea is avascular and therefore clear.[2] A simplified diagram of mass transport flow is shown in Figure 1.11. Considering this important nutrient flow, the inability of an PMMA prosthesis to support epithelial growth is not only compromised by an inappropriate biosurface but also by the absence of solute transport across the cornea.[5]

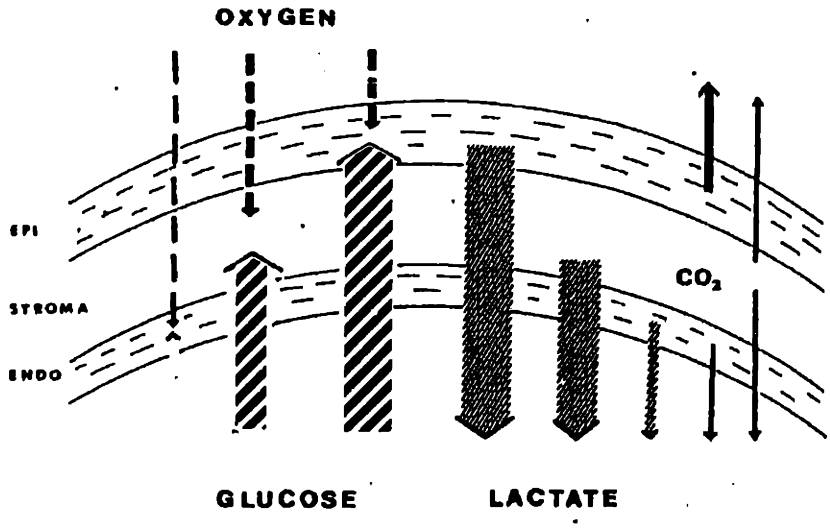

Figure 1.11: Nutritional Vectors in the Cornea

Hydrogel corneal implants were an important advance because they allow the flow of nutrients to the superficial layers and epithelium. Maintainence of glucose flow to the epithelium from the anterior chamber is important for physiological homeostasis. Epithelium is highly active metabolically and the nutrient glucose provides the energy to carry out living processes. Therefore, as a major effort in this study, the mass transport properties of glucose in PEO hydrogels was evaluated in detail.

1.4.3 Epithelial Healing

Ultimately, the goal of the composite hydrogel was to support epithelial healing[5,6,15] over the surface. A major effort was placed on evaluating the growth of cells on these composite material. Important parameters in evaluation of cellular compatibility in vitro range from the qualitative[42] to some quantitative[12] measures. Outright toxicity was the first qualitative measure of compatibility that was readily assessable. PEO by itself is non-toxic. With regard to the process as a whole, bacterial contamination is a complication that could have compromised either *in vitro* or *in vivo implantation*. Irradiation of material always produced sterile non-toxic materials. Corneal epithelial cells were cultured on

composite hydrogels from both primary cell cultures and direct migration of cells from tissue explants. Deposition of basement membrane proteins was noted from week 1 to week 8 for cells grown on composite gels. Composite hydrogel substrates in migration systems showed that epithelial cells would readily migrate onto the hydrogel surface. An artificial ocular system was created to quantitate epithelial cell migration (healing) over the device surface. A compromise in healing rate was noted in diffusion limited cases. This was modelled to generalize the effect of diffusion limitations on healing.

1.4.4 Design Criteria

Currently, there are many different laboratories developing some type of hydrogel prostheses for either refractive or therapeutic intervention. The theoretical models which were developed within this work are amenable to evaluating not only of the function of this particular composite hydrogel prosthesis but others as well. The analysis of in vitro healing was directly extended to the design of a prosthesis for patient use. Providing that the mass transport characteristics of any other hydrogel formulation is known, the analyses of epithelial wound healing and long term health can be evaluated as well.

Chapter 1 References

[1] Frederick S. Brightbill (editor). Corneal Surgery - Theory, Technique, and Tissue, Chapter 31. C.V. Mosby Co., 1986.

[2] Maurice D: The Cornea and Sclera. in The Eye, Vol 1B, Davson H, editor. Florida, 1984, Academic Press, pp 1-158

[3] V. Trinkaus-Randall, J. Capecchi, A. Newton, A. Vadasz, H. Leibowitz, and C. Franzblau. Development of a Biopolymeric Keratoprosthetic Material. In Investigative Ophthalmology and Visual Science. 1985, 29(3), pp 393-400

[4] Hernando Cardona. Keratoprosthesis-Acrylic Optical Cylinder Supporting Intralamellar Plate in Ophthalmology, (1976) pp284-299

[5] CH Dohlman. Discussion: Biology of Complications Following Keratoprosthesis. *Personal Communication*

[6] K.P. Thompson et al. Current Status of Synthetic Epikeratoplasty. Refractive and Corneal Surgery. May/June 1991. Vol 7, pp. 240-248

[7] B. E. McCarey and D. M. Andrews. Refractive Keratoplasty with Intrastromal Hydrogel Lenticular Implants. Investigative Ophthalmology and Visual Science. July 1981, Vol. 21, No. 1, pp. 107-115

[8] Miguel F. Refojo. Artificial Membranes for Corneal Surgery. In J. Biomed. Mater. Res. 1969, Vol 3, pp 393-347

[9] Robert L. Peiffer, TP Werblin, Andrzej W. Fryczkowski. Pathology of Corneal Hydrogel Alloplastic Implants. In *Ophthalmology.* 1985, Vol 92, pp 1294-1304

[10] R. Sipehia, A Garfinkle, W.B. Jackson, and T.M.S. Chang. Towards an Artificial Cornea: Surface Modifications of Optically Clear, Oxygen Permeable Soft Contact Lens Materials by Ammonia Plasma Modification Technique for the Enhanced Attachment and Growth of Corneal Epithelial Cells. In Biomat., Art., Cells, and Art. Org., 1990, 18(5), pp 643-655

[11] Thompson EP, Hana KD, and Gravagna P. et al. Synthetic Collagen IV lendiclue as a biomaterial for epikeratoplasty. ARVO Abstracts. Invest Ophthalmol Vis Sci. 1990. 1990: 31 (suppl): 301

[12] D. K. Pettit et al. Quantitation of Rabbit Corneal Epithelial Cell Outgrowth. Investigative Ophthalmology and Visual Science. Nov 10, Vol 31, No. 11, pp. 2269-2277

[13] Harry S. Geggel, Judith Friend, Richard A. Thoft. Collagen Gel for Ocular Surface. In *Investigative Ophthalmology and Visual Science*. 1985, 26(6), pp901-905

[14] R. Y. Paynter. Chapter 2: Surface Analytical Techniques in Biomaterials Development. Biocompatibility Testing Vol. II, D. F. Williams (editor), CRC Press, Inc., Copyright 1986, pp. 49-80

[15] L. A. McNicol and E. Strahlman. Corneal Biomechanics and Wound Healing. Proceedings from the Workshop on Corneal Biophysics I. National Eye Institute, Bethesda, MD 1989, pp 161-194

[16] Yukitaka Sugimoto. Effect on the Adhesion and Locomotion of Mouse Fibroblasts by the Interacting with Differently Charged Substrates. Experimental Cell Research. 1981, Vol 135, pp. 39-45

[17] T. N. Salthouse and B. F. Matlaga. Chapter 5: Some Cellular Effects Related to Implant Shape and Surface. Biomaterials in Reconstructive Surgery. L. R. Rubin (editor). C. V. Mosby Co., Copyright 1983, pp. 40-45

[18] R. E. Baier et al. Surface Properties Determine Bioadhesive Outcomes: Methods and Results. Journal of Biomedical Materials Research. 1984, Vol. 18, pp. 337-355

[19] Curtis ASG et al: Substrate Hydroxylation and cell Adhesion. Journal of cell Science 86:9. (1986)

[20] S. M. Kirkham and M. E. Dangell. The Keratoprosthesis: Improved Biocompatibility Through Design and Surface Modification. Abstracts-Seventeenth Cornea Research Conference. Sept 19, 1991, p. 23

[21] Rioslahti E, Pierschbacher MD: Arg-Gly-Asp: A Versatile Cell Recognition Signal. Cell; 44 pp. 517-518 (1986)

[22] K. Pandaranga Rao and K. Thomas Joseph. Chapter 3: Collagen Graft Copolymers and their Biomedical Applications. Marcel E. Nimni (editor). Collagen - Volume III Biotechnology. CRC Press, Inc. pp. 63-85

[23] Carl Franzblau et al. Chapter: Cell Growth on Collagen-HEMA Hydrogels. Marcel E. Nimni (editor). Collagen - Volume III Biotechnology. CRC Press, Inc. pp. 191-208

[24] Merrill Lynn. Chapter 1: Inorganic Support Intermediates: Covalent Coupling of Enzymes on Inorganic Supports. Immobilized Enzymes, Antigens, Antibodies, and Peptides. Howard H. Weetal (editor). Marcel Dekker, Inc., New York, pp. 1-47

[25] I.V. Yannas. Collagen and Gelatin in the Solid State. J. Macromol. Sci.-Revs. Macromol. Chem., 1972,C7(1), pp 49-104

[26] R. F. Oliver, R. A. Grant, and C. M. Kent. The Fate of Cutaneously and Subcutaneously Implanted Trypsin Purified Dermal Collagen in the Pig. Br. J. exp. Path. (1972), Vol. 53, pp 540-549

[27] lE. Reichel et al. The Elastic Modulus of Central and Perilimbal Bovine Cornea. Annals of Ophthalmology. 1989, Vol. 21, pp 205-208

[28] Jonathan King. Deciphering the Rules of Protein Folding. In Chemical and Engineering News. 1989, Vol 67, pp 32-54

[29] Joseph E. Wilson. Radiation Chemistry of Monomers, Polymers, and Plastics. Marcel Dekker, Inc. New York. Copyright 1974

[30] J.W. Stafford. The Radiation Induced Reactions of Aqueous Polyethylene Oxide Solutions: I. Theory of Gelation. In Die Makromolekulare Chemie. 1970, Vol 134, pp 57-69

[31] J.W. Stafford. The Radiation Induced Reactions of Aqueous Polyethylene Oxide Solutions: II. Intrinsice Viscosity Changes in the Pregel Region. In Die Makromolekulare Chemie. 1970, Vol 134, pp 71-85

[32] Dennison KA: Radiation Crosslinked Poly(ethylee oxide) Hydrogel Membraes. PhD Thesis, MIT, (1986)

[33] Braams. Rate Constants of Hydrated Electron Reactions with Peptides and Proteins. Radiation Research. 1967, Vol. 31, pp. 8-26

[34] A. R. Shultz et al. Chapter IX: Intermolecular Reactions A. Crosslinking By Radiation. Chemical Reactions of Polymers. E. M. Fettes (editor). Interscience Publishers, Inc. pp 723-755

[35] Merrill EW. et al: Versions of Immobilized Poly(EO) for Medical Applications. Polymers in Medicine: Biomedical and Pharmaceutical Applications, R.M. Ottenbrite & E. Chiellini (eds.) Technomic Publishing (1992), pp 39-56

[36] K. A. Wright and J. G. Trumpp. Co-operative Studies in the Use of Ionizing Radiation for Sterilization and Preservation of Biological Tissues. Sterilzation and Preservation of Biologic Tissues by Ionizing Radiation. International Atomic Energy Agency. Vienna 1970 pp 107-118

[37] Okamura S and Hino T: Silicone Rubber Coated with Collagen. US Patent No 3,955,012

[38] K Pietrucha and J Kroh. Radiation Crosslinking of Poly(butyl acrylate) During Polymerization and Grafted Copolymerization with Cr(III) Crosslinked Collagen. Int. J. Radiat. Appl. Instrum., Part C: 1986, Vol 28, No 4, pp 373-376

[39] K Panduranga Rao, K Thomas Joseph, and Y Nayudamma. Grafting of Vinyl Monomers on to Modified Collagen by Ceric Ion-Studies on the Grafting Site. Leather Science, 1969, Vol 16, pp 401-408

[40] K Pietrucha and M. Lubis. Some Reactions of OH Radicals with Collagen and Tyrosine in Aqueous Solutions. Int. J. Radiat. Appl. Instrum., Part C: 1990, Vol 36, No 6, pp 155-160

[41] Christine A Zurawski, Bernard E. McCarey, and Frederick H. Schmidt. Glucose Consumption in Cultured Corneal Cells. *Current Eye Research*: 1989, Vol 8, No 4, pp 349-355

[42] DT Azar, et al. Reassembly of the Corneal Epithelial Adhesion Structures Following Human Epikeratoplasty. In *Achives of Ophthalmology*, 1991, Vol 109: pp 1279-1284

Chapter 2

Composite Hydrogel Synthesis

This chapter describes the refinements in the methods to synthesize composite hydrogels. Bilayer composite hydrogels are synthetic hydrogels with an ultra-thin surface layer of connective tissue (*a natural hydrogel*) bonded to the surface. In these studies, a composite hydrogel was specifically a poly(ethylene oxide) [PEO] hydrogel grafted onto a layer of corneal tissue. The integral aspect of the synthetic method was the in-situ cross-linking and grafting of the synthetic hydrogel onto the tissue layer. The composite material structure began as a pre-cut, plano, molded layer of tissue onto which aqueous PEO was simultaneously self cross-linked and grafted onto the collagenous tissue by means of electron irradiation induced cross-linking. The development of various refinements to the synthetic procedure are presented here. These are (1) PEO hydrogel synthesis, (2) PEO-Collagen Fixation, and (3) Tissue Layer Preparation.

2.1 PEO Hydrogel Synthesis

A hydrogel network is a water swollen polymeric network. The poly(ethylene oxide) hydrogels used in this study were synthesized by EII (electron irradiation induced) cross-linking of an aqueous solution of PEO. EII cross-linking has been extensively used to cross-link aqueous solutions of PEO molecules into hydrogel networks.[1] Individual PEO molecules are linked to one another via covalent cross-links that arise as a result the irradiation process. During EII irradiation, water is lysed into hydrogen and hydroxyl radicals.

Hydrogen radicals recombine to form hydrogen gas whereas the hydroxyl radicals create macroradicals on polymers (such as collagen and PEO).[2,3,4,5]

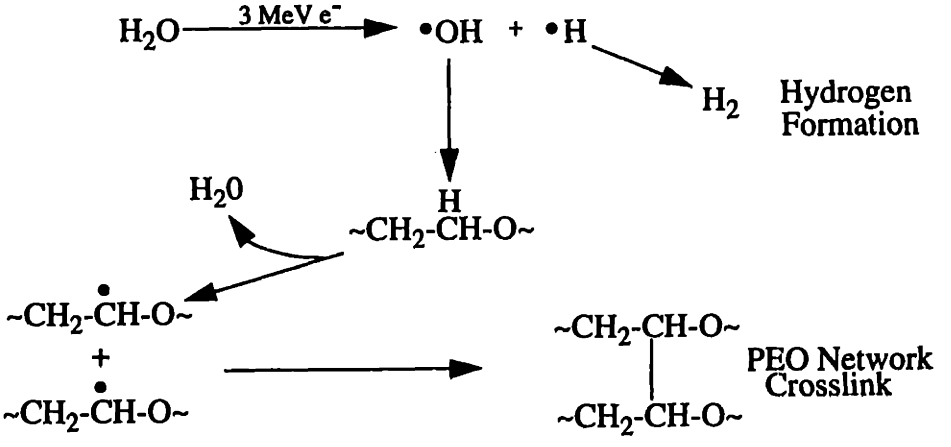

Figure 2.1: Chemistry of Aqueous PEO Irradiation

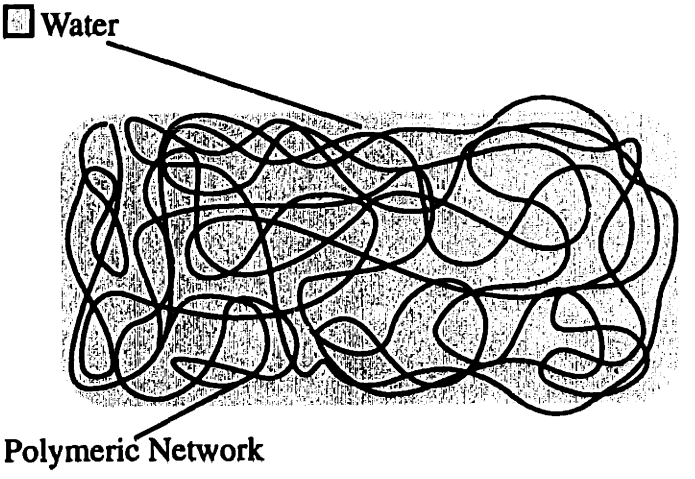

Figure 2.2: Hydrogel Network

For these studies, electron irradiation was performed at the MIT High Voltage Research Laboratory which houses a 3 million electron volt Van de Graaff generator. This Van de Graaff generator provides the electron source (tungsten filament) and accelerating

voltage that creates a 3 inch wide electron beam which irradiates samples conveyed through the beam path by a conveyor belt. Current of up to 10 microamperes flowed through the system. At 3 MeV, this current corresponds to a dose rate of up to 0.25 Mrad/ sec. A schematic of the setup is shown below.

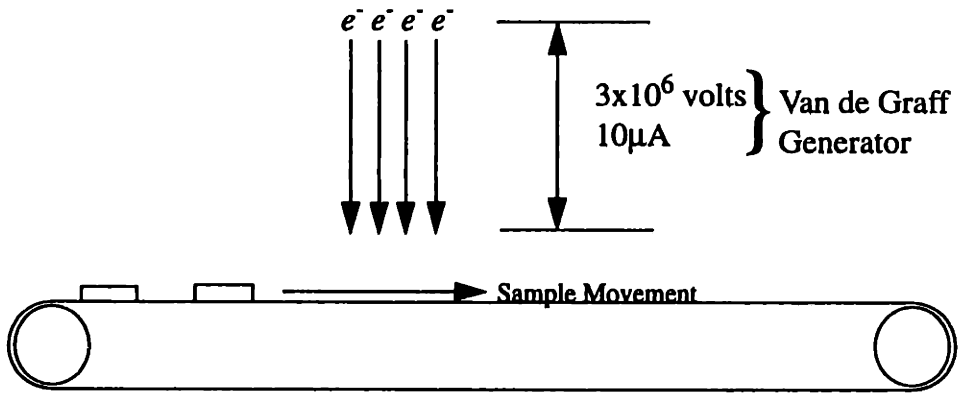

Figure 2.3: Irradiation Setup

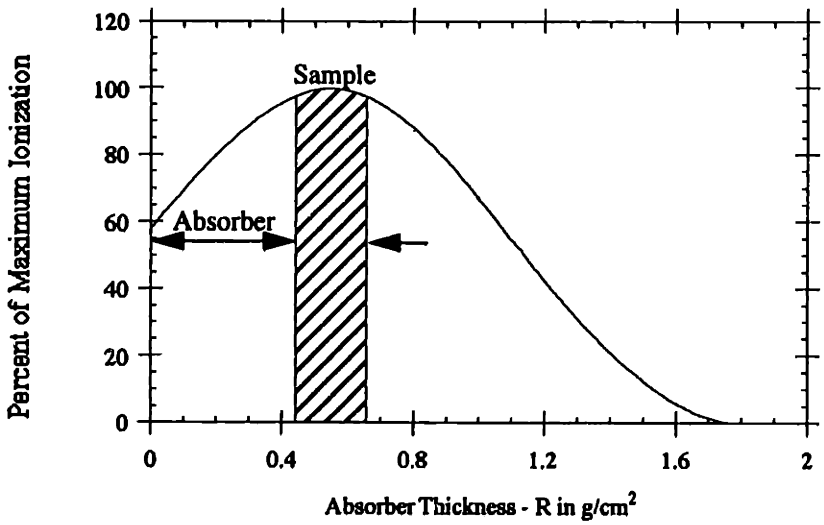

Figure 2.4: Ionization distribution for 3 Million volt Electron Beam

Electron irradiation ionizes material as it penetrates. The ionization distribution of an electron beam has a characteristic broad maximum at about a third of the greatest depth of the electrons. Figure 2.4 shows this generalized ionization profile. This shape of the ionization curve is due primarily to the high scattering tendency of the incident electrons. The depth of penetration (cm) can be found for different materials (copper, lead, and water) if effective thickness (g/cm^2) is converted to depth by dividing by the density (g/cm^3) of the material.[6,7]

The dose delivered to any sample is dependent on the particular depth along the ionization curve where the sample is absorbing. Non-uniform ionization is circumvented by placing an absorber between the sample and the incident beam. The absorber material occupies the ascending portion of the ionization curve and is approximately 0.4 g/cm^2 in effective thickness. Thus, the sample absorbs at the maximum of the ionization curve. At this portion of the curve, the sample receives uniform irradiation. For aqueous solutions of density $1 g/cm^3$, the solution depth can be up to 2mm in thickness.[7,8] Samples conveyed beneath the beam receive a particular dose based on duration of exposure to the beam. The primary manipulatable parameter in this study was dosage (Mrads).

Synthesizing PEO hydrogels by electron irradiation of aqueous solutions contains some inherent drawbacks. Problems such as hydrogen bubble defect formation and swelling of hydrogel materials produced unusable materials for further study or device manufacture. Investigation into the problems of PEO hydrogel synthesis has resulted in the following methods to circumvent those difficultities.

2.1.1 Bolus Dose Irradiation

When a solution of PEO is irradiated, the high energy electrons lyse water to hydrogen and hydroxyl radicals. The hydroxyl radical is the reactive species which causes cross linking. Hydrogen radicals recombine into hydrogen (H_2). The formation of H_2 in solution

can be so fast that nucleation and bubble formation of H_2 will occur in the irradiation process. The process has been circumvented by sequential bolus dose irradiation. The method prevented bubble formation by continuously irradiating only up to the point where nucleation and bubble formation of H_2 is just reached. Irradiation is then stopped and H_2 gas is allowed to diffuse out of the solution (or hydrogel in this case). After hydrogen gas is allowed to diffuse out, the sample can receive more irradiation. The following experiment compared hydrogels made by continuous irradiation and sequential bolus dose irradiation.

Materials and Methods: Solutions of 10% (w/v) were made from 100K (linear PEO (PolySciences, Inc- Lot No. 80036) in MilliQ water containing 0.05% sodium azide. The actual number average molecular weight of this linear polymer was measured as 29,750.[9] The polymer was dissolved overnight with gentle rocking and the flowing agent (silica) was removed by centrifuging the solution at 1,500 rpm for 2 hours. The clarified solutions were cooled to 4°C and degassed 30 minutes prior to irradiation by vacuum application. Clean 100 mm pyrex petri-dishes were used as sample containers for irradiation. Immediately prior to irradiation, 10 cc of PEO solution was placed into each dish. Four samples were continuously irradiated. These four samples had dosages of 4, 6, 8, or 10 Mrads. A companion set of samples received sequential irradiation doses at a dose of 2Mrad per bolus. The samples were sealed with parafilm immediately after irradiation to prevent drying and stored overnight at 4°C. Four sample receiving 4, 6, 8, and 10Mrads were created in this manner.

Results and Conclusions: Continuous irradiation of PEO solutions beyond 2Mrads showed copious bubble formation. Hydrogels formed below 2 Mrads were relatively clear with negligible hydrogen bubble defects. At doses greater than 2 Mrads, bubbles were entrapped in the hydrogel. With continuous irradiation, these entrapped bubbles continued to grow in size. When a solution was sequentially irradiated in bolus doses below 2 Mrad,

high dose materials could be synthesized with minor bubble formation. The figure below is a comparison between two 10 Mrad hydrogels: one synthesized with continuous irradiation and another synthesized in bolus doses. Sequential dose irradiation provided the ability to synthesize high dose hydrogel materials without the accompanying bubble defect formation.

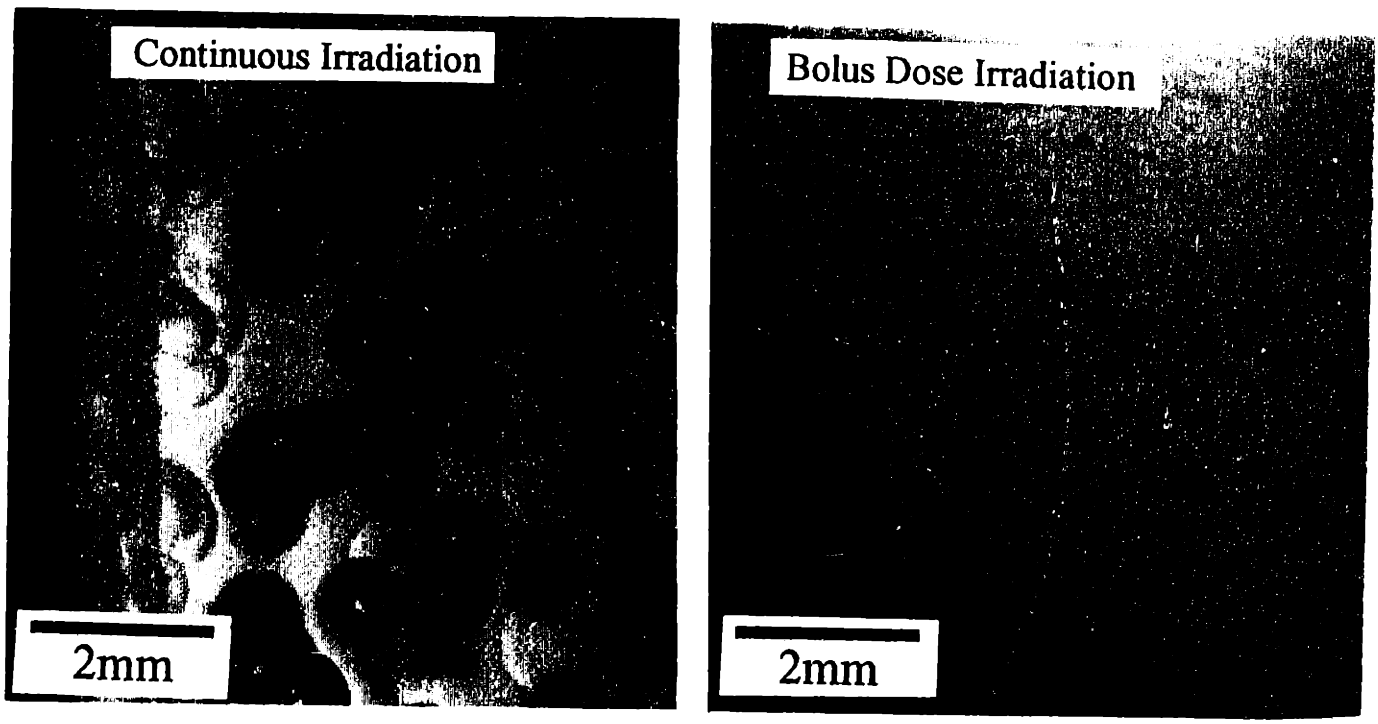

Figure 2.5: Comparison of 10 Mrad PEO Hydrogels

2.1.2 Volume Stable Synthesis

PEO hydrogels made from low molecular weight polymer (<100K) characteristically swell to several times their volume.[1] Yet, it is useful to maintain the PEO hydrogel at a constant volume if it is to be cast in a mold specifically designed for optical correction. In addition, a swelling hydrogel which was bound onto an inextensible layer of tissue led to curling or rolling of the composite. Therefore, hydrogel synthesis at a stable volume was an important refinement in the synthesis of the composites. By creating enough network cross-links, it was possible to create hydrogels which swelled very little. Theoretically, this may be achieved by very high dose irradiation or by utilizing molecules that already

possess intrinsically restrained polymeric chains (i.e. star molecules). An investigation of very high molecular weight PEO (MW=5,000K) revealed that hydrogels produced from this polymer remained stable or contracted with low dosage.

The peculiar swelling behavior of PEO hydrogels made from high molccular weight linear PEO was useful but not altogether obvious, since low molecular weight cross-linked PEO hydrogels characteristically swell to several times their volume. In order to gain some insight into the polymeric network cross-linking in these hydrogels, tensile testing of unswollen cross-linked solutions was performed. As a comparison to high molecular weight linear PEO, star PEO hydrogels of the same approximate molecular weight were synthesized. Electron irradiation induced cross-linking of aqueous star PEO[10] solutions created hydrogels which swelled very little. This result probably occurred because stars acted as hard spheres and are relatively inextensible. Star molecules possibly have less entanglements of PEO chains between individual molecules. In contrast, linear molecules acting as random coils could have a significant amount of entanglement. Star shaped PEO (MW=1,860K- 10K per arm)[10] was obtained to compare its network cross-linking behavior to that of linear PEO (MW=2,000K).

Materials and Methods:

One gram of linear PEO (MW=5,000K, Union Carbide, PolyOX, Cat No. C-014) was dissolved into 50 ml of MilliQ water (0.05% Sodium Azide) by gentle rocking for 24 hours. The solution was cooled to 4°C and degassed by vacuum application prior to irradiation. Clean 60 mm pyrex petri-dishes were used to hold 5cc of solution for irradiation. Samples were continuously irradiated for total doses of 2, 4, 6, 8, and 10 Mrads. Each dose was done in triplicate. After irradiation, the hydrogels were placed in an excess of solvent (10cc of MilliQ water with 0.05% sodium azide) and left at room temperature for 72 hours. After 72 hours, the solvent was decanted off and stored. The hydrogels were

accurately weighed before and after swelling. Volumetric swelling was measured as a ratio of final weight to initial weight. This is equivalent to the ratio of initial to final volume fractions (v_{2S}).

Hydrogels for tensile experiments were synthesized from star PEO (MW=1,860K-10K arm) and linear PEO (MW=2,000K, Union Carbide, PolyOX, Cat No. M-027) irradiation cross-linking solutions of 1% polymer dissolved in MilliQ water with 0.05% sodium azide. The resulting hydrogels were die cut into samples (0.6"x0.2"x0.5") for tensile testing (strain rate=0.000627inches/sec). The tensile modulus (E) was derived from the mechanical testing analysis for each sample. Tensile modulus (E) can be related to moles of elastic chains per unit volume (v_e/V_o) in the network through rubber elasticity theory:

$$f_{\alpha\to 0} = \left(\frac{\tau}{\alpha - \frac{1}{\alpha^2}}\right)_{\alpha\to 0} = \frac{\tau}{3\frac{\Delta l}{l}} = \frac{E}{3} \tag{2.1}$$

$$f = \left(\frac{v_e}{V_o}\right)RT \tag{2.2}$$

$$\frac{E}{3} = \left(\frac{v_e}{V_o}\right)RT \tag{2.3}$$

Where,

E = Tensile Modulus [=] dynes/cm^2
f = reduced modulus[=] dynes/cm^2
(v_e/V_o) = moles of elastic chains per unit volume, mol/cc
τ = tensile stress [=] dynes/cm^2
$\alpha = l/l_o$
T= Absolute Temperature [=] K
R= Gas constant [=] 8.317 x 10^7 dynes/mol·K
l = length[=] cm

The relationship between moles of elastic chains per volume and tensile modulus is given by 2.3. Tensile testing was performed on PEO hydrogels in the unswollen state to

determine the amount of cross-linking present per volume in the original irradiated solution. PEO concentrations were set at 1%, and testing was performed at room temperature.

Results: The swelling behavior of the 2% linear PEO (MW=5,000K) is shown in Figure 2.6. These hydrogels showed some syneresis but in general the contracture was small. At a 2 Mrad dose, an approximate decrease of 7% in volume was noted. With very high doses of 10 Mrad, the contracture approached 30%.

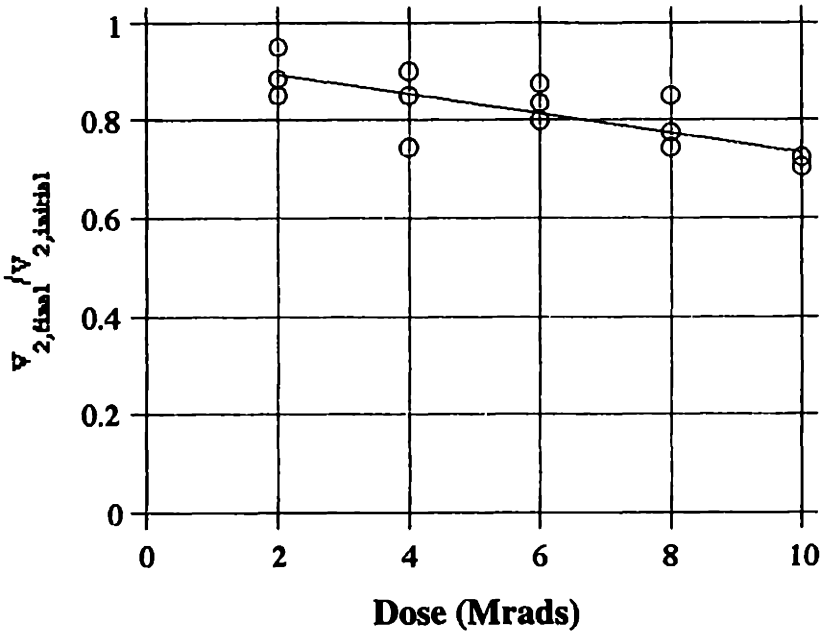

Figure 2.6: Swelling versus Dose for PEO (2%-MW=5,000K)

The tensile testing data of the unswollen hydrogels provided an indication of the cross-linking present within these solutions after irradiation. The relative amount of moles of elastic chains (or effective junctions) showed no difference between the star polymer or the linear polymer at irradiation doses greater than 2.5 Mrad. However, the moles of elastic chains at the lower irradiation dose (1.25 Mrad) was much higher for linear PEO than for star PEO (approximately 5X). Tensile testing on unswollen star polymer networks indicated that ~9 junctions existed within each molecule per 1Mrad of dose. In comparison with star molecules of the same approximate molecular weight, linear molecules pecu-

liarly had a much higher junction density than stars at low irradiation conditions (1.25Mrad). This result could have been due to pre-existing entanglements which thereby created physical junctions. At higher doses these chain entanglements were replaced with chemical crosslinks.

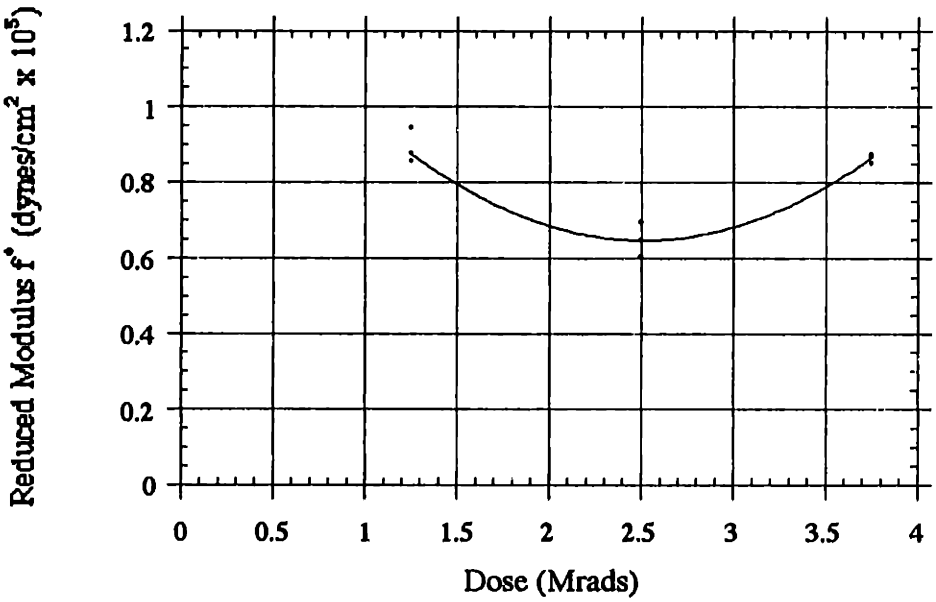

Figure 2.7: Tensile Testing of Unswollen Linear PEO (MW=2,000K), created from a 1% solution

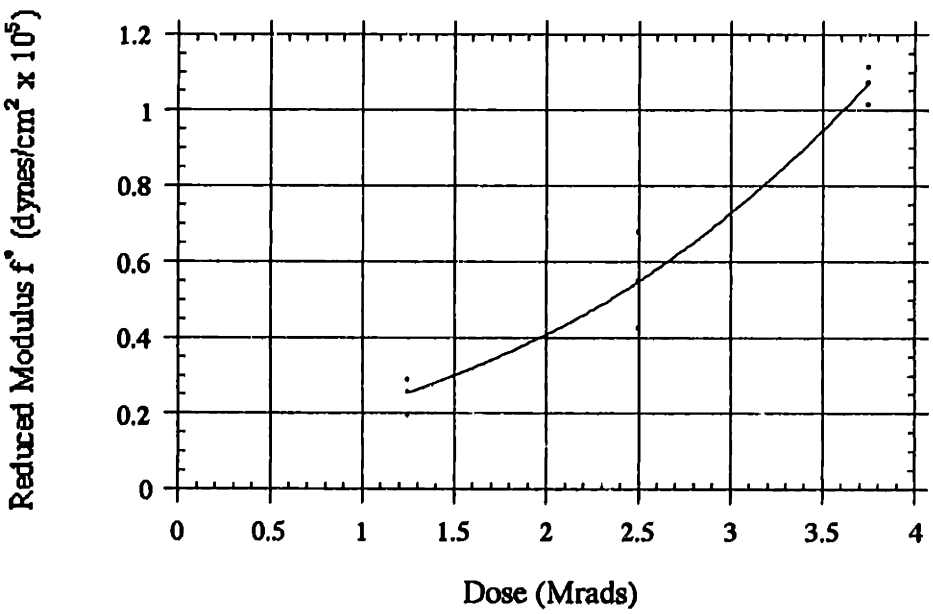

Figure 2.8: Tensile Testing of Unswollen Star PEO (MW=1,860K, arm=10K), created from a 1% solution

Star molecules, in contrast to linear ones, are more compact and do not exhibit this entanglement. The number of effective junctions for star molecule networks approached zero at low doses. This suggested that irradiation of PEO star molecule solutions directly resulted in the genesis of effective network junctions. Thus, it appeared that some pre-existing network junctions may have existed for large molecular weight linear molecules. These pre-existing network junctions may have also accounted for the peculiar swelling behavior of these high molecular weight linear PEO hydrogels..

2.2 PEO-Tissue Fixation

The lamination of the PEO hydrogel surface with a thin layer of corneal tissue was an attempt to physically impart the unique biological characteristics of corneal tissue to the hydrogel surface. The integrity of the composite structure as a single unit was dependent on the permanence of the attachment between tissue and hydrogel. Since the subsequent dehiscence of the tissue layer in the physiological environment can potentially compromise the function of the device, a more detailed understanding of the properties of the tissue-PEO hydrogel interface was sought. Interfacial chemical analyses were performed to obtain this information. The working hypothesis in these interfacial studies was that macromolecular cross-linking induced by electron irradiation can covalently bond tissue to PEO.[2,4,11,12]

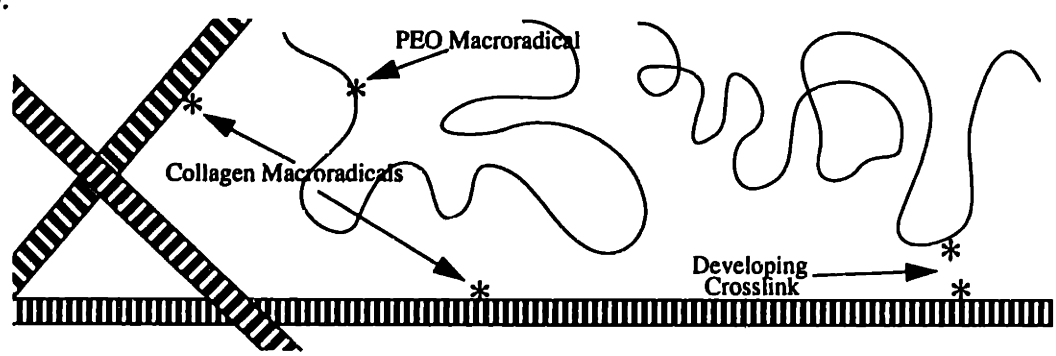

Figure 2.9: Grafting Reaction between Collagen and PEO

The model samples used for these studies consisted of aqueous PEO solutions grafted onto type I collagen with electron irradiation. Collagen in these studies was not soluble but was in solid form. Grafting of PEO molecules to collagen could only occur at the PEO-collagen interface. Thus, a large fraction of collagen present within these model composite hydrogels was not in close proximity to the interface. After hydrogel synthesis, the unbound collagen was hydrolyzed and washed away. Only bound material was detectable after hydrolysis by surface spectroscopic techniques: (Electron spectroscopy for chemical analysis) ESCA and (Multiple Internal Reflectance - Infrared spectroscopy) MIR-IR.

2.2.3 Materials/Methods for PEO-Tissue Fixation Studies

Synthesis of Composite Materials. In the synthesis of these model composites, two forms of collagen were used: films and fine particles. Collagen Type I films were obtained from Collagen Corporation (Palo Alto, CA) as sheets measuring 25 m in thickness. Solid particulate collagen type I was obtained from Medchem Products, Inc. (Woburn, MA). The collagen particles were irregular but averaged *1mm* in diameter. Solutions of PEO were made in MilliQ water containing 0.05% sodium azide and were degassed by short term application of a vacuum. Collagen films were used to make (1) model bilayer composite materials and collagen particles were used to make (2) slurry hydrogels of particles suspended within the PEO hydrogel base.

Collagen films were overlaid with a degassed 10% (w/v) PEO solution (100K, Poly-Sciences, Inc-Lot No. 80036) and irradiated with doses of 7.5 and 10 Mrads. Bilayer collagen/PEO films were irradiated in 60mm pyrex petri-dishes. Collagen-PEO slurries were mixed in an end to end two syringe assembly to form suspensions. The following PEO solutions were used when forming suspensions: 100K-Linear (PolySciences, Inc-Lot No. 80036), 2,000K-Linear (Union Carbide - PolyOX , Cat. No. M-027), Star-1,860K, 10K

arm (Strausbourg)[10] and 5,000K-Linear (Union Carbide - PolyOX , Cat. No. C-014). Table 2.4 shows the model composite material combinations. Irradiation of composites (suspensions or bilayers) took place within 1.5 hours of mixing.

Table 2.4: Model Composite Materials for Analysis

Collagen Material	PEO Solution (w/v)	Doses
Films	10% 100K-linear	7.5 10
Particles (40 mg/ml of solution)	4% 100K - linear	4 6 8 10
Particles (17.5 mg/ml of solution)	4% 100 K-linear	4
Particles (17.5 mg/ml of solution)	4% Star (1,860 K, 10K per arm)	2 4 6
Particles (17.5 mg/ml of solution)	4% 2,000K-linear	2 4 6
Particles (17.5 mg/ml of solution)	2% 2,000K-linear 4% 2,000K-linear 6% 2,000K-linear 8% 2,000K-linear	2 2 2 2
Particles (17.5 mg/ml of solution)	4% 5,000K-linear	4

Exposing the PEO-Collagen Interface (*Removal of ungrafted collagen*):

The resulting composites, either bilayer or suspension, were hydrolytically treated to remove unbound collagen. The resulting hydrogel surfaces, formerly at the collagen-PEO interface, were then amenable to different analytical techniques. Collagen can be degraded by a number of hydrolytic means. Enzymatic removal of collagen I can be accomplished by initial incubation in collagenase and secondly in trypsin. Hydrolytic breakdown of col-

lagen I can be accomplished by using a heated acid bath. Strong hydrolysis with 6N HCl at 110°C will completely free collagen by breakdown into its amino acid constituents. Both methods have drawbacks in that protease treatment introduces another source of nitrogen (from the enzymes), and very strong acid hydrolysis can break down the PEO hydrogel by hydrolysis of the ether linkages.

To preserve the PEO network while dissociating the collagen, a milder degradation of collagen was developed that used 10% oxalic acid.[2] The oxalic acid solutions were made with MilliQ water and with 0.05% sodium azide as a bactericide. Hydrolysis took place at 50°C for 150 hours. Every 24 hours, the oxalic acid and solubilized proteinaceous material was decanted from the hydrogel. Clean oxalic acid solution was added to the digestion container after removing the solubilized material.

Surface Spectroscopy: Surface spectroscopic techniques consisted of Electron Spectroscopy for Chemical Analysis (ESCA) and Infrared Multiple Internal Reflectance (IR-MIR).[13] Both of these methods provide information about the surface chemistry. ESCA is based on the photoelectric effect of x-ray bombardment. It can provide the elemental composition of the top *50* angstroms of the surface by determination of the kinetic energy of surface emitted photoelectrons. IR-MIR provides information on the chemical functionalities present in the surface but can analyze material at much greater depth (order of microns). Both analytical devices worked only with anhydrous samples. Unlike IR-MIR, ESCA must take place in a high vacuum.

ESCA survey spectra on the exposed interface were obtained using a spectrophotometer (Model 101. Surface Sciences, Inc.). Samples which underwent surface spectroscopic analysis were treated as follows: 1) after the oxalic acid removal of collagen, the hydrogels were air-dried for 20 hours in a sterile laminar flow hood; 2) air-dried samples were further dried in vacuum oven at 37°C for 24 hours. For ESCA studies, the exposed inter-

face of a 10 Mrad PEO hydrogel(100K-10%) grafted onto a collagen film was examined. A control 10 Mrad PEO hydrogel was used for comparison. Infrared Multiple Internal Reflectance spectra were obtained using a ZnSe crystal and dual beam infrared spectrophotometer (Perkin Elmer, Model 1430). MIR-IR spectra were obtained for PEO powder (uncross-linked), collagen I film, a 10 Mrad PEO hydrogel (100K-10%) not grafted to collagen, a 10 Mrad PEO hydrogel (100K-10%) grafted to collagen, and a 7.5 Mrad PEO hydrogel (100K-10%) grafted to collagen.

Amine Fluorescence and Fluorimetry: Chemical verification of collagen immobilized on the treated hydrogel surfaces was performed using fluorescence of primary amines. Primary amines specifically react and couple with the compound fluorescamine. The adduct of primary amines and fluorescamine fluoresce at 475 nm with excitation at 390 nm.[14] Amino acid subunits, peptides, and proteins possess abundant primary amines, whereas the PEO hydrogel network alone will not react with fluorescamine to fluoresce. This method of fluorescent labelling was used to detect the presence of primary amines of amino acid residues on the hydrogel interface after acidic removal of collagen for ESCA studies. Hydrogels of 0.2-0.3 mls with exposed PEO-collagen interfaces were buffered in 2 mls of 0.2M $NaBO_3$ (pH = 9.0). An equal volume of a 0.15 mg/ml solution of fluorescamine in acetone was added. After a 15 minute incubation perioad at room temperature, detection of primary amine fluorescence was performed in a fluorescence spectrophotometer (Perkin Elmer, 520M). The detection of primary amine fluorescence was possible with intact hydrogels, but surface quantitation was not possible using this equipment.

Fluorescamine labelling of amino acids from collagen provided a sensitive method of determining the total amount of protein (collagen) in the sample. The protocol for this assay is in Appendix A. For this procedure, collagen had to be completely degraded to the constituent amino acids in solution. To accomplish this complete digestion, the immobi-

lized peptides and hydrogel networks (ranging from 3 to 4 cc in volume) were completely degraded in 6N HCl at 110°C for 24 hours. The hydrochloric acid was removed by evaporation and the *residue* was redissolved in 7.0 mls of buffer (0.2M $NaBO_3$, pH =9.0). This redissolved residue was diluted to 100 fold in more buffer. To one ml of this 100 fold diluted sample, an equal volume of 0.15 mg/ml fluorescamine in acetone was added. The resulting solution of fluorescamine-amino acid conjugates were assayed for fluorescence in a fluorescence spectrophotometer. A linear standard curve of fluorescence versus collagen concentration was used to determine sample concentrations. These studies in particular emphasized low dose irradiation in grafting collagen onto PEO hydrogels. Electron irradiation dosages at 2, 4, and 6 Mrads were evaluated. PEO concentration (2%-8%), molecular weight (100K-5,000K), and molecule type (star vs. linear) were evaluated. Hydrogel samples made from collagen-PEO solutions suspensions possessed 17.5 mg of collagen particles per ml of PEO solution except for a single pilot study which used a suspension of 40 mg collagen particles per ml of PEO solution.

2.2.4 Results from PEO-Tissue Fixation Studies

Surface Spectroscopy: ESCA was used to investigate the presence of residual protein on the surface of the hydrogels. Survey scans (*1000* μm spot size) of the materials included those for PEO hydrogels alone and those with grafted collagen removed. The survey scan of the PEO-Collagen interface in Figure 2.10 shows the presence of carbon, oxygen, and nitrogen. The ratio of carbon to oxygen was roughly 2:1 which is indicative of a high concentration of PEO on the surface. Nitrogen was assumed to arise from the presence of amino acids bound to the surface of the hydrogels. PEO hydrogels not cross-linked in the presence of collagen were also exposed to oxalic acid hydrolysis as a control.

After rinsing and subsequent ESCA examination, these hydrogels had only C_{1S} (carbon) and O_{1S} (oxygen) signals and no nitrogen detected on the surface.

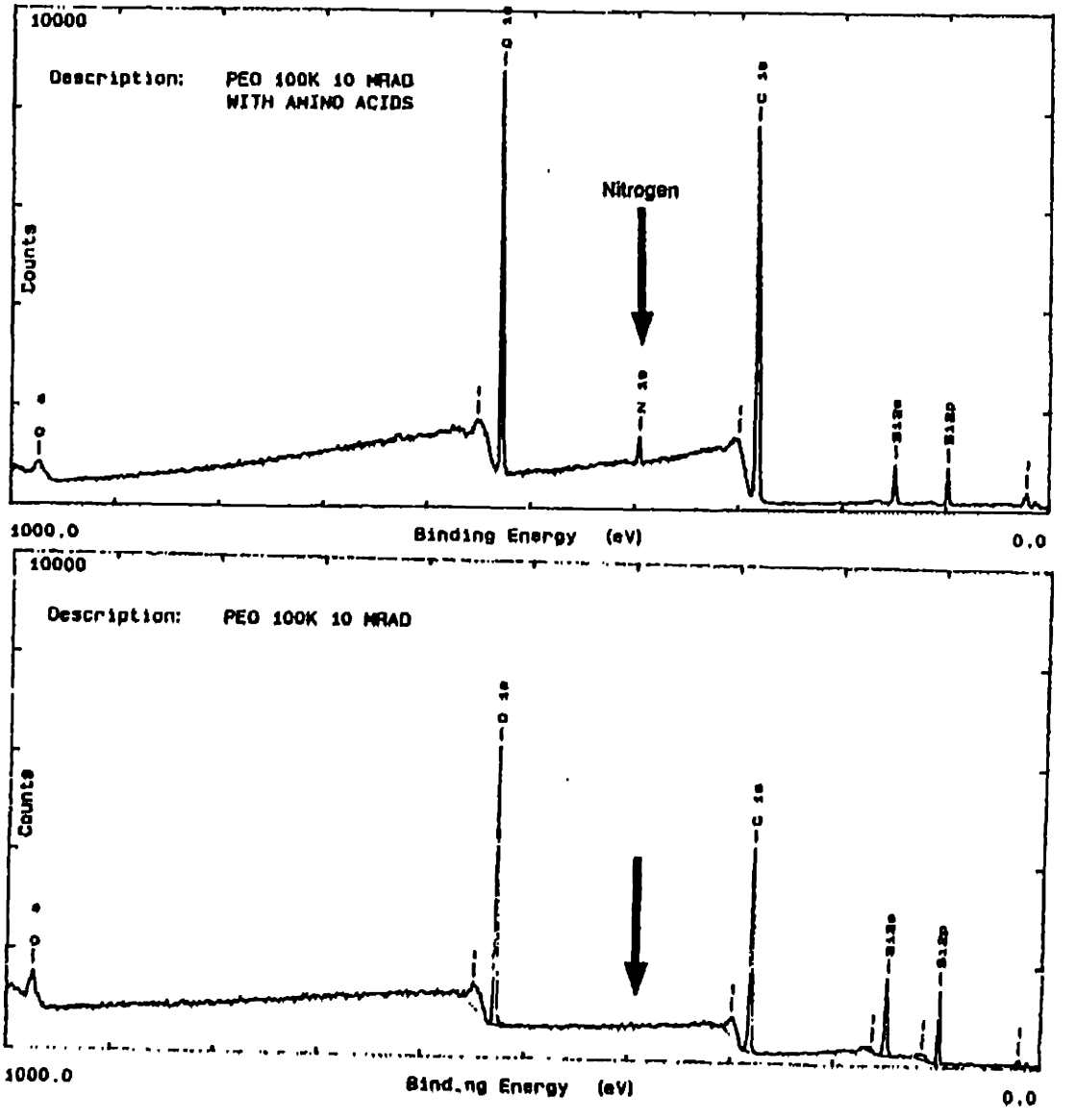

Figure 2.10: XPS Survey Spectra of PEO-Tissue Interface

Surface infrared spectroscopy (IR-MIR) was used to determine the presence of chemical functional groups originating from peptides immobilized on the surface after oxalic acid hydrolysis. Three control spectra were obtained for comparison: (1) Linear PEO

(100K), (2) Collagen Type I, and (3) Pure PEO hydrogel treated with oxalic acid hydrolysis.

The control collagen type I film gave an IR spectrum with characteristic peaks at 1640 cm^{-1} and 1540 cm^{-1} illustrating the Amide I and Amide II bands. This compares identically with published data for collagen.[15] The non-irradiated linear PEO showed the characteristic absorption peaks of C-H vibrations and the distinctive peak at 1080 cm^{-1} due to the C-O ether linkage.[16] Electron beam irradiated PEO showed minor carboxyl formation above 1500 cm^{-1}(shown on Figure 2.13 by ▼).

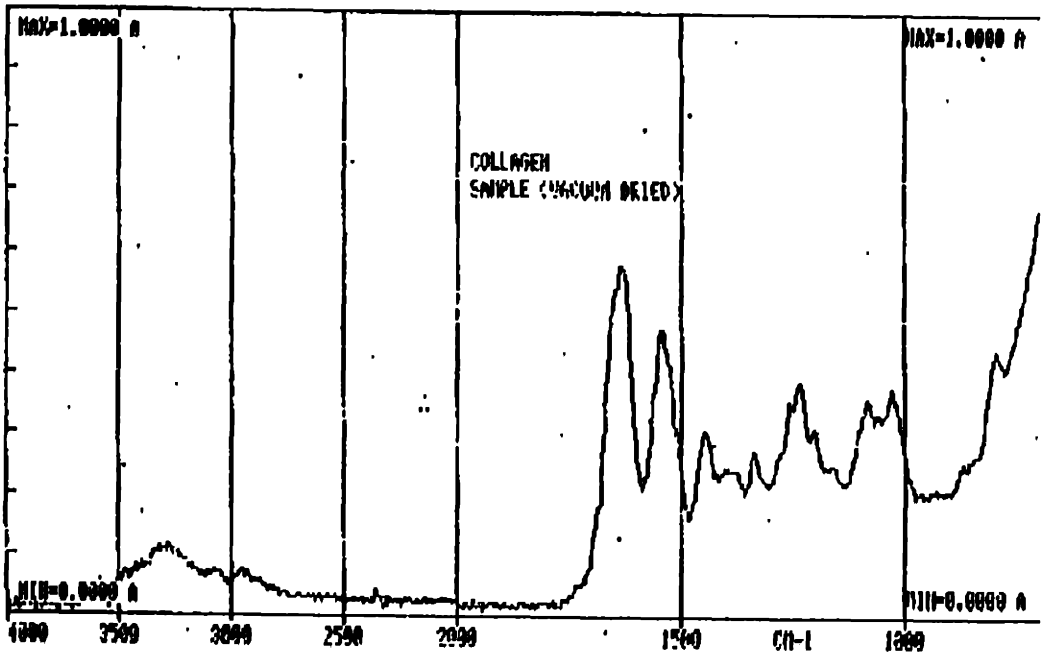

Figure 2.11: MIR-IR Spectra of Grafted Collagen

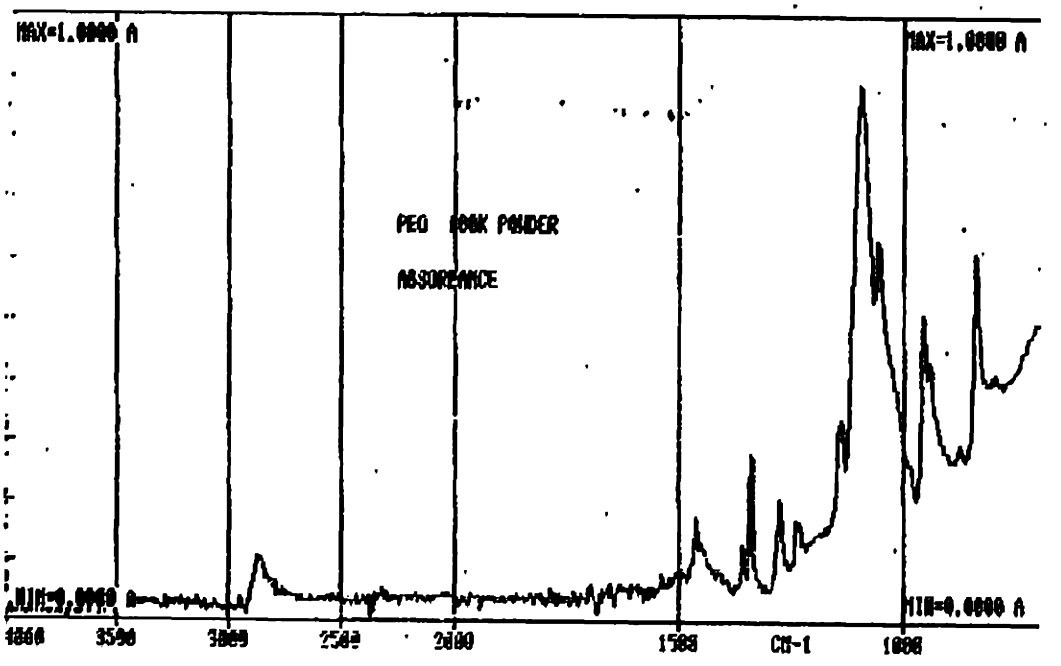

Figure 2.12: MIR-IR Spectra of PEO Solid (not irradiated)

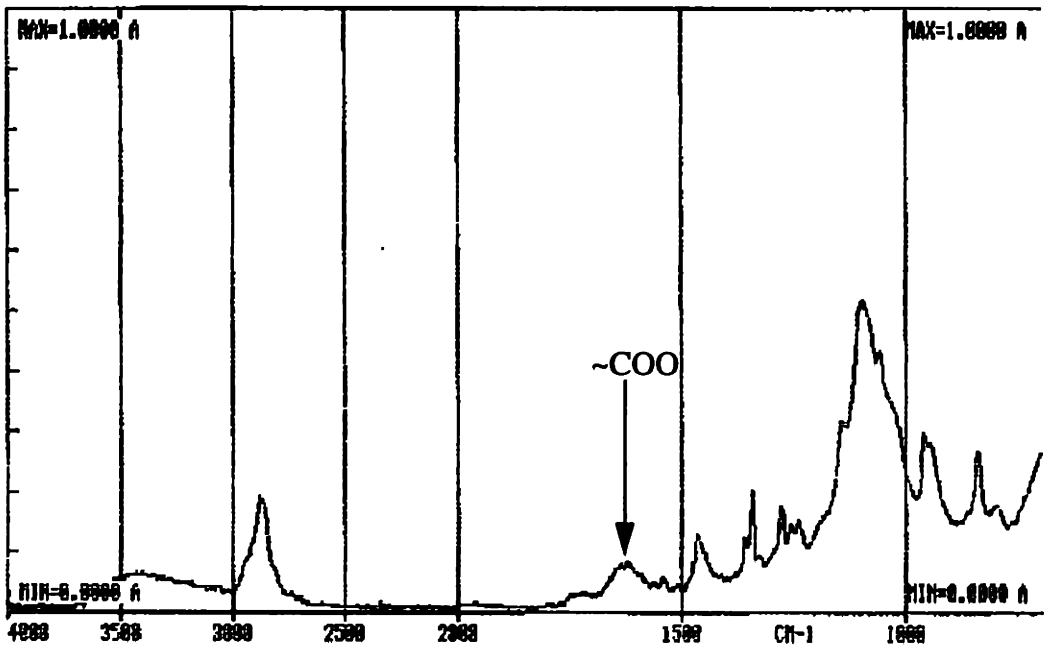

Figure 2.13: MIR-IR Spectra of PEO Hydrogel (Not Grafted to Collagen)

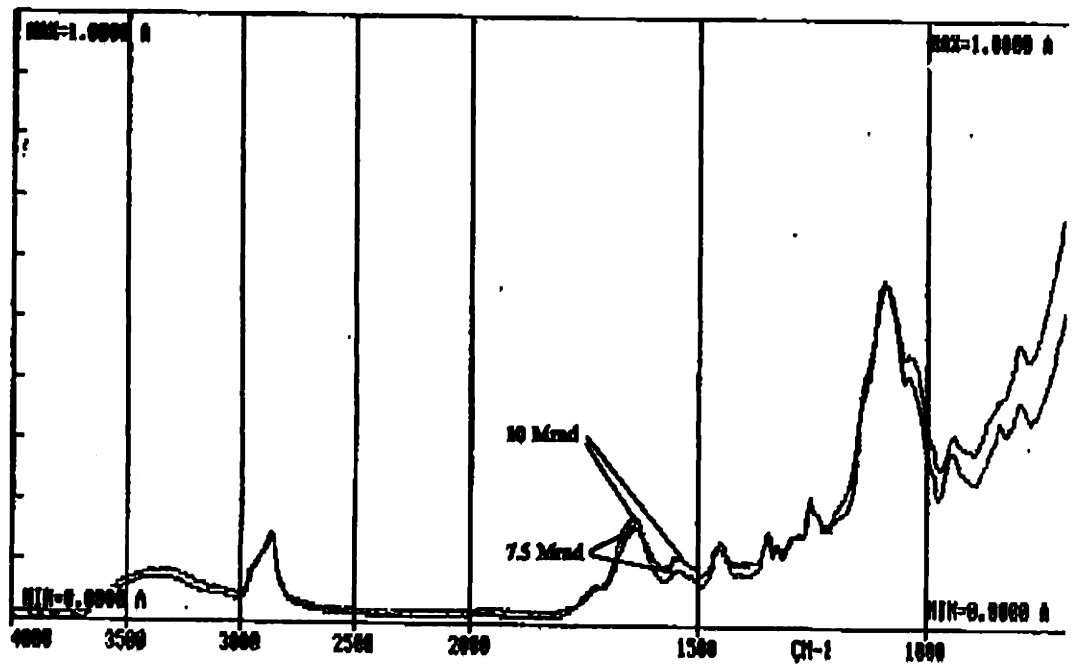

Figure 2.14: MIR-IR Spectra of Collagen-PEO Interface

IR spectra obtained for collagen grafted onto PEO hydrogels confirmed the presence of the thick collagen layer on the surface. After the hydrolytic removal of collagen from the surface of the hydrogels, the IR spectra were similar to that of non-grafted PEO hydrogels. The non-grafted PEO hydrogels served as control specimen. The peak at 1085-1075 cm^{-1} identified PEO as a major constituent of the hydrolytically treated hydrogel surface. The significant differences between the infra-red spectrum of pure cross-linked PEO and the grafted hydrogels with hydrolytically removed collagen were the increased absorption at the Amide I, Amide II regions, and absorption below 1000 cm^{-1}. There also appeared to be a higher IR absorption in those regions for the exposed surfaces 10 Mrad doses hydrogels than those hydrogels grafted at 7.5 Mrad doses. This appeared to indicate some positive dependence on irradiation exists for immobilization of collagen onto PEO.

Fluorescence and Fluorimetry:Hydrolytically treated hydrogels were also reacted with fluorescamine to confirm that the nitrogen present on the surface was in the form of primary amines. Hydrogels grafted onto collagen (7.5 Mrads and 10 Mrads) showed strong positive fluorescence. Pure PEO hydrogels treated with fluorescamine showed no fluorescence. Figure 2.15 shows an image of a fluorescently labeled hydrogel that was hydrolytically treated. The ability to demonstrate fluorescence in these experiments provided the foundation to quantitatively ascertain the amount of collagen bound onto PEO hydrogels.

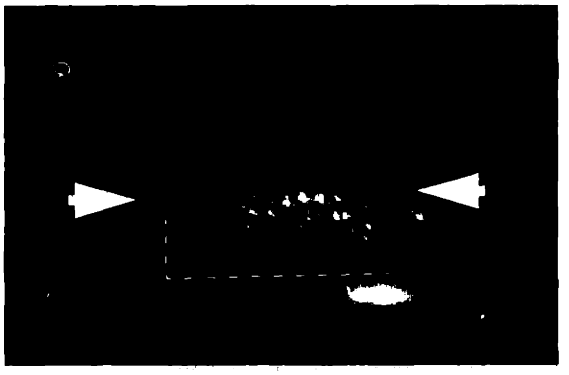

Figure 2.15: Fluorescence of Exposed PEO-Collagen Surface

There was a positive linear relationship between collagen immobilization onto the hydrogel surface and amount of irradiation. Figure 2.16 shows this relationship with a 40mg of collagen per ml of 4% 100K PEO mixture. The amount of collagen immobilized to the hydrogel surface was represented as a percentage of total collagen in the mixture. This normalization of the collagen immobiliation results was performed to provide a parameter indicative of interfacial area. The increase in immobilization with dose is believed to be a reflection of the total amount of hydroxyl radial created.[17]

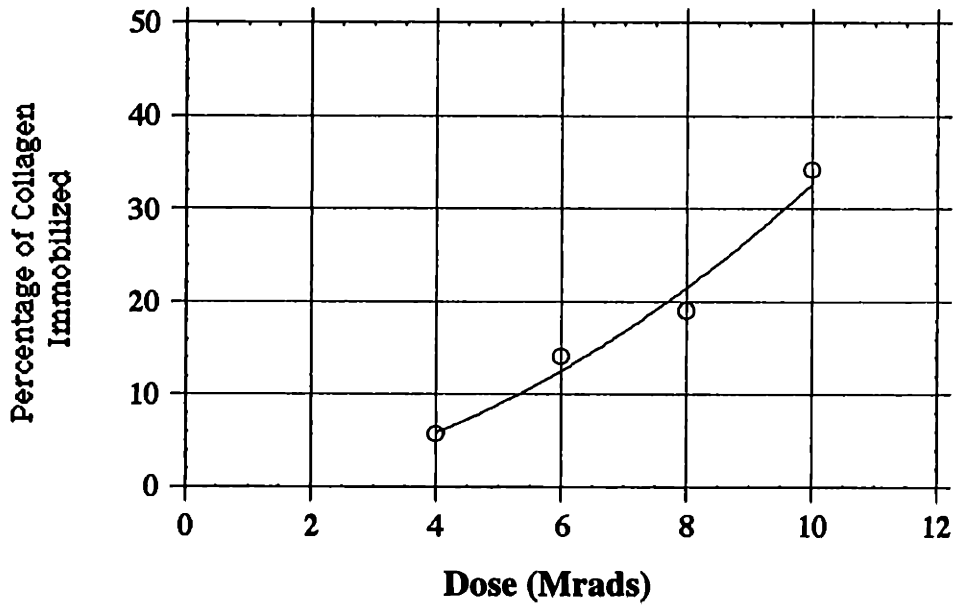

Figure 2.16: Collagen Immobilization in 40mg of collagen per ml of 4% 100K PEO

There was no statistically significant variation between collagen immobilization and the molecular weight of linear PEO molecules. A comparison of composites made with linear PEO of molecular weights: 100K, 2,000K, and 5,000K showed no significant differences. (Figure 2.17) Varying the concentration of PEO from 2, 4, 6, and 8 mg/ml did not appreciably change the amount of collagen immobilization.(Figure 2.18) The percentage

of collagen immobilized was measured for 2, 4, and 6 Mrad irradiation doses as shown in Figure 2.19. Collagen immobilization by star PEO also exhibited a linear dependence on irradiation dose. The most significant finding in this evaluation was that in comparing linear PEO with star-shaped PEO, the star-shaped PEO had significantly lower immobilization than linear PEO.

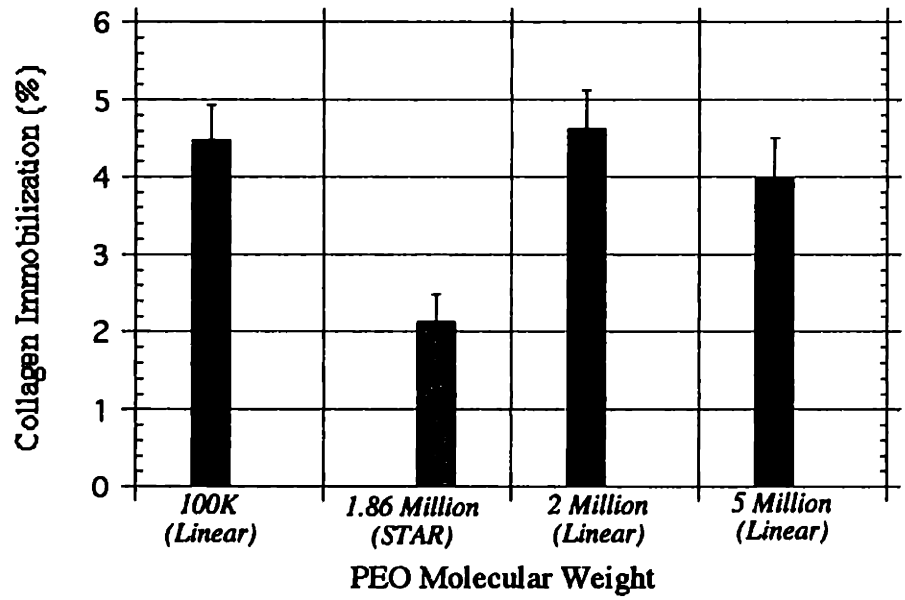

Figure 2.17: Collagen Immobilization versus PEO MW (17.5 mg of collagen per ml of 4% PEO, Dose = 4 Mrad)

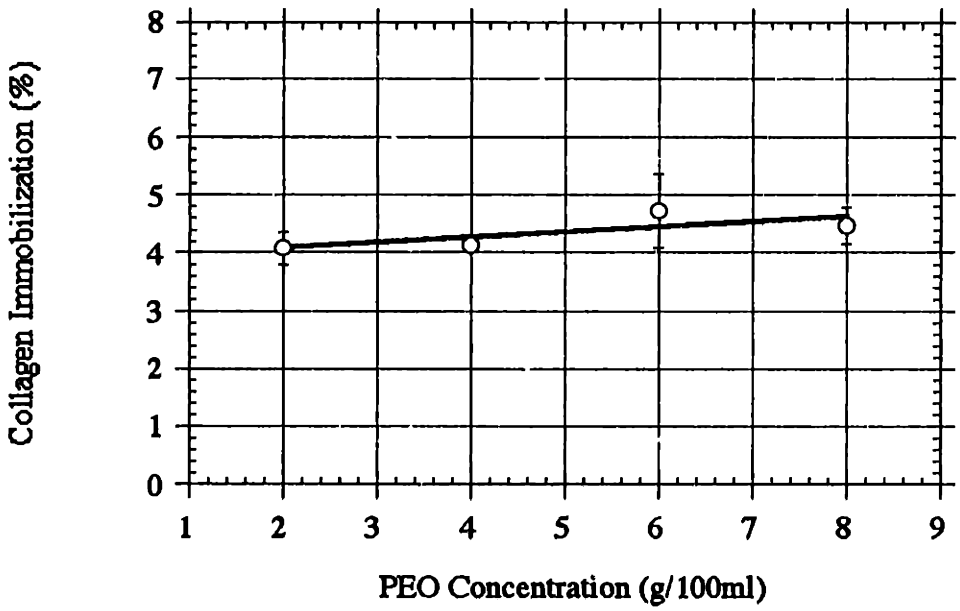

Figure 2.18: Collagen Immobilization versus PEO concentration (17.5 mg of collagen per ml of PEO, at 4 Mrad, MW = 2000K)

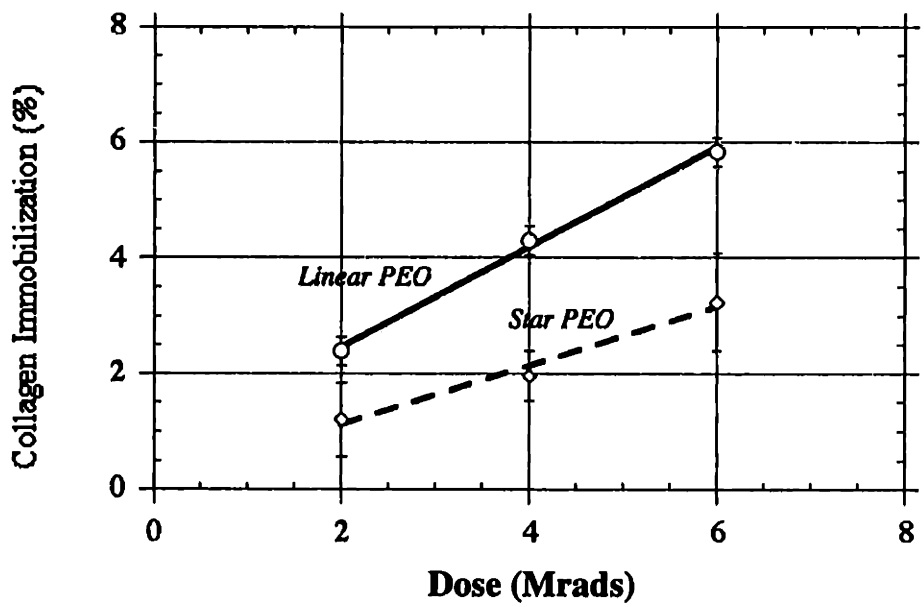

Figure 2.19: Collagen Immobilization and PEO Molecular Shape (17.5 mg of collagen per ml of 4% PEO, MW_{linear}=2000K, MW_{star}=1,860K-10K arm)

The weak effect that concentration of PEO had on immobilizing collagen was understandable in terms of the concentration of macroradicals. Macroradical formation was primarily determined by the concentration of hydroxyl radicals and not by the concentration of PEO. The concentration of hydroxyl radicals created was much less than the concentration of PEO subunits available to participate in macroradical formation. The hydroxyl radical appeared to be the limiting reagent in a very fast reaction. The increasing amount of collagen immobilization was simply a consequence of the total dose (and total amount of hydroxyl radicals created).

Also, the parameter of molecular weight seemed to have little effect on collagen immobilization. This could be explained by noting that segment mobility should be the same for any molecular weight of linear PEO. In this case, the mobility of short segments within any particular molecule was equivalent between different sized molecules. A macroradical on a segment of the linear PEO chain had limited interaction with a radical site on collagen by polymer chain segment mobility. What is interesting is that star shaped molecules (1,860K-10K arm length) immobilized approximately 50% less collagen than linear molecules. Star shaped molecules immobilized less collagen possilbly because PEO segments in star molecules do not have the equivalent mobility all along the PEO arm. Segments of PEO close to the central core are less able to interact with a surface (collagen) than PEO segments at the periphery. Therefore, radicals generated at or near the star molecule core could not participate in immobilizing collagen. Only those radicals generated near the end of the arms could immobilize collagen.

2.3 Stromal Tissue Layer Preparation

The layer of stroma which "coats" or covers the synthetic hydrogel portion of the composite hydrogel was obtained directly from fresh corneal tissue that was cut on a freezing microtome.[18] Corneal tissue was harvested from NZW rabbits or from bovine sources. These procedures are in accordance with the Association for Research in Vision and Ophthalmology (ARVO) Resolution on Animal Care. The specific protocol approved by the MIT division on animal care is in Appendix B.

The epithelial layer of cells was removed from the cornea in order to securely immobilize the tissue on a specimen holder. This was best done by abrading the epithelial layer off of the cornea with a scalpel. Once the epithelium was removed, an approximately 12mm diameter disc was free-hand excised from the globe. Freezing embedding compound was sparingly applied to the surface of the cornea which was then pressed and mounted onto the specimen holder held at a temperature of -20°C. A flat press was applied to the cornea and holder for at least one minute. The sample and tissue were then affixed to the cryostat chuck where it could oscillate against the advancing cutting blade. The entire cutting environment was held at -20°C to maintain the corneal tissue as a rigid structure. The cryostat can cut contiguous tissue layers from 5μm to 120μm. These layers were kept from curling during cutting by using a special suppression attachment and were handled with cold forceps (-20°C). The tissue layers were then placed into the molds that served as PEO solu-

tion containers during cross-linking into hydrogels. Once the layers were lined onto the internal surface of the mold, the molds were ready to hold solution and be irradiated.

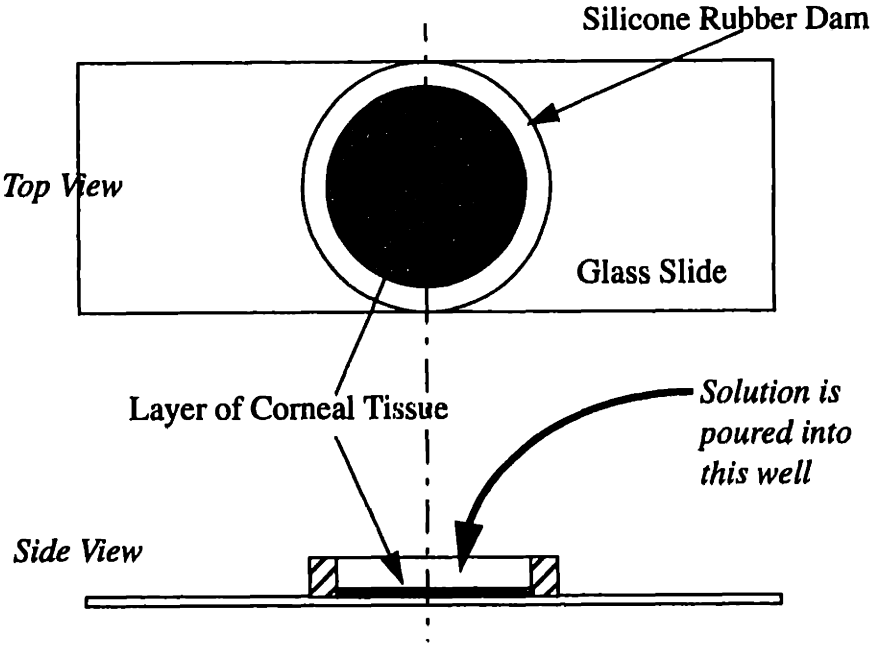

Figure 2.20: Mold for Composite Hydrogel

2.4 Conclusions

The information presented in this chapter summarizes refinements in the synthesis of PEO hydrogels for the additional studies in this thesis. The production of bubble defects within hydrogel membranes rendered them useless for diffusion studies. Inclusion of large and numerous bubble defects created conduits through which forced transfer of solute could occur producing erroneously high hydrogel solute diffusivities. Primarily, bolus-dose irradiation allowed the creation of high dose hydrogels that were virtually defect free.

Refinements in the methods to create non-swelling hydrogels at low doses was important in the synthesis of material for cell study. In addition, insight into the greater collagen immobilization of linear PEO directed the methods to employ high molecular weight linear material instead of stars to maximize PEO-tissue union. All cell studies subsequently reported were performed using 2% solutions of PEO (MW=5,000K) cross-linked at 2 Mrads.

Chapter 2 References

[1] Kathleen A. Dennison. Radiation Cross-Linked Poly(ethylene Oxide) Hydrogel Membranes. Ph.D. Thesis Massachusetts Institute of Technology, Cambridge, MA March 1988

[2] K Pietrucha and J Kroh. Radiation Crosslinking of Poly(butyl acrylate) During Polymerization and Grafted Copolymerization with Cr(III) Crosslinked Collagen. Int. J. Radiat. Appl. Instrum., Part C: 1986, Vol 28, No 4, pp 373-376

[3] J.W. Stafford. The Radiation Induced Reactions of Aqueous Polyethylene Oxide Solutions: II. Intrinsice Viscosity Changes in the Pregel Region. In Die Makromolekulare Chemie. 1970, Vol 134, pp 71-85

[4] K. Panduranga Rao et al. Grafting of Vinyl Monmers on to Proteins. Journal of Scientific and Industrial Research, 1970, Vol. 29, No. 12, pp559-567

[5] M. S. Matheson, A. Mamou, J. Silverman, and J. Rabani. Reaction of Hydroxyl Radicals with Polyethylene Oxide in Aqueous Solution. The Journal of Physical Chemistry, 1973, Vol. 77, No. 20, pp. 2420-2424

[6] J.G. Trump, K.A. Wright, and A.M. Clarke. Distribution of Ionization in Materials Irradiated by Two and Three Million-Volt Cathode Rays. Journal of Applied Physics: 1950; Vol 21, No 4, pp 345-348

[7] J.G. Trump, R.J. Van de Graaff, and R.W. Cloud. Cathode Rays for Radiation Therapy. American Journal of Roentgenology and Radium Therapy. Vol. 43, No. 5, May 1940, pp 728-734

[8] J.G. Trump and R.W. Cloud. The Production and Characteristics of 3,000 Kilovolt Roentgen Rays. American Journal of Roentgenology and Radium Therapy: 1943 Vol XlIX, No 4, pp 531-535

[9] L.G. Cima and S.T. Lopina. Network Structures of Radiation-Crosslinked Star Polymer Gels. *Submitted to Macromolecules.*

[10] Remmp, P. Institute Charles Sadron, Strausbourg France. *Private Communication*

[11] Woonza Rhee, et al. Collagen-Polymer Conjugates. United States Patent, No. 5,162,430; November 10, 1992

[12] K Pietrucha and M. Lubis. Some Reactions of OH Radicals with Collagen and Tyrosine in Aqueous Solutions. Int. J. Radiat. Appl. Instrum., Part C: 1990, Vol 36, No 6, pp 155-160

[13] R. Y. Paynter. Chapter 2: Surface Analytical Techniques in Biomaterials Development. Biocompatibility Testing Vol. II, D. F. Williams (editor), CRC Press, Inc., Copyright 1986, pp. 49-80

[14] S Udenfriend et al. Fluorescamine: A Reagent for Assay of Amino Acides Peptides, Proteins, and Primary Amines in the Picomole Range. Science. Vol 178, Nov 1972, pp 871-872

[15] I.V. Yannas. Collagen and Gelatin in the Solid State. J. Macromol. Sci.-Revs. Macromol. Chem., 1972,C7(1), pp 49-104

[16] The Infrared Spectroscopy Committee. An Infrared Spectroscopy Atlas for the Coatings Industry. Federation of Societies for Coatings Industry. Philadelphia, Pennsylvania, p. 268

[17] Reiner Braams. Rate Constants of Hydrated Electron Reactions with Peptides and Proteins. Radiation Research. 1967, Vol. 31, pp. 8-26

[18] M. Hirsch et al. Quick-freezing Technique Using a 'Slamming' Device for the Study of Corneal Stromal Morphology. Exp. Eye. Res. 1982, Vol. 34, pp. 841-845

Chapter 3

Nutrient Diffusion in PEO Hydrogels

This chapter presents an analysis of glucose diffusion through linear PEO, star PEO and HEMA hydrogels. These experiments were performed in order to evaluate the mass transport characteristics of important nutrients in potential synthetic hydrogel materials to be used in making corneal implants. Synthetic materials within the cornea must be able to permit the normal physiologic nutrient and solute flow. The disruption of nutrient flux through the cornea is considered to be an important cause of tissue necrosis over impermeable implants. Clear bubble-free poly(ethylene oxide) hydrogels were made by sequential bolus dose electron beam irradiation. HEMA hydrogels were obtained from Bausch and Lomb, Inc. Time lag analysis was used to determine the diffusion coefficient of these materials. A solute depletion method was used to determine the partition coefficient separately. Glucose diffusion was measured for linear PEO hydrogels, star PEO hydrogels, and HEMA hydrogels.

3.1 Introduction

Poly(ethylene oxide) hydrogels are generally considered excellent biomaterials because of their high biocompatibility. In the research and clinical community, PEO hydrogels are utilized as a synthetic substrate for cell encapsulation technology, scaffolding for cell transplantation, and drug delivery. In all of these cell dependent applications, nutrient and metabolite flux is an important factor in biocompatibility. In the formulation of PEO hydrogels as a non-resorbable ocular implants, the transport properties of glucose in PEO hydrogels was of concern.[1] Glucose diffusivity in PEO hydrogels is usually

assumed to be the same as it is in water. This study was undertaken to more accurately define the diffusivity and partition coefficient of glucose in pure PEO hydrogels.

3.2 Materials and Methods

3.2.1 Hydrogel Samples

Hydrogels created by electron beam irradiation of aqueous solutions are usually flawed by formation of hydrogen gas bubbles. These bubbles form as a consequence of the water irradiation chemistry. In the previous chapter, a method of hydrogel synthesis was presented to circumvent this problem. In this method, partial doses of irradiation were delivered to the sample. Between each partial dose, the samples were stored for a period of time (~24 hrs) so that accumulated hydrogen gas could diffuse out of hydrogel. Defect-free or bubbleless hydrogel samples were necessary for these experiments. A comparison of hydrogels that were created using continuous irradiation and sequential bolus-dose-irradiation is shown in Figure 3.1. A range of varied concentration poly(ethylene oxide) hydrogels were created in this manner. Solutions of linear PEO (100K Aldrich Chemical) at 10% wt/vol were cross-linked in bolus doses of electron irradiation from 2 Mrad to 10 Mrad. Solutions of star PEO (MW=1.86 Million, 10K arm) (Strausburg)[18] at 10% wt/vol were cross-linked in bolus doses of electron irradiation from 2 Mrad to 6 Mrad. The hydrogels were swollen, rinsed in MilliQ water to remove uncross-linked polymer. Clean 1cm diameter disks were cut and placed in the diffusion cell apparatus. After the assay was finished, the gels were weighed, dried and reweighed to determine the exact concentration of the PEO in each sample. The hydrogel samples after swelling ranged from 2% to 8% polymer at equilibrium. Thicknesses of samples ranged from.7mm to 1.5 mm. Hydroxyethyl methacrylate lenses obtained from Bausch and Lomb were 21%, 30%, and 61.4% water.

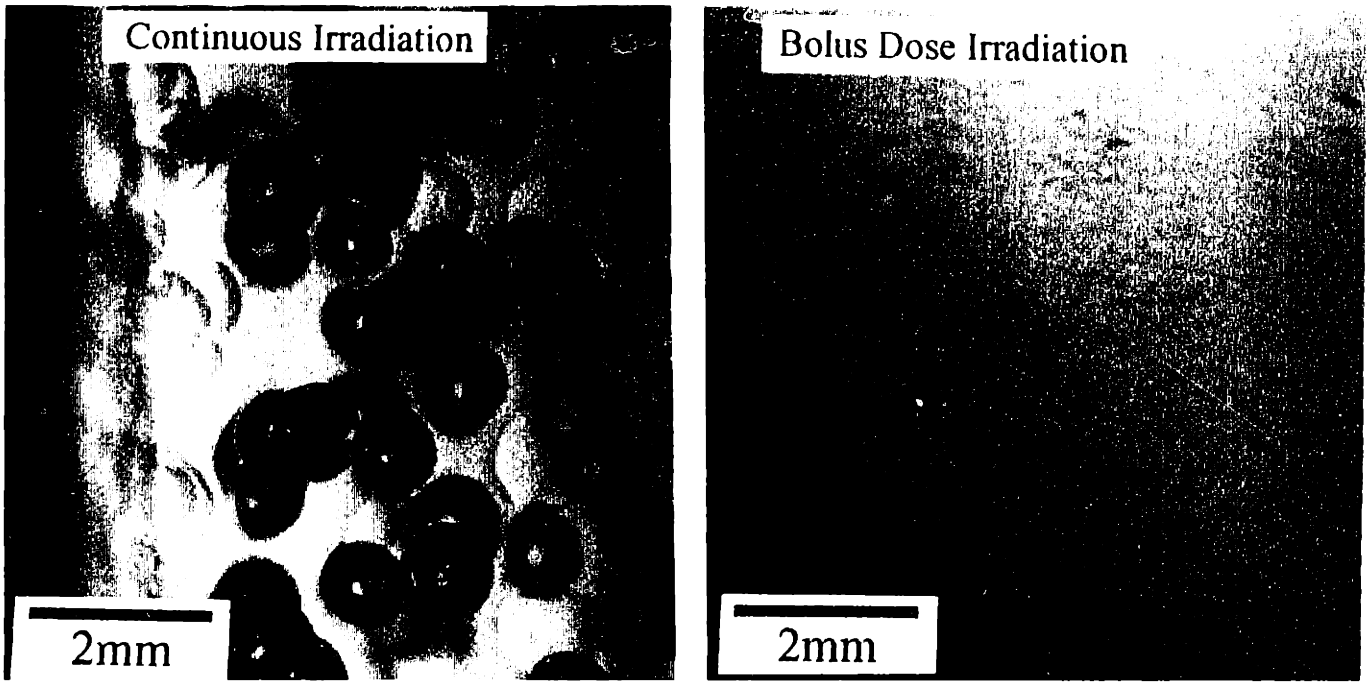

Figure 3.1: Defective and Defect Free Hydrogels

3.2.2 Diffusivity Measurement

The determination of diffusion coefficients in stable water-swollen materials has been addressed in a number of earlier publications.[2-8] The approach to diffusivity determination that was taken in this study is time-lag analysis. Time lag analysis is based on the system transition from unsteady state diffusion (after an instantaneous change in membrane concentrations) to steady state mass transport. At time zero, the concentration on the high solute side is changed from zero to C_l (2 mg/ml). As time proceeds, the concentration profile changes from an unsteady state non-linear profile to a linear steady state profile.[7,9,10]This is demonstrated with superimposed axes in Figure 3.2

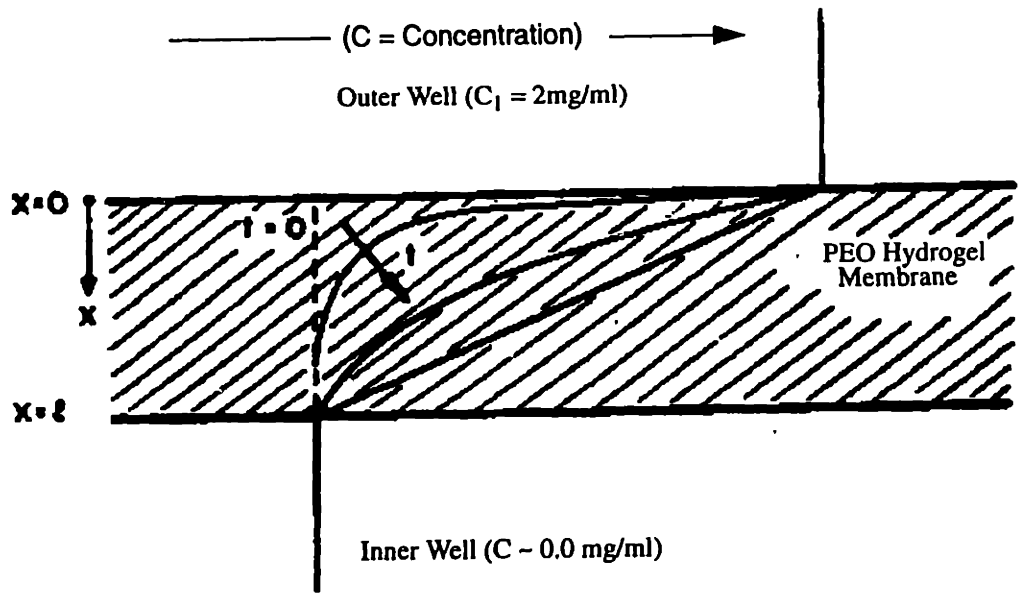

Figure 3.2: Concentration profile within hydrogel

Thus, the flux (mg) of glucose that passed through the hydrogel (at x = *l*) over time, was initially small but then grew to a constant rate. For example, a plot of the flux versus time is shown in Figure 3.3.

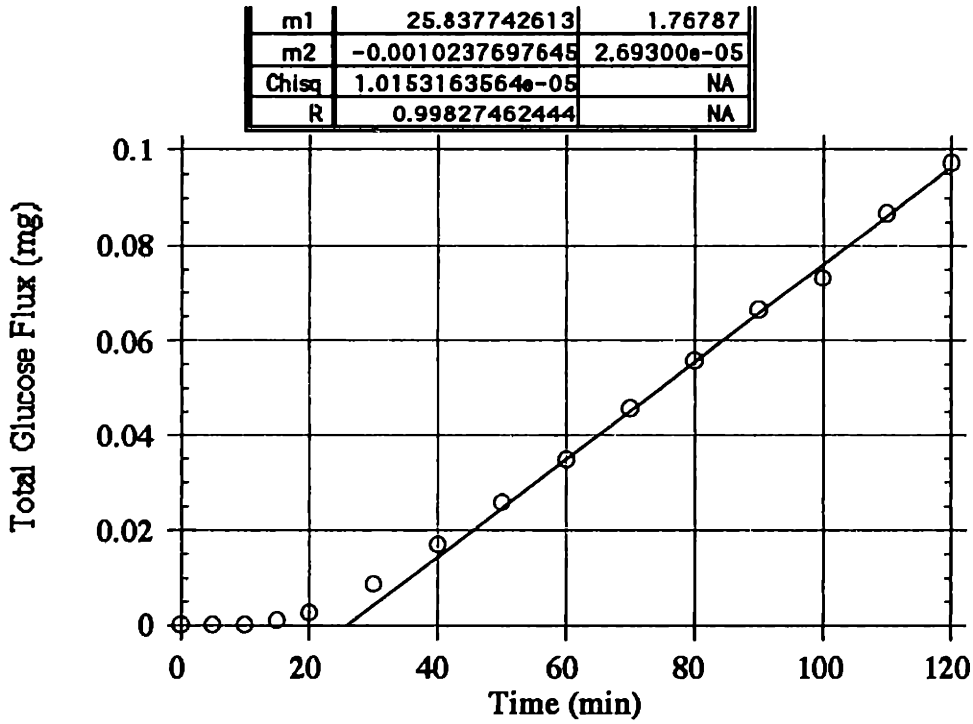

Figure 3.3: Flux of glucose across 3% PEO Hydrogel in time-lag experiment

The linear portion of the flux curve is described by the following equation:

$$Q|_t = \frac{ADC_1}{l}\left(t - \frac{l^2}{6D}\right) \tag{3.1}$$

Where:

$Q|_t$ =Total flux of solute at time (t) [=] mg
A = Area of membrane [=] cm^2
l = Thickness of the membrane [=] cm
C_1 = Concentration of solute [=] mg/cm^3
t = Time [=] sec
D = Diffusivity of solute in the membrane [=] cm^2/sec

From this graphical analysis, the x-intercept gives t_o. This lag time can be related to the diffusivity by determining the thickness of the hydrogel membrane.

$$D = \frac{l^2}{6 \cdot t_o} \tag{3.2}$$

t_o = Lag time (obtained by graphical analysis) [=] sec

An additional method of determining the mass transport properties involved taking the slope (dQ/dt) of the regression line which was fit to the steady state portion of flux (Q) versus time curve. The apparent diffusivity ($D \cdot K_p$) in equation 3.3 includes partition effects if any are present.

$$(DK_p) = \frac{l}{A \cdot C_1}\left(\frac{dQ}{dt}\right)_{ss} \tag{3.3}$$

Where,

$(D \cdot Kp)$ = Apparent Diffusivity [=] cm^2/sec
Q = Flux [=] mg
A = Area [=] cm^2
C_1 = Concentration [=] mg/cm^3
t = time [=] sec
l = membrane thickness [=] cm

3.2.3 Diffusion Cell and Setup

The diffusion cell was a modification of a commercially available membrane holder which is used in cell culture work. This cell was a modified Milli-Cell cup for use in a 24 well cell culture plate. The cell was comprised of a free-standing plastic cylinder supported by three small feet (clearance = .05 mm) and had a membrane spanning the bottom of the cylinder. In these experiments, the commercial membrane was removed and a circular hydrogel disc (10mm diameter) was inserted in the bottom of the cell where it was suspended between two snug-fitting rings. The rings were made of silicone rubber (80 durometer) 0.5 mm in thickness and 10mm OD and 7 mm ID. The complete set-up is shown in Figure 3.4

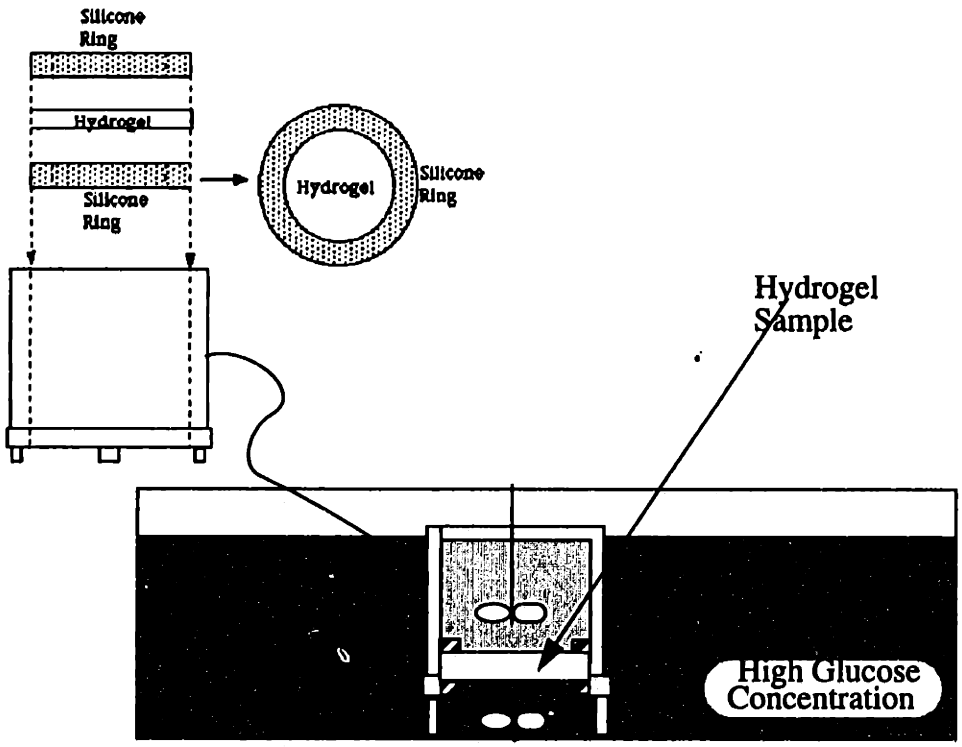

Figure 3.4: Diffusion Test Cell

The bottom-end closed cells were placed in a 60mm polystyrene petri-dish (1.5 cm deep) whose lid had been modified to hold a magnetically driven impeller. On the bottom of the petri-dish, a free standing micro stir bar (2mmx7mm) resided in depression created by a layer of silicone rubber with an 8mm hole cut out of it. The whole assembly, diffusion cell and petri-dish, was placed on a 1" thick styrofoam sheet which was affixed to a magnetic stirrer to keep the system at room temperature. Thus, the diffusional setup was maintained at room temperature. A micro-thermocouple was used to determine the actual temperature of the diffusion cell. All experiments were performed at 19°C $\pm$ 1°C. The setup created a system with two compartments separated by a hydrogel membrane. Each side of the membrane was well stirred magnetically to remove boundary layer effects.

The nutrient of interest in this mass transport analysis was glucose. The concentration of glucose (C_1) in the high-solute side of the diffusion test cell was 2 mg/ml. The solute deficient chamber had no glucose. The internal membrane concentrations should have ranged from approximately 0 to 2mg/ml over the course of the experiment. These particular glucose concentrations were chosen to reflect the normal physiologic values of glucose concentrations (~1 mg/ml). The total volume in the central sample well was 300 µl. Two hundred microliter samples from each reservoir were taken at 10 minute intervals and replaced with an equal volume of MilliQ water (0.05% sodium azide). The flux was calculated using the following algorithm:

$$Q\big|_t = (V_T - V_S)\, C_n + V_S \sum_{i=0}^{n} C_i \tag{3.4}$$

Where,

$Q\big|_t$ = Flux at time t [=] mg
V_T = Total volume in test cell [=] cm^3
V_S = Sample volume from central well[=] cm^3
C_n = Concentration of the nth sample[=] mg/cm^3
n = Index denoting sample chronology (i.e 1st, 2nd, etc.)

The glucose in the samples was enzymatically converted to a quinone moiety and the concentrations determined colorimetrically.[11,12] The protocols for these procedures are included in Appendix C and Appendix D.

3.2.4 Partition Coefficient Determination

The extent of glucose partitioning into PEO hydrogels was an important parameter in understanding the dynamics of glucose transport. The protocol in these experiments was designed to separate the evaluation of two defining parameters for PEO hydrogels: diffusivity (D) and partition coefficient (K_p). The partition coefficients in these gels were determined by a simple mass balance analysis. A volume of hydrogel (V_{Gel}) is placed in a

volume of incubation solution (V_{Sol}) at an initial glucose concentration (C_o). The equilibration of glucose between the hydrogel and the incubation solution gave a new concentration (C_S) in the solution, which was indicative of the partition coefficient of the hydrogel. Hydrogel samples (0.5-0.7g) were placed in 1.5 ml air-tight polypropylene tubes and incubated at room temperature with a 1mg/ml (Co) solution. After one night of incubation, a *200 μl* sample was assayed to determine the concentration (C_S). The partition coefficient was determined using equation 3.7

$$K_p \equiv \left(\frac{C_G}{C_s} \right) \tag{3.5}$$

$$V_{Sol}C_o = V_{Sol}C_s + V_{Gel}C_G \tag{3.6}$$

$$K_p = \left(\frac{V_{Sol}}{V_{Gel}} \right)\left(\frac{C_o}{C_G} - 1 \right) \tag{3.7}$$

Where,

K_p = Partition Coefficient
C_G = Concentration in Hydrogel Sample
C_S = Concentration in Surrounding Solution
C_o = Initial Concentration of Incubation Solution
V_{Sol} = Volume of Solution
V_{Gel} = Volume of Hydrogel

3.3 Results and Analysis

3.3.5 Glucose Diffusion

A typical glucose flux versus time profile was shown below in Figure 3.3. In general time lag values ranged in between 10 and 20 minutes. Glucose diffusivity measurements for PEO hydrogel polymer concentrations of 2% -8% were performed. Also presented with the experimental glucose diffusivities is the theoretical diffusivity of glucose based

on simple obstruction from the PEO network. The diffusivity results are show in Figure 3.5

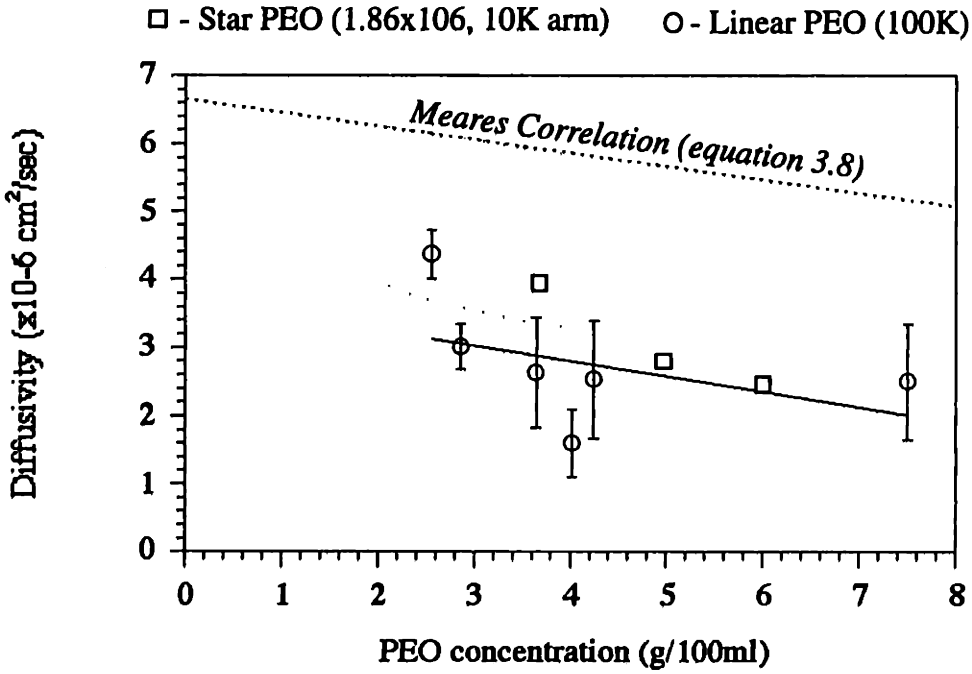

Figure 3.5: Glucose Diffusivity in PEO Hydrogels

Hydroxylethyl Methacrylate (HEMA) lenses were obtained from Bausch and Lomb, Inc. to evaluate glucose transport in another potential prosthetic material. These lenses were too thin to evaluate diffusivities (D) using time lag experiments. Total flux of glucose was used to ascertain the apparent glucose diffusivities (DK_p). HEMA lenses of 21%,

30%, and 61.4% polymer were evaluated. The results for these experiments are shown in the figure below.

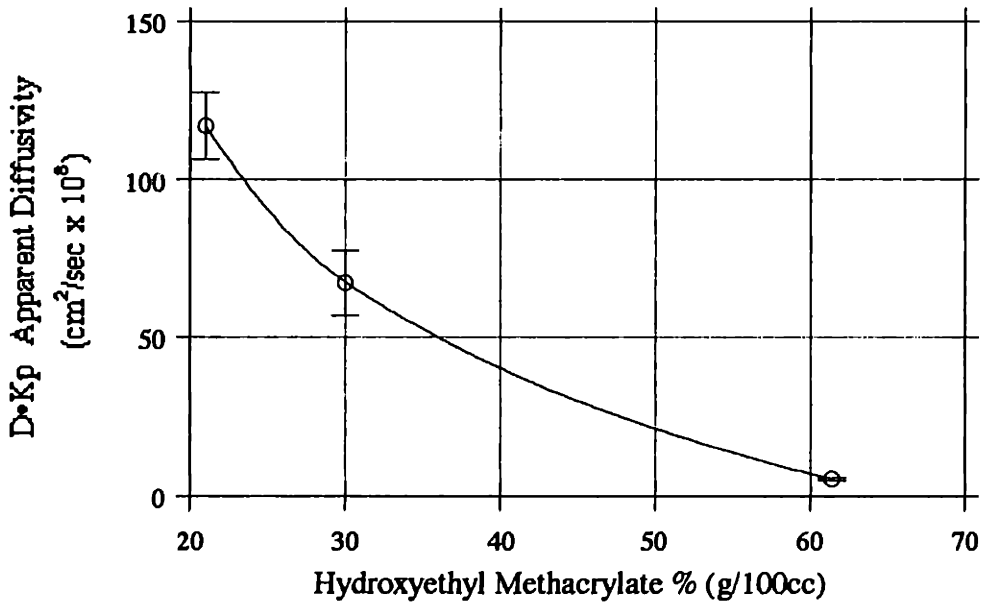

Figure 3.6: Apparent Glucose Diffusivity in HEMA Hydrogels

Figure 3.7 shows how the partition coefficient varied with the concentration of PEO in the hydrogels. There was a positive correlation between the partition coefficient and the PEO concentration in the polymer. The least squares linear regression equation of the data for the glucose partitioning is:

$$K_p = 0.145 C_{PEO} + 1.282$$

Where, K_p = Partition Coefficient
C_{PEO} = Concentration of PEO in Hydrogel [=] g/100ml

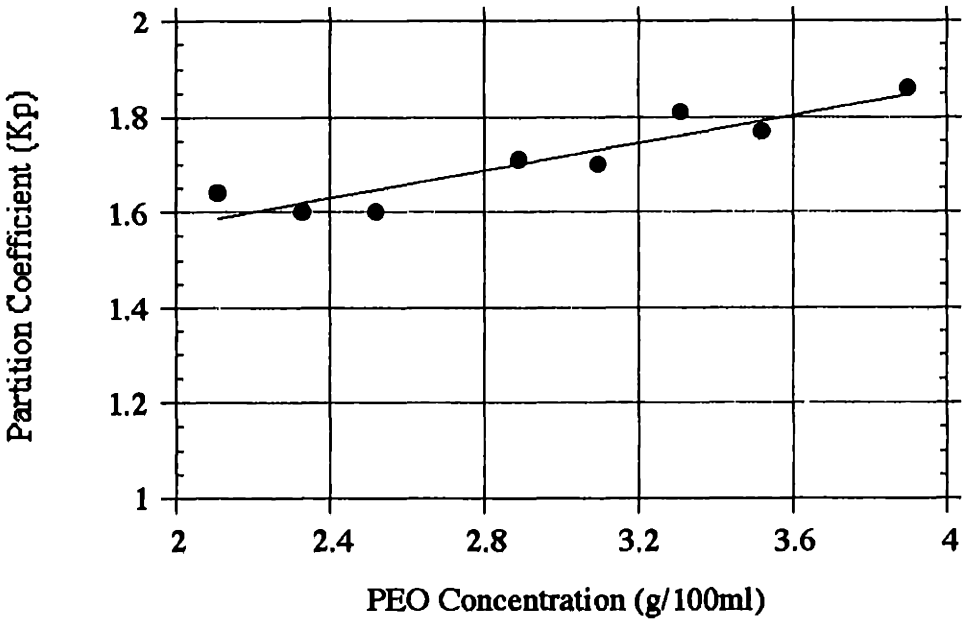

Figure 3.7: Glucose Partitioning in PEO Hydrogels

3.4 Discussion of Glucose Transport

Partitioning of glucose into the PEO hydrogel membrane suggested some unexpected phenomena for glucose transport. In these high water content hydrogels, one would expect the mass transport behavior to be similar to the characteristics of water.[13] Indeed, partition coefficients (K_p) slightly less than unity would have been expected since the concentration of water was 96%-98%.[14,15] The partition coefficients, which ranged from 1.6 to 1.9, directed attention towards the possibility that glucose was somehow interacting with the polymer in hydrogel.[9,16]

Hydrogel networks have been described as having water in three states: bound, bulk (free), and intermediate.[6] Explanations of partitioning small solutes into hydrogel networks have used this line of reasoning to explain partition coefficients less than unity. For these cases, Kp has a negative correlation with polymer volume fraction. In the PEO hydrogel--glucose system, Kp is greater than unity and consequently glucose is being cor-

centrated into the hydrogel. Paul et. al. considered the case of solute partitioning into swollen polymeric networks. An extension of that reasoning proposes a positive correlation of Kp and v_{2s} for systems appreciable polymer solute affinity.[13] In in the PEO hydrogel--glucose system, glucose may directly interact with the polymer subunits.

By considering the diffusivity of small solutes in highly swollen membranes, small (in comparison to pore size) solutes would simply experience an obstruction effect in the absence of any specific interaction between polymer and solute. Therefore, the entire role of the polymer can be specified by the volume fraction of polymer (v_{2s}).[17] A simple yet accurate model which predicts diffusivities in high solvent content gels is shown in equation 3.1. This relation is plotted along with the experimentally determined diffusivities for PEO in Figure 3.5 and Figure 3.8.

$$D_{obst} = D_o\left(\frac{1 - v_{2,S}}{1 + v_{2,S}}\right)^2 \tag{3.8}$$

Where,

D_o = Diffusion Coefficient in Solvent, cm^2/sec
D_{obst} = Diffusion Coefficient in Swollen Polymer membrane, cm^2/sec
$v_{2,S}$ = Polymer volume fraction, swollen membrane

The experimental values for diffusivity of glucose were lower than those predicted by this correlation (see Figure 3.5). At a volume fraction of 0.032, the expected diffusivity of glucose should be 5.7×10^{-6} cm^2/sec. The values for glucose diffusion (2.0×10^{-6} cm^2/sec) were 3 times lower than the calculated values. These discrepancies are postulated to have resulted from the interaction of glucose directly with the PEO polymer chain. In addition to an obstructional effect of PEO for glucose, PEO may serve as a site for glucose sorption and desorption. Glucose diffusion in the PEO hydrogels probably occurred by simple dif-

fusion through bulk H_20 which was impaired by glucose entrapment by sorption and desorption phenomena.

Consider the following reversible reaction:

$$Glucose_{(soluble)} + Site \leftrightarrow Glucose_{(adsorbed)}$$

Let:

C = Concentration of Glucose $_{(soluble)}$
S = Concentration of Glucose $_{(adsorbed)}$
and
R = Equilibrium ratio of S to C, a constant

If we consider that adsorption to the network[9] was very fast with respect to diffusion, then:

$$S = R \cdot C \tag{3.9}$$

$$\frac{\partial C}{\partial t} = D_{obst} \cdot \frac{\partial^2 C}{\partial x^2} - \frac{\partial S}{\partial t} \tag{3.10}$$

$$\frac{\partial C}{\partial t} = D_{obst} \cdot \frac{\partial^2 C}{\partial x^2} - \frac{R\partial C}{\partial t} \tag{3.11}$$

$$\frac{\partial C}{\partial t} + \frac{R\partial C}{\partial t} = D_{obst} \cdot \frac{\partial^2 C}{\partial x^2} \tag{3.12}$$

$$\frac{\partial C}{\partial t} = \frac{D_{obst}}{(1+R)} \cdot \frac{\partial^2 C}{\partial x^2} \tag{3.13}$$

A model of solute partitioning within the hydrogel can be formulated by considering the amount of solute (glucose) adsorbed to the network. An expression for the concentration of glucose within the hydrogel (C_G) can be determined by summing up the glucose

adsorbed to the network and that remaining in the bulk solvent (H_2O) phase. The following expression for C_G is written in terms of: (1) glucose adsorbed onto the network (S) and (2) glucose that remained in solution and excluded by the volume fraction ($v_{2,S}$) of the polymeric network.

$$C_G = S + C(1 - v_{2,s}) \tag{3.14}$$

Inserting this expression into the definition for partition coefficient (equation 3.5) the equilibrium constant (R) can be related directly to the partition coefficient and the volume fraction of polymer.

$$K_p \equiv \frac{C_G}{C} = \frac{S + C(1 - v_{2,s})}{C} \tag{3.15}$$

$$K_p = \frac{RC + C(1 - v_{2,s})}{C} \tag{3.16}$$

$$K_p = R + 1 - v_{2,s} \tag{3.17}$$

$$K_p + v_{2,s} = R + 1 \tag{3.18}$$

Substituting equation 3.18 into the expression for obstructed diffusion in equation 3.13, the following expression for diffusion is obtained:

$$\frac{\partial C}{\partial t} = \frac{D_{obst}}{(K_p + v_{2,s})} \cdot \frac{\partial^2 C}{\partial x^2} \tag{3.19}$$

$$D_{Theoretical} = \frac{D_{obst}}{(K_p + v_{2,s})} \tag{3.20}$$

From Figure 3.7, the partition coefficient (K_p) was seen to have a positive linear correlation with the polymer hydrogel concentration (C_{PEO}) over the range of interest. The linear regression of K_p onto C_{PEO} provided the following relationship:

$$K_p = 0.145C_{PEO} + 1.282$$

Using equation 3.20 a theoretical diffusivity that considers network adsorption was calculated. This theoretical curve is shown in Figure 3.8, which is highly correlated with the experimentally derived data.

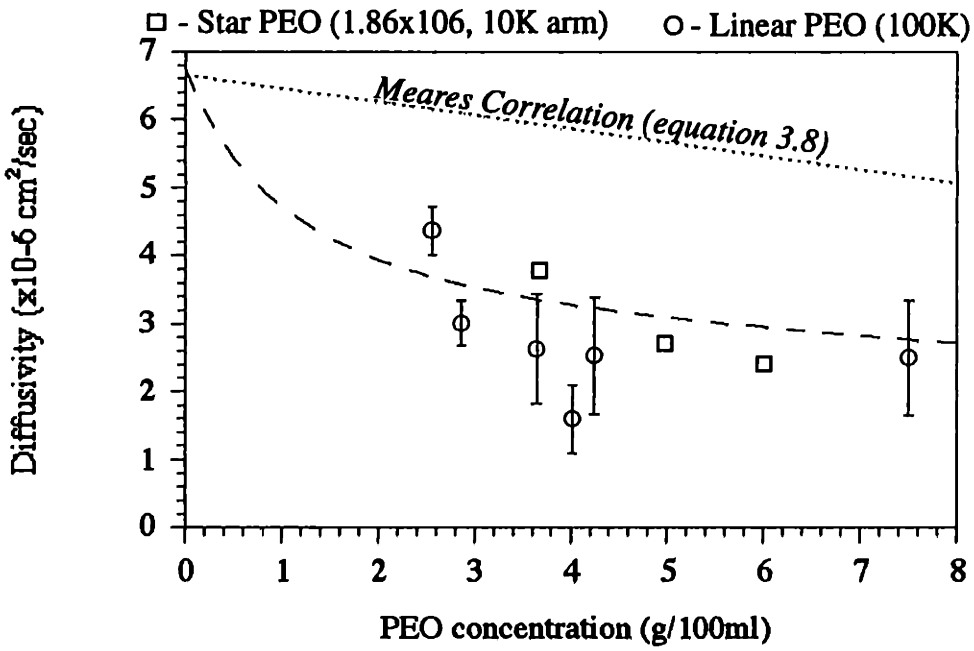

Figure 3.8: Theoretical Diffusivity of Glucose in PEO Hydrogels

Glucose diffusion through HEMA hydrogels is already well characterized and presented in the literature.[2] From that body of scientific work, 41% HEMA hydrogels are reported to have apparent glucose diffusivities of 2.0×10^{-7} cm^2/sec. The apparent glucose diffusivities presented here are in good agreement with established values. Specifically the values in this study ranged from 67.4×10^{-8} cm^2/sec (30% HEMA) to 5.3×10^{-8} cm^2/sec (61.4% HEMA).

3.5 Summary

PEO hydrogels were swollen to equilibrium in water with the resulting volume fraction polymer which ranged from 0.016 to 0.064 (2-8 wt/vol%). Glucose partitioned into poly(ethylene oxide) hydrogels (K_p=1.6-1.9) and showed a positive correlation with the volume fraction polymer in the hydrogel. Glucose diffusivity was decreased ($D = 4.2 \times 10^{-6} - 1.8 \times 10^{-6}$ cm^2/sec) and showed a negative correlation with volume fraction polymer in the gel. These results indicated that glucose was interacting with the poly(ethylene oxide) network. This sorption and desorption of glucose onto the poly(ethylene oxide) introduced an additional barrier to diffusion. This additional barrier to diffusion is in addition to the simple inert obstructional effect of the polymer in swollen networks. There appeared to be no difference in glucose diffusivities between hydrogels made from star PEO molecules or linear PEO molecules. This implies that the molecular structure of PEO in these high water content hydrogels does not affect the mass transport properties of small solutes. The information on glucose mass transport in PEO hydrogels and HEMA hydrogels has been incorporated into some design criteria presented in Chapter 5.

Chapter 3 References

[1] B. E. McCarey and D. M. Andrews. Refractive Keratoplasty with Intrastromal Hydrogel Lenticular Implants. Investigative Ophthalmology and Visual Science. July 1981, Vol. 21, No. 1, pp. 107-115

[2] Wisniewshi S and Kim SW, Permeation of Water-Soluble Solutes Through Poly(2-Hydroxyethethyl Methacrylate) and Poly(2-Hydroxyethyl Methacrylate) Crosslinked with Ethylene Glycol Dimethacrylate, Journal of Membrane Science, 6(1980) pp. 299-308

[3] Pu HT and Yang RYK, Diffusion of Sucrose and Yohimbine in Calcium Alginate Gel Beads with or Without Entrapped Plant Cells, Biotechnology and Bioengineering (1988) (32) pp891-896

[4] Hendrix M, Vandeen Abiele C, Engels C and Tobback P., Diffusion of Glucose in Carrageenan Gels, Journal of Food Science (1986) 51(6) pp1544-1546

[5] Hendrix M, Ooms C, Engels C, VanPatten C. Obstruction Effect of Carageenan and Gelatin on the Diffusion of Glucose. Journal of Food Science. (1987) Vol 52 (4) pp1113 - 1114

[6] Peppas NA (editor), Hydrogels in Medicine and Pharmacy. Volume 1, © 1986 CRC Press, Inc

[7] Hannoun BJM and Stephanopoulous G. Diffusion Coefficient Glucose and Ethanol in Cell Free and Cell Occupied Alginate Membranes. Biotechnology and Bioengineering (1986) 27 pp 829-835

[8] Brito E, Don Juan J, Dominguez F, and Casas LT. Diffusion Coefficient of Carbohydrates in modified k-Carrageenan Gels with and without Escherichia Coli. Journal of Fermenation and Bioengineering. Vol 69 (2) 1990, pp 135-139

[9] Crank J. The Mathematics of Diffusion. 5th Ed. Oxford University Press. Ely House

[10] Rogers WP, Buritz RS, and Alper D. Diffusion Coefficient, Solubility, and Permeability for Helium in Glass. Journal of Applied Physics. Vol 25 (7) pp 868-876

[11] Young DS, et al: Clinical Chemistry. 21:304D, 1975 (Special Issue)

[12] Howanitz PJ, Howanitz JH. IN Clinical Diagnosis and Management by Laboratory Methods, 17 ed., JB Henry Ed., WB Saunders, Philiadelphia 1984 , p 168

[13] Paul DR, Garcin M, and Garmon WE, Solute Diffusion Through Swollen Polymer Membranes, Journal of Applied Polymer Science.

[14] Ogston AG, The Spaces in a Uniform Random Suspension of Fibres, Trans of the Faraday Society, No 54, 1754-1757

[15] Ogston AG, Preston BN, Wells JD. On the Transport of Compact Particles Through Solutions of Chain Polymers. Proceedings of the Royal Society of London. A. Vol 33 (1973), pp 279-316

[16] Okar RS. Solute Adsorption and Concentration Dependent Permeability in Certain Polymer Films. Journal of Pharmaceutical Pharmacology. (1989) 41 pp 483-484

[17] P. Meares. Journal of Polymer Science., Vol 20, 1956, p. 507

[18] Remmp, P. Institute Charles Sadron, Strausbourg France. *Private Communication*

Chapter 4

Biocompatibility Studies

Prosthetic devices and implantable materials have classically been scrutinized in terms of inflammatory potential, foreign body responses, or outright toxic sequelae due to breakdown or byproducts. Poly(ethylene oxide) hydrogels by themselves are considered highly non-inflammatory materials.[1,2] Recently, specific cellular interactions have become a consideration in device performance (ie vascular, bone, liver, cartilage, nerve, skin). The most important cellular interaction with a keratoprosthesis is the interaction with epithelial cells resulting in the subsequent coverage of the implant.[3,4] As such, further developments in keratoprostheses focus on the device outer surface which apposes the external environment. (see Chapter 1). The surface must be enclosed in epithelium to maintain the protective boundary of the body. Thus the restoration and maintainence of an epithelial cell layer was the foundation of these compatibility studies presented in this chapter.

4.1 The Biological System

4.1.1 Corneal Epithelium

Epithelium is the outermost layer of a living organism. It serves as a protective boundary between the organism and the environment.[5] In vertebrates, the epithelium is a mulitlayered cellular structure where cells are tightly adhered to one another to form a contiguous boundary. Corneal epithelium has some unique features which separate it from other epithelial types. Epithelial cells from cornea do not produce keratin and remain living from the most superficial layers to the basal layer. The corneal epithelium also has a very high metabolism which requiries more energy than other epithelial types.[6,7,8] The structure of

corneal epithelium is shown schematically in Figure 4.1.

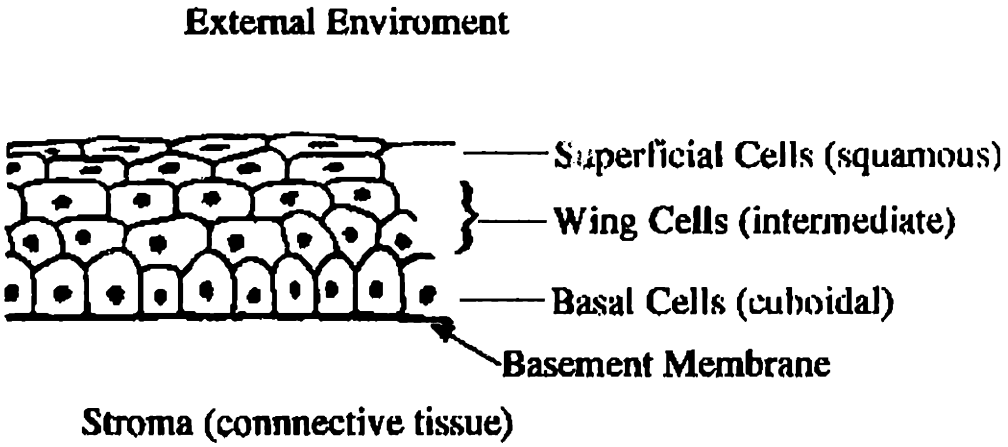

Figure 4.1: Cellular Structure of Corneal Epithelium

Epithelium has a stratified structure. The basal epithelial cells are cuboidal and directly appose the basement membrane and connective tissue below. The cellular layers above the basal layer are the wing cells. These epithelial cells make a gradual morphologic transition to squamous cells from the basal layer to the outermost surface of the epithelium.

Between the collagenous connective tissue of the stroma and the basal epithelial cells is the basement membrane zone (BMZ). The basement membrane is an acellular proteinaceous structure that serves as a boundary and an attachment site for epithelial cells over connective tissue. It is composed of laminin, type IV collagen, and type V collagen to which subcellular elements such as hemidesmosomes attach. These components of the BMZ are deposited and maintained by the basal epithelial cells and the keratocytes (stromal fibroblasts).[9]

4.1.2 Corneal Epithelial Healing

Wounding of the epithelial cell layer is potentially a very serious condition. The restoration of an epithelial surface over the denuded surface of a corneal prosthesis is therefore an important consideration in device performance. Healing or recovery of the epithelial

integrity must take place completely (if not expediently) to maintain this protective boundary and the smoothness of the tear film. Epithelial wound closure (healing) takes place in two phases: (1) Early migratory phase and (2) Late proliferative phase. This initial "early" phase of epithelial wound healing is characterized by rapid movement of epithelial cells over the denuded area to initially close the wound. The epithelium during this early phase is usually seen as one or two cell layers in thickness with no cell division. The cells in this phase move rapidly from the wound margin by a process of active horizontal movement. In epithelial wound healing, there is an inverse relationship between migration and mitosis. There is no growth pressure from dividing cells although there can be some cell division distant from the wound edge to supply cells for movement. These aspects of epithelial wound healing are shown in Figure 4.2

With the wound now covered, the basal layer of epithelial cells assumes the mophologic appearance of stationary cuboidal cells. Active mitosis is then apparent as the epithelial cells attempt to restore the multilayered epithelial structure. This late phase of epithelial wound healing takes place many days after the initial insult. The repairing epithelial cells reassemble the basement membrane components as the surface is reepithelialized. The sequence of immunologically distinct structures that appear are: (1st)-hemidesmosome structures, (2nd)-type IV collagen, and lastly laminin.[9]

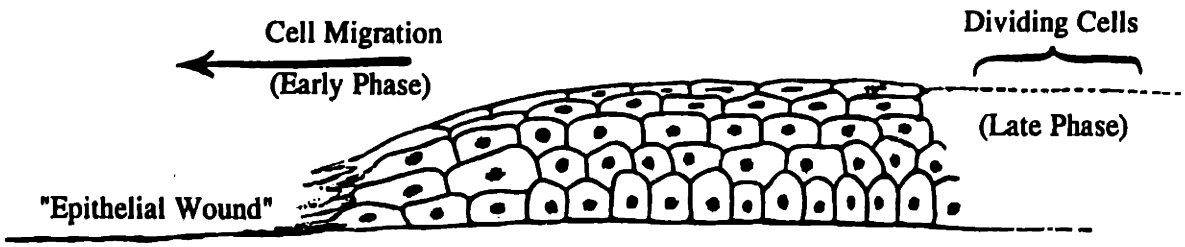

Figure 4.2: Schematic of Epithelial Wound Healing

4.1.3 Criteria for Evaluation

In the previous chapters, the focus was on the non-biologic material properties of the corneal PEO composite hydrogels. For this chapter, the goal was to quantify the behavior of cellular interactions with the composite hydrogel. In light of the epithelial healing process, parameters for evaluating the device performance have been established in these studies. In the early phase, the radial rate of epithelial migration was evaluated. Outgrowth rates could be evaluated in situ (living cells in culture). This was primarily a quantitative assessment. In the late phase, cellular differentiation and morphology was evaluated. In late phase analyses, assessments were mainly qualitative and static. Instead of in situ evaluation, histological analyses were used to understand the differentiation and functioning of epithelium. Light microscopy was used to examine the morphology of migrating epithelium and development of multilayer structures. Transmission electron microscopy was also used to examine the adherence of cells to the stromal tissue layer. Differentiation and functioning of epithelial cells was evaluated by examination of the basement membrane proteins by deposited by basal epithelial cells. This was performed by immunohistochemicial analysis. The morphology of adherent cells was compared between different substrates.

4.1.4 *In vivo* versus *In vitro*

A biological system can vary from a solution of proteins, a defined cell population *in vitro*,[10,11,12,13] an *in vitro* organ system,[14] and lastly by *in vivo* implantation.[15,16] In choosing an experimental system, the ability to quantify variables was considered most important. The clinical standard of performance is to implant the device or material into a host cornea and observe the clinical outcome.[17,18,19] Yet, surgical implantation has relatively little quantifiability other than success or failure and is costly. A more defined, cost effective, and potentially quantifiable system involves the an organ or cell culture environ-

ment.

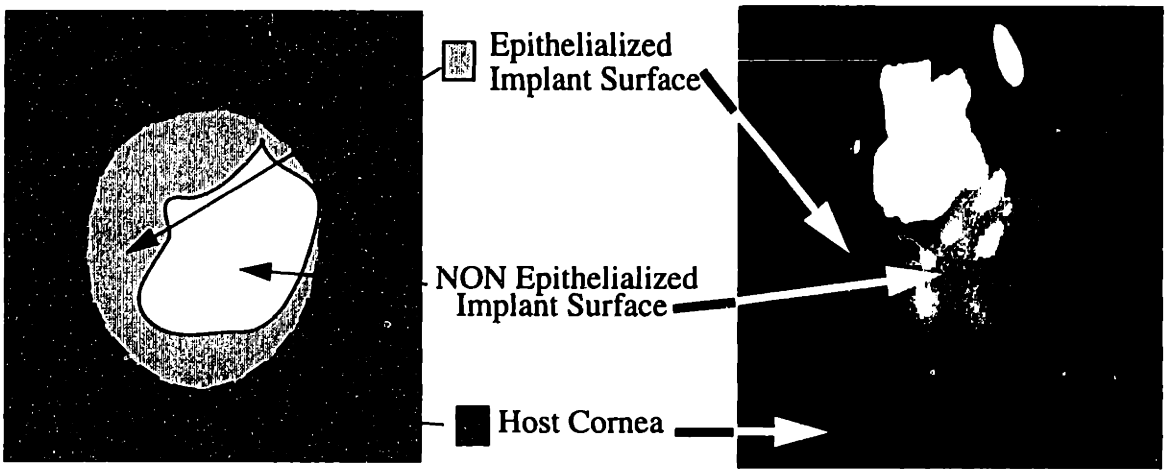

Figure 4.3: Appearance of Fluoroscein stained Rabbit Eye Implant

Mammalian cells from the tissue of interest (e.g., cornea) were used in the organ and cell culture systems, and maintained in an aqueous medium. This liquid medium environment supplied nutrient support to the living cell population. In vitro systems were maintained at 37°C with a mixture of air and 5% CO_2 to maintain the proper pH. Cell culture systems are attractive in that cellular behavior is readily observable in situ through microscopy. Since the population of cells can be well defined, aberrations in results due to the complexities in implantation techniques etc. can be avoided. Thus cell culture and organ culture became a major emphasis of the compatibility testing performed

4.2 In vitro Epithelial Migration Assays

Several different *in vitro* assays that have been designed to elaborate kinetics of epithelial cell migration have been published.[10,20,21] In general, these methods place a source of epithelial cells in close proximity to the test surface in question. Simmons et. al. created a system of subcultured epithelial cells where a defect was created in the confluent layer of cells, whereas Tanelian used an elaborate system of perfused whole corneas with the denuded central cornea as the test surface. Additionally, Nishida presented a system

where 3 mm corneal trephinations served dually as sources of epithelial cells and as test surface. Configurations of these assays present difficulties in changing the test surfaces and difficulties in evaluating diffusion of important solutes through the material in question. Recently, a corneal epithelial migration assay by Petit et. al., was presented that allows the testing of differing substrates. In this assay epithelial cells from 5 mm corneal tissue buttons were observed as they migrated onto the test surface in vitro. This assay configuration is shown below in Figure 4.4.

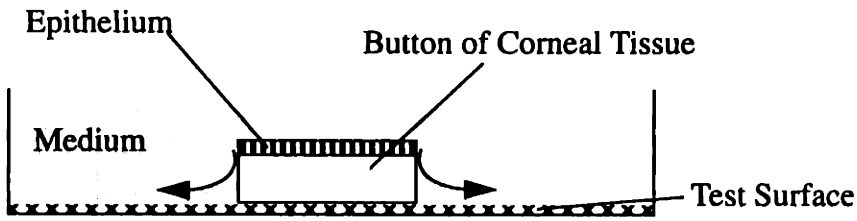

Figure 4.4: Schematic of Petit Migration Assay

The importance of this particular migration assay is that epithelial cells migrate from host corneal tissue (as they would normally during healing) down the cut edge of the button outward in a radial manner. The perimeter of this expanding epithelial cell population delineates an area of cell coverage: the new epithelialized surface. The kinetics of epithelializatin for the Petit assay is presented below.

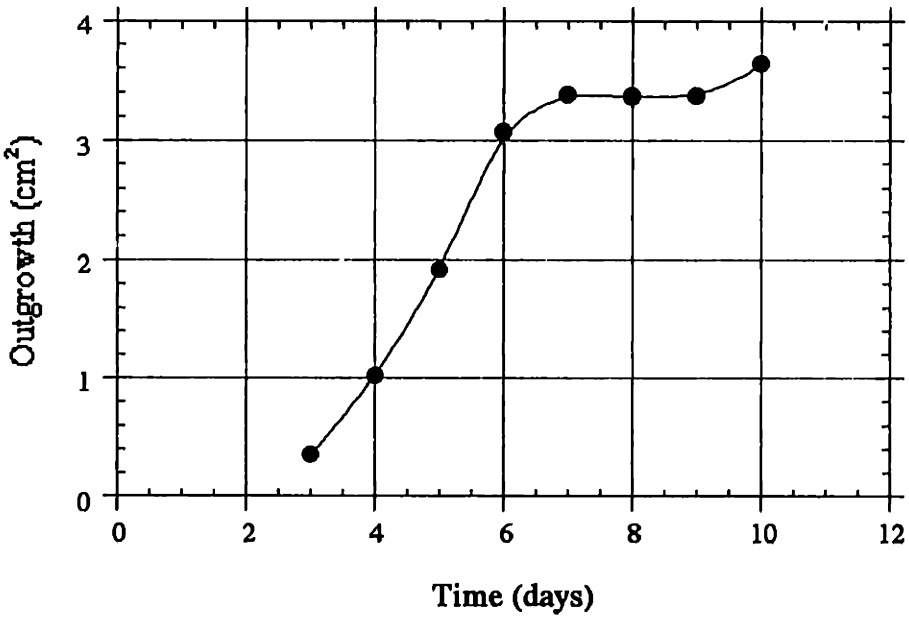

Figure 4.5: Kinetics of Migration in Petit Assay

4.2.5 Suspended Hydrogel System

Adaptation of the outgrowth assay presented by Petit[20] was necessary in order to evaluate the mass transport processes involved in epithelial wound healing over the composite hydrogels. Although the outgrowth assay was attractive in that the epithelial cells population could be placed in contact with various surfaces, the substrate in the assay presented by Petit was completely submersed in medium and the epithelial cells were in direct contact with the nutrients and soluble factors. This direct contact between cells nutrients is a non-diffusion limited situation. Therefore, the Petit assay arrangement can not evaluate the diffusion limitations of nutrient and soluble factors on healing. A more physiologic system was developed in this study to test these limitations.

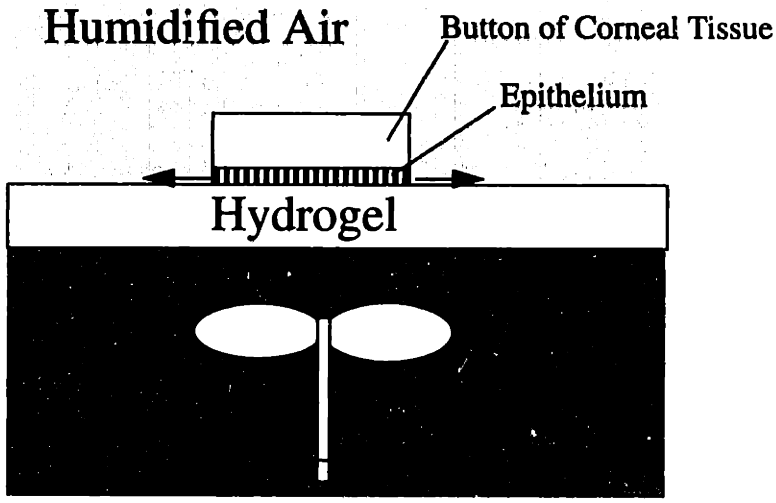

Figure 4.6: Suspended Hydrogel System

Anatomically, epithelial cells derive their nutrients from the aqueous humor which lies beneath the cornea in the center of the eye.[6,7] A system to evaluate diffusive flows must mimic this normal arrangement of trans-corneal nutrient flow. A new experimental design was developed in this work to evaluate mass transport considerations. This system that simulated the natural anatomic arrangement and is shown in Figure 4.6. The test composite hydrogel lenticule was suspended in a upright plexiglass cylinder between a medium compartment and a humidified air chamber. Epithelial cells could migrate onto the composite hydrogel surface much in the same way that the epithelial cells in normal epithelial wound healing can grow over the abraded cornea. This process was observed in situ through inverted phase contrast microscopy. The apparatus used to magnetically stir the medium during the experiments is shown in Appendix E.

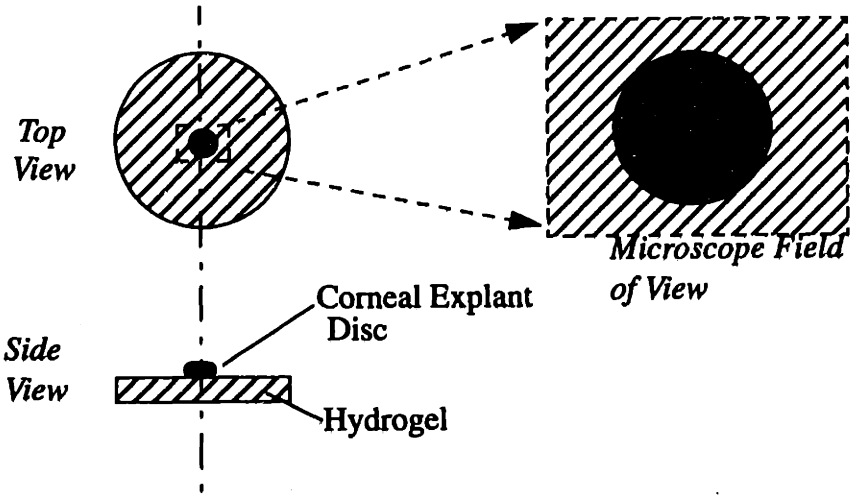

Figure 4.7: Microscope Field of Observation

The appearance (as seen through the microscope) of the suspended hydrogel system is drawn schematically Figure 4.7. The top view shows a dashed line indicative of the field of view of the microscope. Figure 4.8 shows the initial appearance of a 2mm button of corneo-scleral limbal tissue for outgrowth. No medium was added to the surface of the hydrogel and the entire system was grown in a 100% humidified chamber at 37C. Figure 4.9, seven days after assay initiation, illustrates the appearance of epithelial cell out-growth. The rate at which these cells grew radially outward was measured to evaluate and model the mass transport effects on epithelial wound closure.

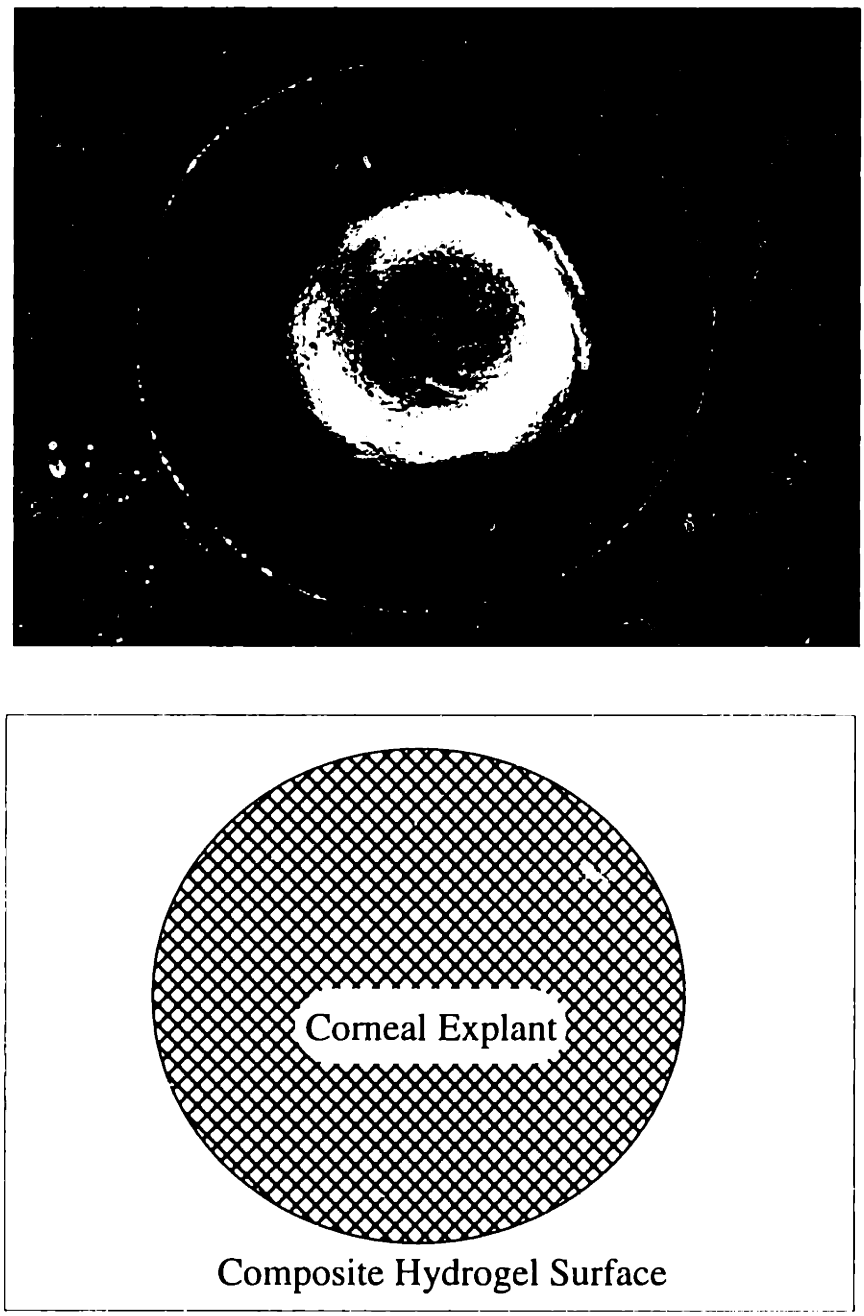

Figure 4.8: In vitro: 2 mm Button of Corneal Tissue on Composite Hydrogel (0 days)

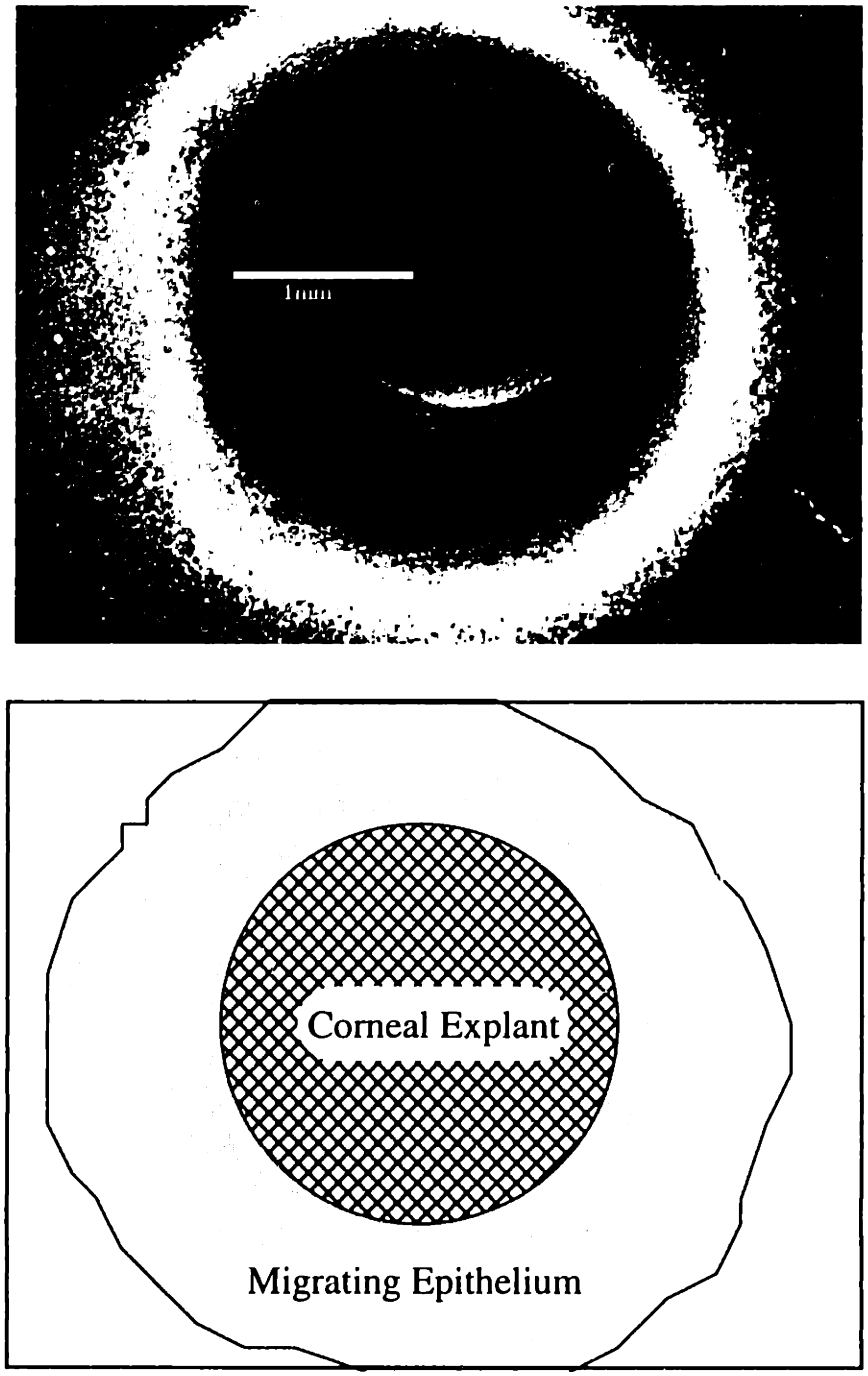

Figure 4.9: In vitro: 2 mm Button of Corneal Tissue on Composite Hydrogel (7 days)

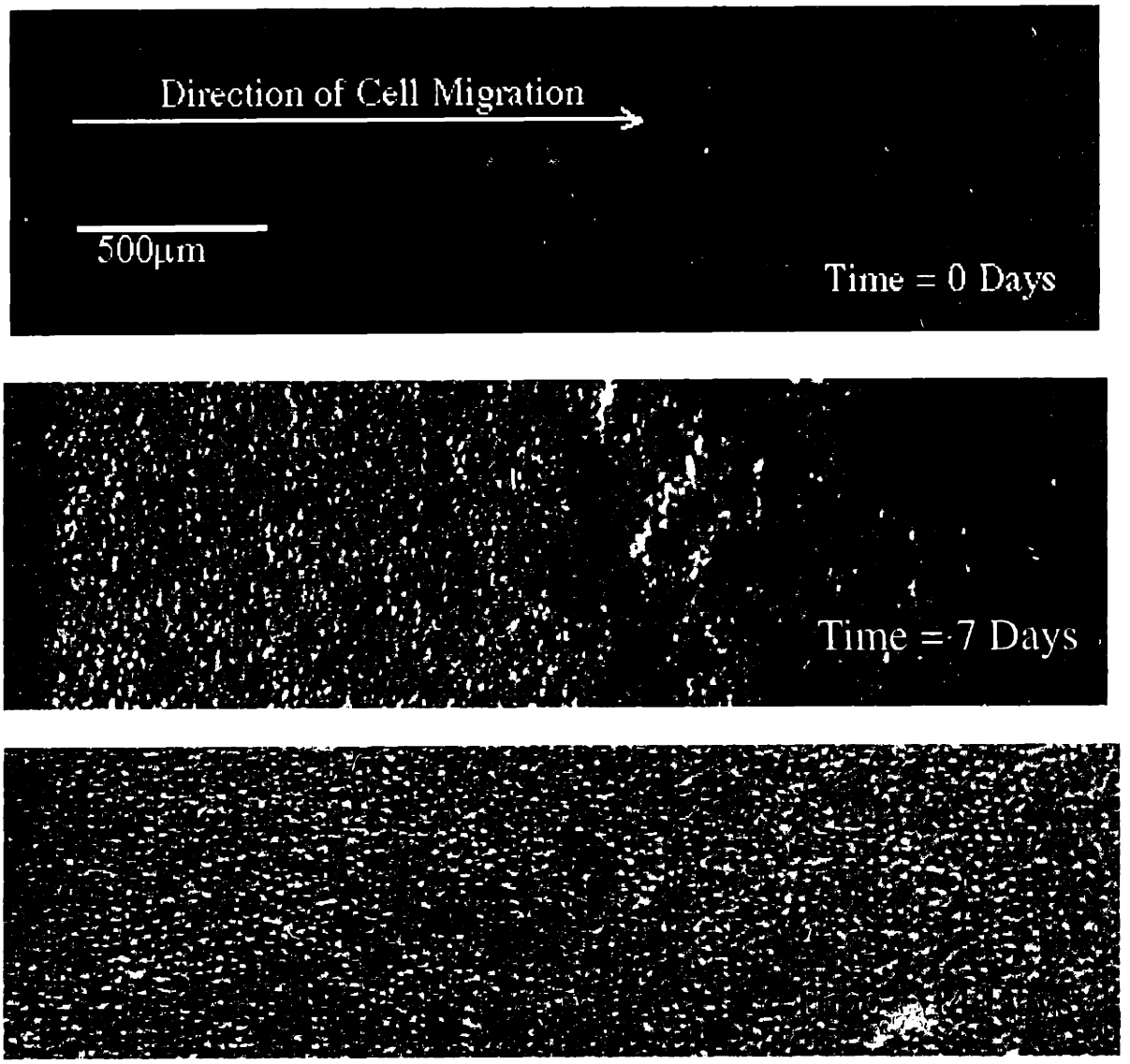

Figure 4.10: Epithelial Migration onto Composite Hydrogel over time

4.3 Epithelial Wound Healing on Composite Hydrogels

Using this artificial corneal system, an experimental demonstration of compromised epithelial wound healing was sought. In particular, the effect of introducing a significant barrier to diffusion was of interest. This barrier was the composite hydrogel. Wound healing was measured as the distance between the wound edge of the corneal tissue implant and the edge of the migrating epithelial cells. Typical outgrowth as observed through phase contrast microscopy is shown in Figure 4.10. The migrating epithelial margin appeared as the densely confluent cells on the left side of the 7 day window. Each epithelial wound healing sample can be followed throughout the course of the experiment in situ without resorting to histological preparation. The following experiment was designed to elaborate the effect of composite hydrogels on epithelial wound healing in the suspended hydrogel system.

4.3.6 Materials and Methods for in vitro epithelial healing

The experimental setup was identical to that presented in the previous section. Test composite hydrogels were suspended between a healing epithelial cell population and a nutrient medium. Thick composite hydrogels (2mm) served to create the diffusion limited scenario. Thin sections (40 microns) of corneal stroma without hydrogels were used as NON diffusion-limited controls.

Wound Healing Substrates: Bovine corneal stroma was sectioned into 40 μm sections using a cryostat maintained at -20C. These stromal layers to be grafted onto hydrogels were placed into flat molds (glass slides with circular silicone rubber dam, 15mm ID). Approximately 600 μl of a 2% aqueous solution of 5,000K PEO (Union Carbide, PolyOX Cat. No. C-014) was placed over the stromal layers 15 minutes prior to irradiation. Control substrates layers of stroma (40 μm) were also prepared. All samples were irradiated to

a total dose of 2 Mrad in one exposure. The composite materials and controls were then ready for in vitro wound healing tests.

Epithelium: Corneal epithelium for wound healing studies was obtained from euthanized NZW rabbits (3-5 kg).[22] The entire intact globes were removed and incubated for 3 hours in a rinse of Hank's Balance Saline Solution that contained polymixin (200 μg/ml) and gentamicin (100 μg/ml). The corneas were removed from each globe in a sterile fashion within a laminar flow hood. The endothelium of the cornea was removed by scraping with a sterile cotton-tipped applicator. Two mm discs of corneal tissue were punched out from the tissue using a sterile corneal trephine. These 2 mm tissue explants contained the wound healing epithelium that was placed in contact with suspended test substrates (composite hydrogels or control stroma).

Table 4.1: Epithelial Cell Media Compositions

Supplemented Hormonal Epithelial Medium (SHEM)	**Petit Assay Medium (w/o DMSO & Cholera Toxin)**	**Keratinocyte Serum Free Medium (K-SFM)** (Gibco Cat # 320-7005PJ)
DMEM/HAMS F12	DMEM/HAMS F12	DMEM/HAMS F12
Fetal Calf Serum (5%)	Fetal Calf Serum (5%)	Bovine Pituitary Extract (1μg/ml)
Dimethyl Sulfoxide (0.5%)	———	———
Gentamicin (1μg/ml)	Penicillin (50U/ml) Streptomicin (50μg/ml)	Gentamicin (5μg/ml)
Epidermal Growth Factor (10 ng/ml)	Epidermal Growth Factor (10 ng/ml)	Epidermal Growth Factor (10 ng/ml)
Cholera Toxin (0.1μg/ml)	Insulin (5μg/ml)	———
Glucose (1mg/ml)	Glucose (1mg/ml)	Glucose (1mg/ml)

Cell Culture: In vitro wound healing epithelial cultures were maintained at 37°Cwith 5% CO2. A commercial form of serum-free medium (Keratinocyte-SFM, Gibco Laboratories, Inc Cat. No.320-7005PJ) was used to support these cells during the experiment.

This particular medium contained a minimal amount of supplementation with respect to other media used for corneal epithelial cell culture. (See Table 4.1) Wound healing cultures were given fresh media everyday (1.25 ml/day). Epithelial outgrowth was noted at 0 days, 3 days, and 5 days. Observations were perfomed with an inverted phase contrast microscope and documented with 35 mm photographs.

4.3.7 Results for in vitro epithelial healing

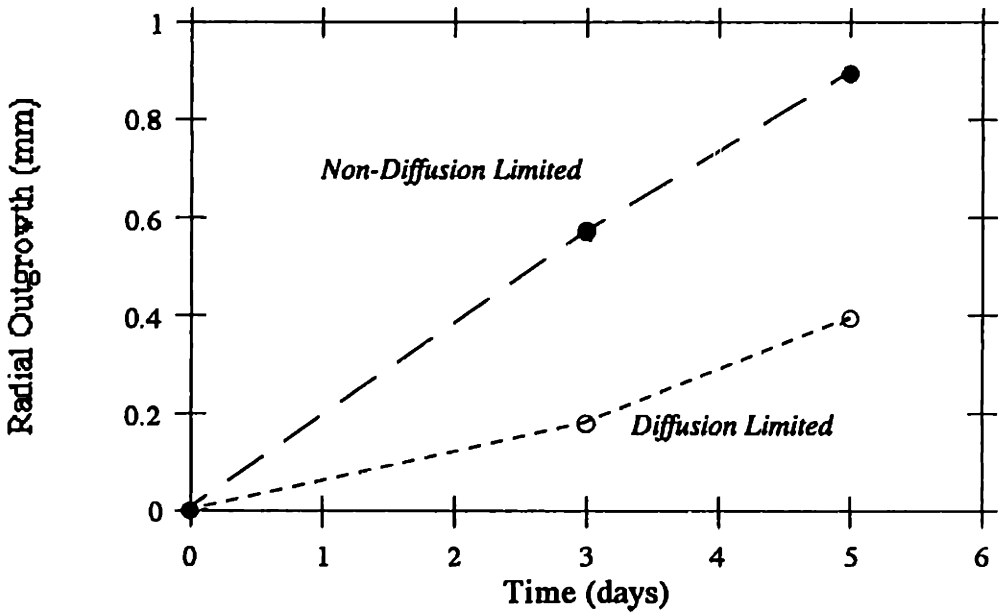

Figure 4.11: Epithelial Wound Healing (In Vitro)

As is shown in the outgrowth figure, the non-diffusion limited case showed a linear progression of epithelial cells during the first week. When a hydrogel was placed between the stroma and the epithelial cells, the rate of outgrowth was decreased significantly. The diffusion limited (hydrogel) outgrowth rate eventually reached approximately the same outgrowth rate as the non-diffusion-limited control at day 5. This outgrowth response lag is thought to have arised from the impedance of the hydrogel to diffusion of a soluble factor important in stimulating migration.

4.3.8 Analysis of Epithelial Wound Healing Results

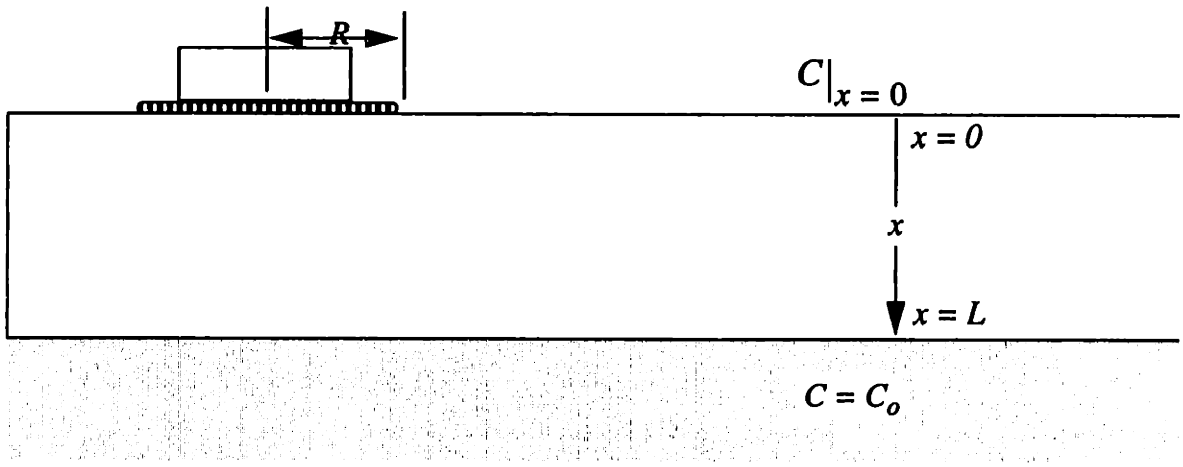

These wound healing experiments were constructed to elucidate how perturbing the diffusion through the material could affect the clinical performance of a corneal prosthetic device. The results from the in vitro experiments indicated that with the introduction of a hydrogel, there was a reduction in the rate of radial outgrowth. Initially, the amount of outgrowth was much less than the control which had very little diffusive limitations. If the situation is modeled as cell behavior (migration) that is promoted by an important solute, the observed migration kinetics can be theoretically interpreted.

$$Migration \propto Solute\ \ Concentration$$

$$\frac{dR}{dt} = h \cdot (C|_{x=0}) \tag{4.2}$$

This relationship is an approximation congruent with the experimental results. In the absence of the hydrogel, the radius R increased linearly with time (h is a constant at a given concentration). Many investigators have noted the apparent constant velocity migration of the corneal epithelium in wound healing studies. Classical kinematics of individual moving cells show multi-directionality in their movment. This would not be consistent

with a constant velocity epithelial front observed in the cornea. Interestingly, videomicroscopic studies have shown that individual corneal epithelial cells in the epithelium migrate in a *uni-directional* manner.[23] As a population, the cells at the wound margin move fastest and in total cells move in a synchronous and interconnected fashion. These characteristics may give rise to the constant velocity migration observed in these in vitro wound healing experiments.

Secondarily, with the composite hydrogel, the outward migration rate of cells was diminished. This is presumably due to an initial absence of an important soluble factor in the media. In this analysis, that decrease in migration rate is interpreted as having a linear relationship with concentration. The presence of a specific corneal epithelial chemotactic or chemokinetic factor is still in controversy. In vitro systems which have demonstrated chemotactic activity of fibroblast growth factor (FGF) and epidermal growth factor (EGF) used non-physiologic isolated cell systems.[24] Still, the chemotactic dose response to both FGF and EGF in that study was linear at low concentrations (*0-10ng/ml*) and then quickly reached a constant. At low surface concentrations (or equivalently early times in this system), migration can be within the linear portion chemotactic dose response.*

From the data acquired we can estimate (*hCo*) to be:

$$(hC_o) = \left(\frac{dR}{dt}\right)_{NoHydrogel} \tag{4.3}$$

The diffusion of a migration factor to the hydrogel surface is presented as follows:

* Although a specific activity of a particular molecule was not evaluated in these experiments, the serum free medium used contained 10 ng/ml of EGF.

$$\frac{\partial C}{\partial t} = D \cdot \frac{\partial^2 C}{\partial x^2} \tag{4.4}$$

Initial Condition: C = 0 at t = 0 for all x, 0<x<l

Boundary Condition 1: C = Co at x= L for all t>=0

Boundary Condition 2: $\frac{dC}{dx} = 0 \quad \text{at} \quad x = 0 \forall (t \geq 0)$

The boundary condition, $\frac{dC}{dx} = 0$ @ $x = 0$, is meant to describe the concentration of the migration stimulator solute *on the unepithelialized surface*. Only 1.77% of the surface was in contact with cells from the explant. Most of the surface was not epithelialized. Furthermore, in wound healing of the corneal epithelial cells, the leading edge of the healing front set the rate of wound closure.[23] This rate setting edge borders and moves into the unepithelialized surface region, which is governed by an absence of interfacial flux. This is only an approximation because there is likely to be some uptake solute by the cells. But analysis based on the unepithelialized surface seems plausible when one considers that chemotactic signals in vivo would most likely originate from cells beneath the unepithelialized surface.[24]

Solution:[25]

$$\frac{\left(C|_{x=o}\right)}{C_o} = 1 - \sum_{n=0}^{\infty} \frac{(-1)^n}{(2n+1)} \cdot exp\left(\frac{-D\left((2n+1)^2 \cdot \pi^2 \cdot t\right)}{4 \cdot L^2}\right) \tag{4.5}$$

Hence,

$$\frac{dR}{dt} = hC_o\left(1 - \sum_{n=0}^{\infty} \frac{(-1)^n}{(2n+1)} \cdot exp\left(\frac{-D\left((2n+1)^2 \cdot \pi^2 \cdot t\right)}{4 \cdot L^2}\right)\right) \tag{4.6}$$

Integrating we get:

$$\frac{R}{R_o} = 1 + \left(\frac{h}{R_o}\right)t - \left(\frac{16hL^2C_o}{\pi^3 R_o D}\right)\left(\sum_{n=0}^{\infty}\frac{(-1)^n}{(2n+1)^3}\cdot\left(1-exp\left(\frac{-D((2n+1)^2\cdot\pi^2\cdot t)}{4\cdot L^2}\right)\right)\right) \tag{4.7}$$

Now defining dimensionless variables:

$$\phi = \frac{hC_oL^2}{R_oD} \qquad \tau = \frac{tD}{L^2} \qquad and \qquad \theta = \frac{R}{R_o}$$

$$\theta = 1 + \phi\tau - \left(\frac{16\phi}{\pi^3}\right)\left(\sum_{n=0}^{\infty}\frac{(-1)^n}{(2n+1)^3}\left(1-exp\left(\frac{-(2n+1)^2\pi^2\tau}{4}\right)\right)\right) \tag{4.8}$$

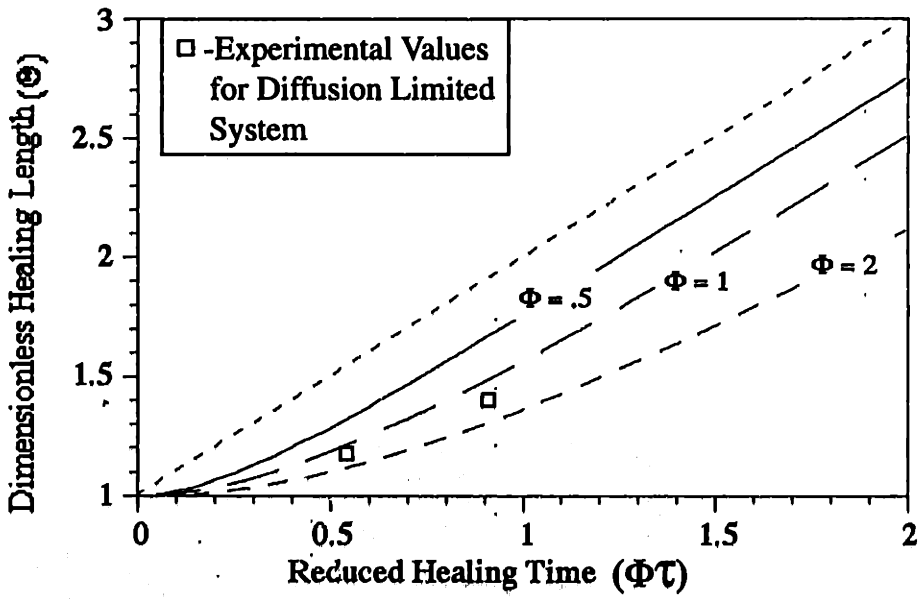

Figure 4.12: Theoretical Healing Curves

A mathematical model of epithelial wound healing was formulated to relate observed biological activity with mass transport properties of the hydrogel. Ideally, this model can enhance the explication of experimental results and give insight into the validity of the model's assumptions by comparing theoretical and experimental results. Overall thesolution followed a pattern very similar to that of the experimental results. For the in vitro results, the calculated value of the healing time scale (h*Co/Ro) gave a value of 133 hours. Experimental results for the diffusion limited case (introduction of the hydrogel) are between the family of healing curves $\phi = 1.0$ and $\phi = 2.0$ as shown in Figure 4.12. Approximating the value of $\phi \sim 1.5$, a diffusion time scale value was calculated to be 200 hours.

Much concern has existed over whether purely nutrient limitations affect the behavior or health of the corneal epithelium-prosthetic system.[4,26] In this particular experimental corneal system and phase of epithelial healing, it was unlikely that the introduction of mass transport limitations to glucose affect the epithelial healing dynamics. The diffusion time scale (L^2/D) value for glucose through hydrogels used in these epithelial wound healing experiment was 3.7 hours. This time scale was too small to be congruous with this model. The theory indicated that the diffusion time scale was approximately ~200 hours. Still, this theoretical analysis did suggest the presence of some diffusion limitation to a migration stimulation factor.

To date, a single "factor" which promotes the rate of epithelial wound closure has not been identified. Growth factors such as eye derived growth factor (EDGF) and basic fibroblast growth factor (bFGF) have proven to be potent mitogenic factors, but in vitro and clinical trials have not demonstrated increased rate of healing.[27-28] Interestingly enough, in vitro experiments with keratinocytes (skin epithelial cells) have shown a migration stimulation potential of the medium supplement bovine pituitary extract (BPE).[29] A spe-

cific migration stimulatory factor has not been identified within BPE, however, many of the growth factors present have been tested. BPE was a supplement that is used in these biocompatibility studies.

In general, the molecular weight of regulatory proteins (hormones and growth factors) is 5000~10,000. In order to test the hypothesis that a protein factor within the supplemented media could demonstrate the mass transport dynamics that are present within the system, a time lag experiment was performed with the hydrogels used in the healing experiment. The transport of fluorsceinated insulin was tested in diffusion cells used for testing glucose transport (see Chapter 3). The diffusion time scale for insulin in the composite hydrogel,(L^2/D), was 93 hours. (See Appendix F.) This time scale was less than that predicted by the theoretical model by a factor of 2, but this result suggested that a large molecule was the soluble mediator. Although research has not defined a specific molecule that accelerates epithelial migration, these results are highly supportive in the hypothesis that mass transport limitations present in this system can affect healing.

This theoretical analysis provided an additional means of assessing permeable corneal prosthesis design using clinical and physical data from the biological scenario and the device material itself. In the next chapter, this analysis is expanded into design parameters for the assessment of a hydrogel prosthesis design.

4.4 Long Term Epithelial Cell Functioning of Materials

Other more qualitative measures of the biological performance of these materials can be assessed through histologic evaluation. Histologic light microscopy can demonstrate the cellular or extracellular structure indicative of healthy epithelial function. For example, morphology is observable through both light and transmission electron microscopy. After initial migration in wound healing, multilayered epithelium formation occurs . (Fig-

ure 4.16) After epithelial wound closure, basal epithelial cells form anchoring filaments to the basement membrane which they deposit and maintain. This activity is representative of the normal cellular function of basal cells. Immunohistochemistry (in relation to light microscopy) can provide functional definition to the extracellular structural matrix such as the basement membrane. Immunologic localization of proteins such as laminin, vitronectin, fibronectin, and other integrins identify the reformation of a basement membrane on a previously "new" surface.[30]

4.4.9 Epithelium Regeneration

In another attempt to observe epithelial growth over a bilayer composite hydrogels, implantable lenticules were synthesized in concave glass molds and placed in excised rabbit corneas. This system was originally formulated to simulate an actual implantaion.[31,32] Epithelial cells readily migrate to heal the exposed central area of the implant in the same manner as they do in the quatiative in vitro wound healing assay. TEM was unable to identify hemidesmosomal formation in the early migratory phase. Nevertheless, migrating epithelial cells appeared to be healthy and well-adherent to the underlying tissue layer of the composite. The healing epithelium was not subjected to diffusion limitations of the hydrogel in this setup.

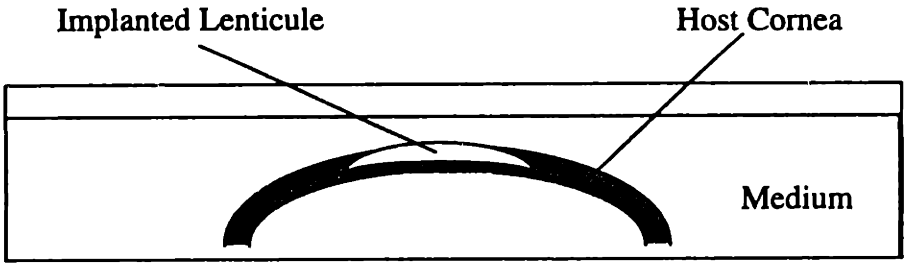

Figure 4.13: Implanted lenticule in Organ Culture

Figure 4.14: TEM of Migrating Epithelium (in vitro)

These organ culture results confirmed that the lenticule provided a surface conducive to epitheliazation. Still, the whole system did not lend itself easily to in situ observation. Additionally during the incubation period, the host tissue swelled and became opaque. After a sufficient amount of time, the host cornea and synthetic lenticule were fixed and processed for light microscopy. Cells grown in this system could only be observed through classic histological preparations performed in plastic embedding compound. Once cells reached confluence, multilayered epithelial formation occured at approximately one week. Photomicrographs of epithelium regeneration are shown in the following figures.

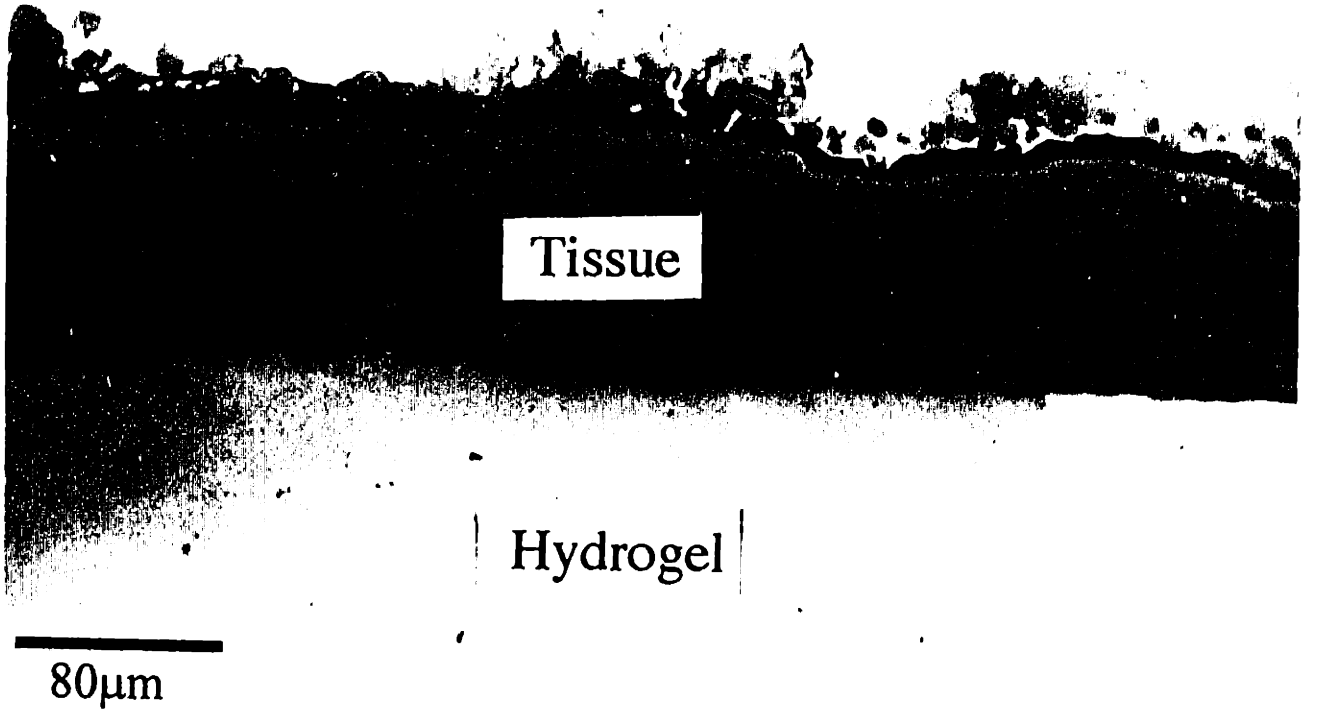

Figure 4.15: Continuous Layer of Basal Epithelium on Composite Hydrogel

Figure 4.16: Multilayered Epithelium Grown on Composite Hydrogel

4.4.10 Deposition of Basement Membrane Matrix

Other investigators have demonstrated that epithelial cells grown on renatured collagen materials erode material beneath the basal cells.[33] The deposition of an intact basal lamina (basement membrane) is an indication that cells are remaining resident and not resorbing or remodeling their substrates. These studies utilized immunohistochemical staining for laminin to detect the deposition of basal lamina by epithelial cells. Epithelial cells grown over composite hydrogels deposited and maintained a basal lamina containing laminin up to eight weeks. Positive immunohistochemical staining for laminin was detected in these "living" composites as early as one week after multilayer epithelium formation. The following photomicrographs show positive laminin staining in "living" composites and a negative control *de novo* composite hydrogels.

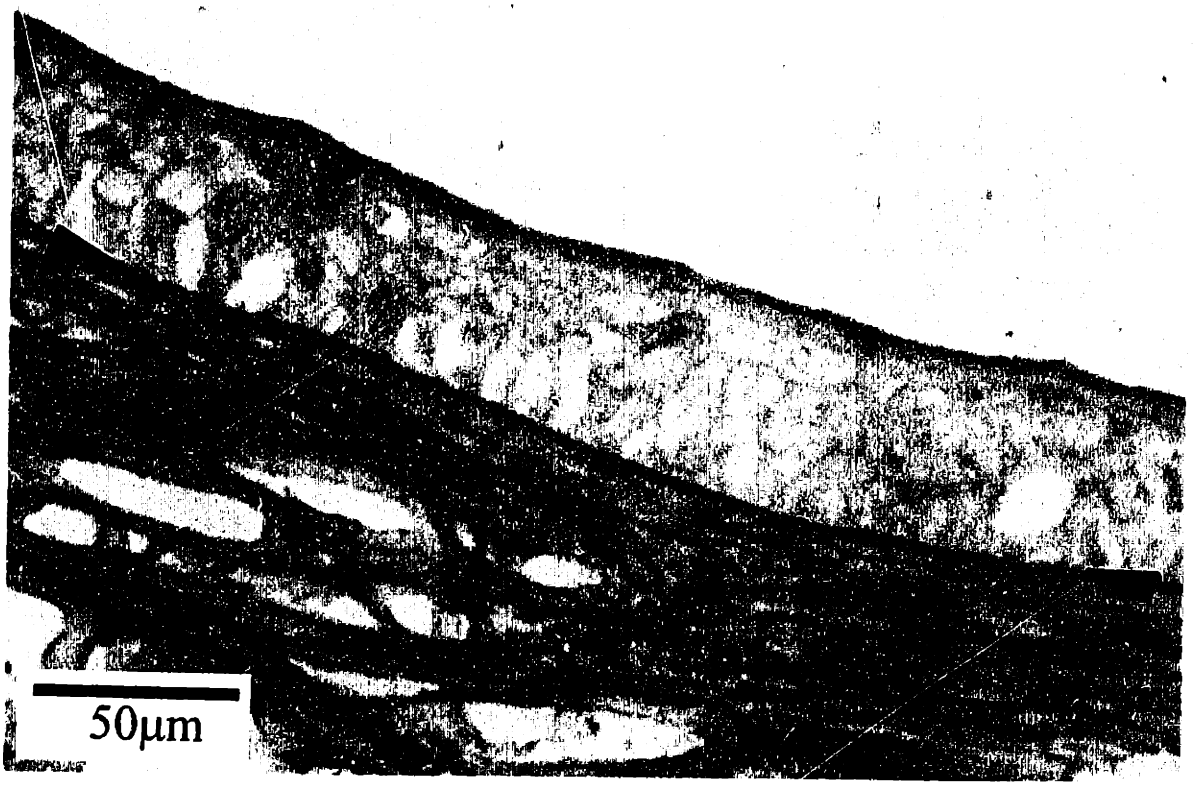

Figure 4.17: Anti-Laminin Stained Normal Rabbit Cornea (positive)

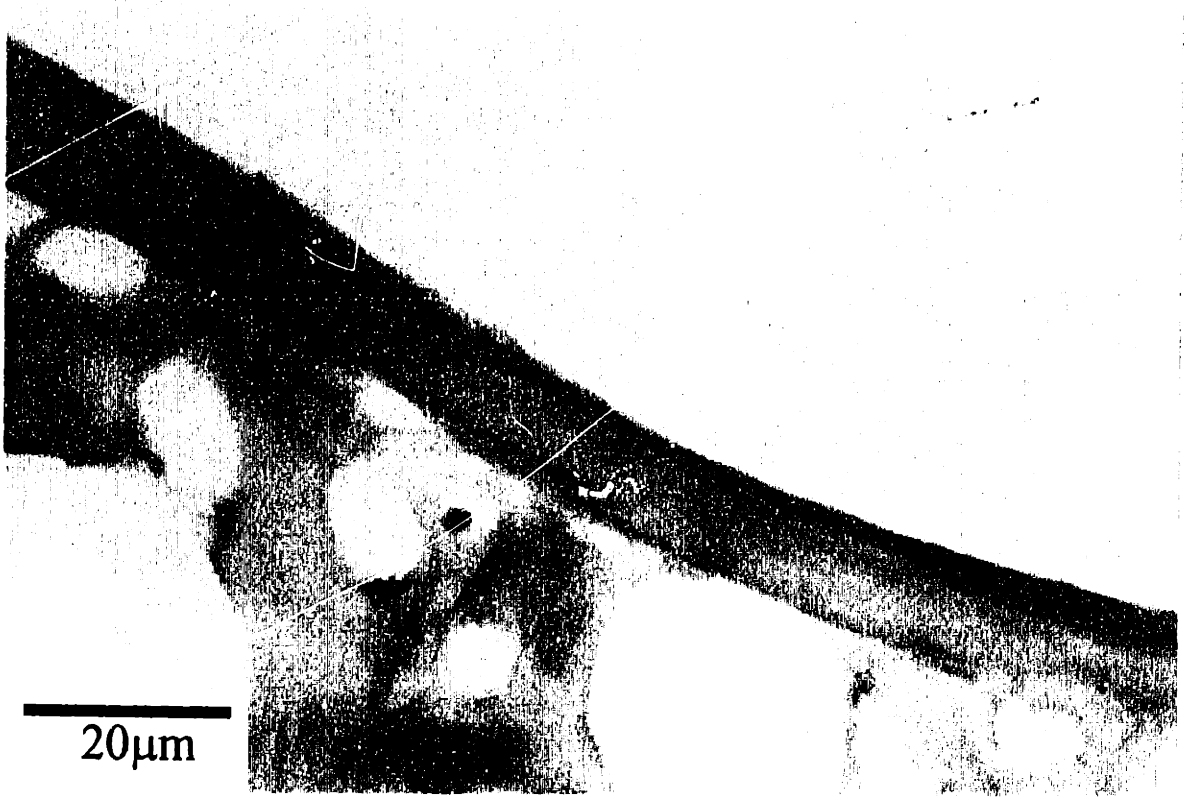

Figure 4.18: Anti-Laminin Stained *de novo* Composite Hydrogel (negative)

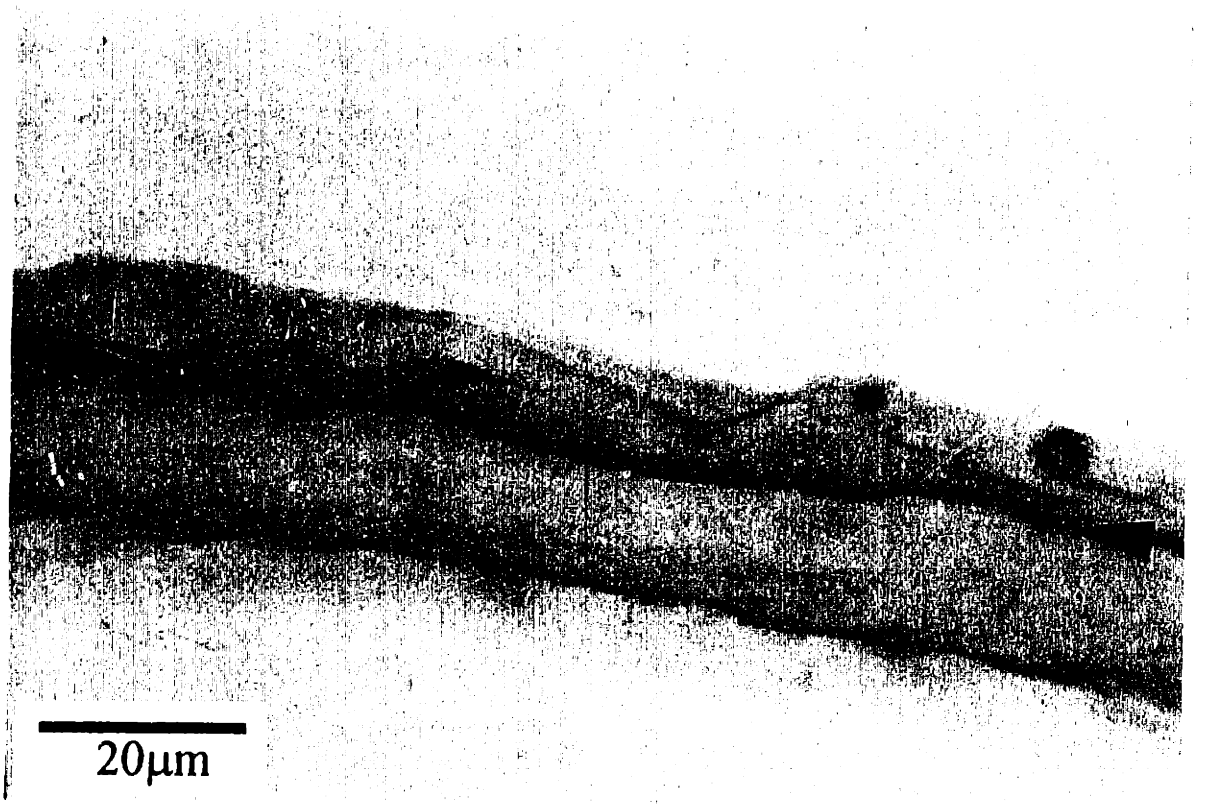

Figure 4.19: Anti-Laminin Stained *cultured* Composite Hydrogel (8 wks) (positive)

4.4.11 Epithelial Morphology After Outgrowth

Differences between cell growth on tissue culture plastic (TCP) versus growth on composite hydrogels was readily noted. Epithelial cells grown on TCP exhibited a flattened shape with denritic pseudopodia during growth. Multilayered growth of these TCP cultured cells resulted in epithelium thicknesses of 2-3 cell layers in thickness. In contrast, epithelial cells growing on composite hydrogels were rounded or polygonal in nature. Cell thicknesses up to 8-9 cell layers thick were commonly observed (as shown in Figure 4.16). As a further comparison to composite hydrogels, hydroxyethylmethacrylate (HEMA) lenses coated with soluble collagen I (Vitrogen®) also exhibited the fibroblast-like morphology consistent with the TCP epithelial cell growth. Although these were only qualitative comparisons, the morphology of normal epithelial cells was more like that grown on composite hydrogels than on these comparison substrates.

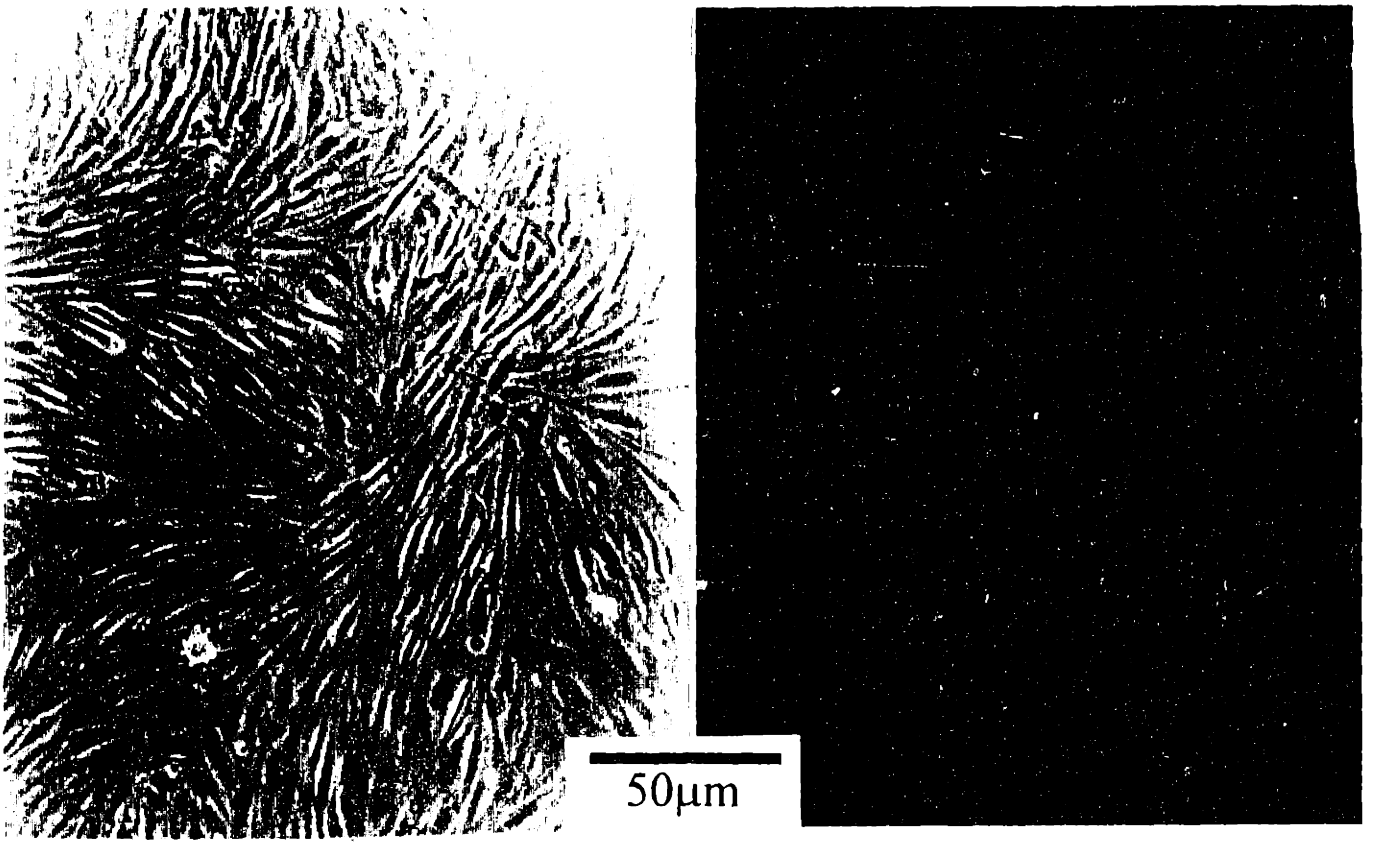

Figure 4.20: Comparison of Epithelial Growth on Different Substrates

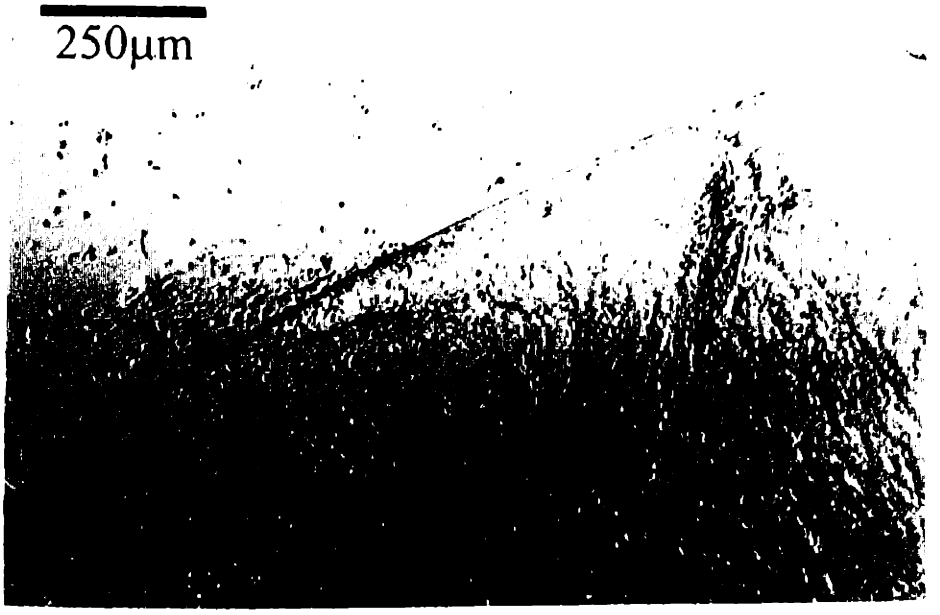

Figure 4.21: Epithelial Growth on Vitrogen Coated HEMA hydrogels

4.5 Summary of Biocompatibility Studies

Bilayer composite hydrogels appeared to provide a suitable stable substrate for growth of corneal epithelial cells. Other investigators have also noted the enhanced growth of epithelium on connective tissue coated synthetic materials.[34] Much attention has been placed on the ability of hydrogels to permit normal physiological solute flux in a corneal prosthesis. An in vitro ocular system designed to elucidate limitations in nutrient mass transport was developed and tested. Epithelial cell functioning in this system was used as an index of biocompatibility in relation to sufficient solute transport. The experimental results confirmed that it was possible to compromise epithelial wound healing by introducing mass transport limitations within the corneal environment. A theoretical model was developed to relate the cell behavior to non-steady state diffusion of solutes within a hydrogel corneal prosthesis. Theortical predictions of wound healing trends correlate well with experimental in vitro healing results. The model also indicated that the kinetics of epithelial wound healing was compromised by a larger solute than glucose. More qualitative measures of cell function indicated that epithelial cells grown on composite hydrogels were morphologically similar to those in vivo. After wound healing (migration), in vitro growth demostrated multilayered epithelium formation and deposition of basement membrane proteins. In general, composite hydrogels provided adequate support for growth of corneal epithelial cells. The model for epithelial wound healing has been expanded in the next chapter to establish some design criteria.

Chapter 4 References

[1] E.W. Merrill and Edwin Salzman. Polyethylene Oxide as a Biomaterial. In American Society for Artificial Internal Organs. 1983, 6(2), pp60-64

[2] E.W. Merrill, E.W. Salzman, K.A. Dennison, S-W Tay, and R.W. Pekala. Nonadsorptive Hydrogels for Blood Contact. Progress in Artificial Organs. ISAO Press, Cleveland,1986 pp 909-912

[3] R. Sipehia, A Garfinkle, W.B. Jackson, and T.M.S. Chang. Towards an Artificial Cornea: Surface Modifications of Optically Clear, Oxygen Permeable Soft Contact Lens Materials by Ammonia Plasma Modification Technique for the Enhanced Attachment and Growth of Corneal Epithelial Cells. In Biomat., Art., Cells, and Art. Org., 1990, 18(5), pp 643-655

[4] K.P. Thompson et al. Current Status of Synthetic Epikeratoplasty. Refractive and Corneal Surgery. May/June 1991. Vol 7, pp. 240-248

[5] K. S. Stenn and L. Depalma. Chapter 14: Re-epithelialization. in The Molecular and Cellular Biology of Wound Repair. edited by R.A.F. Clark and P.M. Henson, Plenum Press, New York and London, pp 321-353

[6] Frederick S. Brightbill (editor). Corneal Surgery - Theory, Technique, and Tissue, Chapter 31. C.V. Mosby Co., 1986.

[7] D. M. Maurice. Chapter 1: The Cornea and Sclera. in The Eye, Vol 1B, Davson H, editor. Florida, 1984, Academic Press, pp 1-158L.

[8] S. D. Klyce and R. W. Beuerman. Chapter 1: Structure and Function of the Cornea. The Cornea, pp. 3-54

[9] A. McNicol and E. Strahlman. Corneal Biomechanics and Wound Healing. Proceedings from the Workshop on Corneal Biophysics I. National Eye Institute, Bethesda, MD 1989, pp 161-194

[10] S. J. Simmons, M. M. Jumblatt, and A. H. Neufeld. Corneal Epithelial Wound Closure: an in Vitro Model of Ocular Irritancy. Toxicology and Applied Pharmacology, 1987, Vol. 88, pp 13-23

[11] J. Fantani, et al. Suramin-treated HT29-D4 cells grow in presence of glucose in permeable culture chambers from electrically active epithelial monolayers. A comparative study with HT29-D4 cells grown in the absence of glucose. European Jounal of Cell Biology. 1990, Vol 51, pp 110-119

[12] W. M. Minuth, G. Stockl, S Kloth, R. Dermietzel. Construction of an apparatus for perfusion cell cultures which enables in vitro experiments under organotypic conditions. European Jounal of Cell Biology. 1992, Vol 57, pp 132-137

[13] I. J. Hidalgo, K.M. Hillgreen, G. M. Grass, and R. T. Borchardt. A New Side-By-Side Diffusion Cell for Studying Transport Across Epithelial Cell Monolayers. In Vitro Cell. Dev. Biol. Sept-Oct 1992, 28A: pp 578-580

[14] D. L. Tanelian and K. Bisla. A New In Vitro Corneal Preparation to Study Epitelial Wound Healing. Investigative Ophthalmology and Visual Science, Vol. 33, No. 11, Oct 1992, pp 3024-3029

[15] H Kobayashi et al. Collagen-Immobililized Hydrogel as a Material for Lamellar Keratoplasty. Journal of Applied Biomaterials. 1991, Vol 2, pp 261-267

[16] R. Jeyanthi and K. Panduranga Rao. In vivo biocompatibility of collagen-poly(hydroxyethyl methacrylate) hydrogels. 1990, Biomaterials, Vol. 11, pp 238-243

[17] M. B. Moore, B. M. Gebhardt, S. M. Verity, and M. B. McDonald. Fate of Lyophilized Xenogeneic Corneal Lenticules in Intrastromal Implantation and Epikeratophakia. Investigative Ophthalmology and Visual Science. 1987, Vol 28, pp 555-559

[18] Ray P. Galitis et al. Laser Welding of Synthetic Epikeratoplasty Lenticules to the Cornea. Refractive and Corneal Surgery. Nov/Dec 1990, Vol 6, pp 430-436

[19] S. Amudeswari et al. Short-term biocompatibility studies of hydrogel-grafted collagen copolymers. Journal of Biomedical Materials Research. 1986, Vol. 20, pp 1103-1109

[20] D. K. Pettit et al. Quantitation of Rabbit Corneal Epithelial Cell Outgrowth. Investigative Ophthalmology and Visual Science. Nov 10, Vol 31, No. 11, pp. 2269-2277

[21] T Nishida et al. Fibronectin Promotes Epithelial Migration of Cultured Cornea In Situ. The Joural of Cell Biology. Nov 1983. Vol 97. pp 1653-1657

[22] Committee on Animals in Research. Handbook on the Use of Animals in Biomedical Research. The Association for Research in Vision and Ophthalmology, Inc., Copyright 1990, pp. 1-15

[23] Kwan Y. Chan, Dorothy L. Patton, Yvonne T. Cosgrove. Time-Lapse Videomicroscopic Study of In Vitro Wound Closure in Rabbit Corneal Cells. *Investigative Ophthalmology and Visual Science*, Vol. 30, No. 12, Dec 1989, pp 2488-2498

[24] Maria B. Grant et al. Effects of Epidermal Growth Factor, Fibroblast Growth Factor, and Transforming Growth Factor-β on Corneal Cell Chemotaxis. *Investigative Ophthalmology and Visual Science*, Vol. 33, No. 12, Nov 1992, pp 3292-3301

[25] J. Crank. The Mathematics of Diffusion (2nd Ed.). Copyright Oxford University Press, Inc. 1975

[26] B. E. McCarey ad H. E. Kaufman. Improved Corneal Storage. Investigative Ophthalmology and Visual Science. March 1974, Vol. 13, No. 3, pp. 165-173

[27] Y Ando, G. S. Lazarus, and P. J. Jenson. Activation of Protein Kinase C Inhibits Human Keratinocyte Migration. Journal of Cellular Physiology. 1993, Vol 156, pp 487-496

[28] D. K. Olivero and L.T. Furcht. Type IV Collagen, Laminin, and Fibronectin Promote the Adhesion and Migration of Rabbit Lens Epithelial Cells In Vitro. Investigative Ophthalmology and Visual Science. September 1993, Vol 34, No. 10, pp. 2825-2834

[29] Y. Sarret et al. Human Keratinocyte Locomotion: The Effect of Selected Cytokines. Journal of Invest. Dermatol. 1992, Vol 98. pp 12-16

[30] D. T. Azar et al . Reassembly of Corneal Epithelial Adhesion Structures following Human Epikeratoplasty. Arch Ophthal. September 1991. Vol 109. pp 1279-1284

[31] M. H. Friedlander et al. Keratophakia Using Preserved Lenticules. Ophthalmology. 1980, Vol. 87, pp 687-692

[32] Committee on Ophthalmic Procedures Assessment. Epikeratoplasty. Ophthalmology, Sept. 1990, Vol. 97, No. 9, pp. 1225-1231

[33] Harry S. Geggel, Judith Friend, Richard A. Thoft. Collagen Gel for Ocular Surface. In *Investigative Ophthalmology and Visual Science*. 1985, 26(6), pp901-905

[34] B Chehroudi, T. R. L. Gould and D. M. Brunette. The role of connective tissue in inhibiting epithelial downgrowth on titanium-coated percutaneous implants. Journal of Biomedical Materials Research. (1992), Vol. 26, pp493-515

Chapter 5

Physiologic Based Design

Up to this point this thesis has focused on the development and analysis of a particular corneal prosthesis. This chapter summarizes the information gathered from previous chapters and incorporates the results into some theoretical design criteria. In fact, a number of different corneal hydrogel prosthesis[1,2,3,4,5,6,7] formulations are currently being proposed and evaluated by other laboratories. The criteria outlined here can be adapted to predict the clinical performance of those devices. The implications of device geometry and material transport characteristics will be examined in terms of optical correction (for refractive surgery), epithelial wound healing, and nutrient homeostasis. Lastly some evaluations on the surgical performance of a bilayer hydrogel corneal prosthesis will be made.

5.1 Prosthesis Design based on Optical Correction

For therapeutic intervention, most of the entire thickness of the cornea must be replaced. Thus the implant thickness in this case should be at least (*~500μm*). For optical intervention, an onlay prosthesis also mandates a thickness requirement based on achieving a proper outer curvature. The spherical curvature of the human cornea is approximately *7.5 mm* in radius. Refractive surgery requires that postoperative correction be $\pm$ *6.0 diopters.* As illustrated in figure 5.1 below, the outer curvature of the eye is primarily responsible for the power of magnification to the cornea due to the significant change in the index of refraction between the cornea and air. This relationship is shown mathematically in equation 5.1 below:[8]

$$D = \frac{n_1 - n_2}{r} \tag{5.1}$$

Where, D = Magnification (diopters) [=] m^{-1}
n = index of refraction
r = radius of curvature [=] m

To determine the requisite amount of curvature change necessary to accomplish a 6 diopter change in refraction, the derivative of equation 5.1 can be taken as an approximation.

$$\frac{dD}{dr} = \frac{n_2 - n_1}{r^2} \approx \frac{\Delta D}{\Delta r} \tag{5.2}$$

Substituting values for dioptric change (*0.006 mm^{-1}*), corneal radius (*7.5mm*), and index of refraction change, a necessary radius change of *0.925mm* is calculated.

$$\Delta r \approx \frac{(7.5)^2}{0.413} \cdot 0.006 = 0.925mm$$

For myopic correction, the thickest section of an onlay prosthesis is at the edge as shown in Figure 5.1. Approximately, the central 4 mm of the of cornea is used to focus images.[9] Based upon this *4 mm* diameter window and the radii r_1 and r_2, the angles $\theta_1$and θ_2 can be determined and inserted into equation 5.3. This relation describes the edge thickness of a lenticule designed to correct myopia.

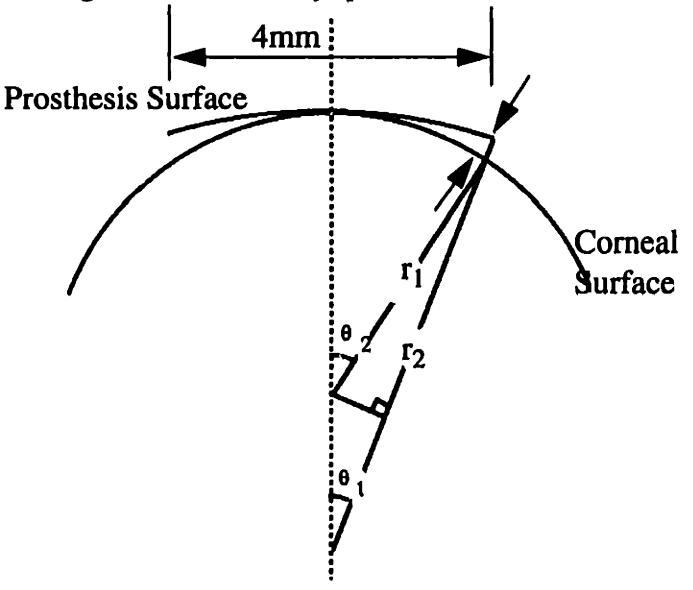

Figure 5.1: Myopic Correction for Prosthetic Corneal Onlay

$$L^2 = 2r_1^2(1-\cos\theta_1) + 2r_2^2(1-\cos\theta_2) \\ -2r_1r_2(1+\cos(\theta_1-\theta_2) - \cos\theta_1 - \cos\theta_2) \tag{5.3}$$

Where,

L = thickness of lens [=] m
r_1 = radius of curvature of lens [=] m
r_2 = radius of curvature of eye [=] m
θ_1= angle from vertex of lens
θ_2 = angle from vertex of eye

The edge thickness for these parameters indicates that thickest portion of the hydrogel prosthesis must be at least *266μm* to achieve a refractive correction of *6 diopters*. This information is useful in assessing whether physiological allowable thicknesses for hydrogels are satisfactory for maximum surgical refractive interventions.

5.2 Prosthesis Design based on Epithelial Wound Closure

In vitro wound healing was analyzed in Chapter 4. This theoretical analysis of epithelial wound closure was derived to reflect diffusion limitations for a protein factor which stimulates migration. The non-dimensional relation governing this situation is presented below in equation 4.7

$$\theta = 1 + \phi\tau - \left(\frac{16\phi}{\pi^3}\right)\left(\sum_{n=0}^{\infty}\frac{(-1)^n}{(2n+1)^3}\left(1-exp\left(\frac{-(2n+1)^2\pi^2\tau}{4}\right)\right)\right) \tag{4.7}$$

Where:

$\phi = \dfrac{hC_oL^2}{R_oD} \equiv$ Dimensionless Healing Efficacy

$\theta = \dfrac{R}{R_o} \equiv$ Dimensionless Wound Radius

$\tau = \dfrac{tD}{L^2} \equiv$ Dimensionless Time

L = Thickness of the membrane [=] cm

C_o = Concentration of migration factor [=] mg/cm^3
t = Time [=] sec
D = Diffusivity of factor in the membrane [=] cm^2/sec
R = Wound Radius [=] cm
h = ratio of migration rate:concentration of factor
[=] cm^4/(gm·hr)

The *in vitro* experiments performed on composite hydrogels led to the development of this analytical expression. In contrast to the well defined *in vitro* conditions, the actual healing rates were higher than those exhibited *in vivo*. The *in vitro* experiments were designed to demonstrate a diffusion limited compromise in healing rates. In reality, the thicknesses of the hydrogels were substantially larger than would be employed in vivo. Because of its non-dimensional character, this analysis can be used to make design specifications for a hydrogel corneal prosthesis destined for in vivo use.

The sufficient transport of a migration factor is the basis of assessing corneal prosthesis design parameters with respect to establishing wound healing criteria. The dimensionless group (Φ) describes the health of the system in terms of mass transport properties and the biological demands of healing epithelium. The proportionality (h) which relates healing rate to concentration of factor is determined from the observable linear migration rate. There is no need to directly measure the concentration of the possible factors: bFGF, EGF, etc., because the product of factor concentration and (h) is equal to basal migration rate. The derivation of the short term healing equation is based on an assumption that the migration (dR/dt) is proportional the concentration of a factor (C).

$$h = \frac{\frac{dR}{dt}}{C} \tag{5.4}$$

The quantity (hC_o) is readily assessable by determining the linear healing rate in the absence of a hydrogel. This is simply the normal epithelial healing rate and is easily observed clinically.

$$(hC_o) = \frac{dR}{dt}_{Normal} \tag{5.5}$$

The normal in vivo epithelial healing rate, $\frac{dR}{dt}$, is *0.05 mm/hr.*[10,11] The size of a prosthetic lenticule must provide a window no less than *3.0 mm* in diameter, which is the actual area of the cornea used for sight. Radial keratotomy operations usually provide a *4.0 mm* diameter optical zone. Therefore, an initial wound radius (R_o) of *2.0 mm* is used as a worst case scenario criterion. Diffusivity of proteins within hydrogels can vary widely leading to a varied range of permeabilities. In addition to PEO as a potential hydrogel material, many other synthetic hydrogel material may be used as the base. In order to compare these materials directly, albumin diffusivities were tabulated with some common hydrogel materials.

In order to make an assessment of allowable hydrogel thickness for these potential materials, some limiting time for healing must be chosen. Arbitrarily, this analysis assumed a *10%* increase in time to heal, and was an estimate of the error in measurement for normal epithelial migration rates. For a *10%* increase in time to heal, Φ is approximately equal to *0.25*. The maximum hydrogel thickness was calculated below:

$$\Phi = \frac{hC_o L^2}{R_o D} \tag{5.6}$$

$$0.25 = \frac{0.05\frac{mm}{hr} \cdot L^2}{2.0mm \cdot D} \tag{5.7}$$

$$3.16hr^{\frac{1}{2}}\sqrt{D} = L \tag{5.8}$$

Table 5.1 shows the allowable thicknesses of corneal prosthetic lenticules for different materials:

Table 5.1: Design Specifications based on Epithelial Healing

Material	Albumin Diffusivity (cm^2/sec)	Allowable Thickness (microns)
Corneal Tissue[12]	$1.125x10^{-7}$	636
PEO (2%)[13]	$3.6x10^{-9}$	114
PEO (8%)[13]	$1.5x10^{-11}$	7
PVA (9%)[14]	$1.8x10^{-8}$	254
pHEMA (80%)[15]	~0	*not feasible*

On average, proteins have diffusivities in water on the order of $1x10^{-6}$ cm^2/sec and hydrogels further reduce the diffusivity of proteins by 1- 2 orders of magnitude. Therefore, allowable hydrogel thicknesses on the *order of ~100* μm are within the dimensions necessary to achieve refractive correction. If these criteria derived from early wound healing are imposed in this design, then hydrogel materials such as high polymer content pHEMA pose problems because of their poor protein transport properties.

Accelerated healing by exogenous delivery of a healing (migration) promotion factor has yet to be addressed in this assessment. Hypothetically, it should be possible to load a poorly transporting hydrogel with a postulated healing factor such as bovine pituitary extract.[16] Alternatively, delivery of healing factors could be accomplished by using degradable bandage contact lenses loaded with healing factors or other topical application. Thus, materials with low protein diffusivities can theoretically be utilized if one or more of the above strategies is employed.

5.3 Prosthesis Design Based on Long term Nutrient Homeostasis

This section addresses the assessment of the physical limitations of a hydrogel prosthesis based on nutrient homeostasis. The information on glucose transport across hydrogels was of primary importance in this analysis. The introduction of a barrier to diffusion of nutrients through the cornea has been known to cause tissue loss anterior to the implant.[17,18,19,20] Of particular concern is the loss of complete epithelial integrity by necrosis of the epithelial layers. In order to use the information that describes the mass transport properties of the hydrogel, measures to assess the effects of transport properties on metabolic homeostasis must be formulated.

The analysis of heterogenous reaction kinetics in catalysis[21] provides well established methods for assessing the effectiveness of reaction systems limited by mass transport. In heterogeneous reactions, gradients in concentration which exist between the "source" and "sink" can have significant effects on the overall kinetics of the reaction. The analysis of external (interphase) gradients can quantitatively define an effectiveness factor (η) that is based on the tissue metabolism combined with the geometric and mass transport parameters of an implant.

The figure below depicts two regions of the cornea--prosthesis scenario with a concentration profile of reactant superimposed over these two regions. The interphase region is inert while the intraphase region is converting reactant to product. The intraphase region is the reactive interface, which in this case is the multilayered epithelium. It is assumed that

intraphase limitations are negligible in light of the facilitated diffusion[22] of glucose within epithelium.

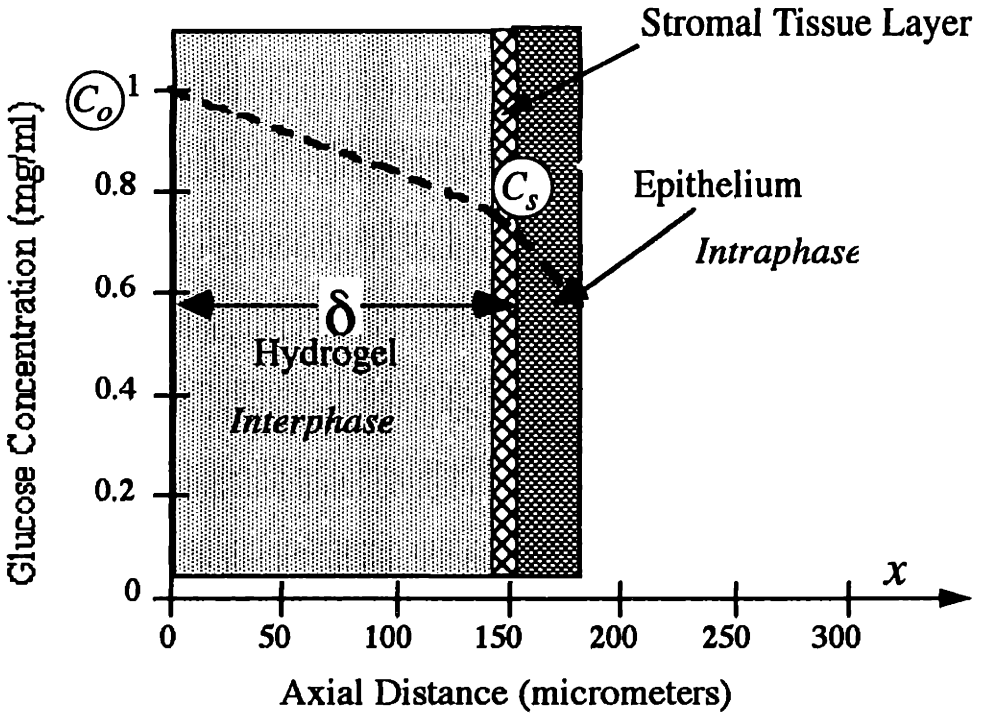

Figure 5.2: Profile of Glucose Concentration in Implanted Corneal Prosthesis

The epithelium can be considered to be a reactive interface which metabolizes glucose. For long term biocompatibility, the system can be considered to be at steady state. At the epithelial--hydrogel interface, the metabolism of glucose equals the diffusive flux:

$$D\frac{dC}{dx}\bigg|_{x=\delta} = DK_p \cdot \frac{C_O - C_S}{\delta} \quad \text{(Diffusion of Glucose through Hydrogel)} \qquad (5.9)$$

Where,

D = Diffusivity of Hydrogel Prosthesis [=] cm^2/sec
K_p = Partition Coefficient
C_O = Glucose Concentration entering Hydrogel [=] gm/cc
C_S = Glucose Concentration at Epithelium interface[=] gm/cc
δ= Thickness of Hydrogel Prosthesis

$$\frac{dC}{dt} = k_o x C_S \qquad \text{(Metabolism of Glucose)} \tag{5.10}$$

Where,

k_o = Reaction rate constant for epithelial glucose consumption
[=] $\frac{\text{cm}}{\text{sec·cell-layer}}$
x = Number of epithelial cell layers over implant
C_S = Glucose Concentration at Epithelium interface[=] gm/cc
C = Glucose Concentration [=] gm/cc
t = time [=] sec

After algebraic manipulation, the concentration of nutrient (glucose) at the epithelial--prosthesis interface is described by equation 5.11:

$$C_S = \frac{C_O}{\frac{k_O x \delta}{DK_n} + 1} \tag{5.11}$$

The consumption of glucose in the absence of a hydrogel prosthesis can be assumed to an optimal rate or flux of glucose to the epithelium (R_o). In the presence of a hydrogel prosthesis, the actual rate of glucose metabolism (R) is limited by the concentration of glucose at the epithelium. Considering catalyst particle reaction rate analysis, an effectiveness of this situation can be determined by a ratio of reaction rates.

$$\text{Efficiency} = \eta = \frac{R}{R_O} = \frac{k_O x C_S}{k_O x C_O} = \frac{1}{\frac{k_O x \delta}{DK_n} + 1} \tag{5.12}$$

This value $\left(\frac{k_O x \delta}{DK_n}\right)$ is actually a dimensionless group, the Dämkohler number (Da), that characterizes an intraphase limited system. Da expresses the ratio of chemical reaction velocity to mass transport velocity. The effectiveness factor (η) expresses at what fraction (of the optimum performance) a system is operating. In this case the intraphase

limited system is the epithelium and hydrogel prosthesis. Figure 5.3 is a graphical representation of the effectiveness factor (η) which is derived for a first order system (epithelium). Of course, with no hydrogel in place in the normal anatomic arrangement the effectiveness will be 1.0. If we assume that a 10% decrease in function is tolerable, some estimates of prosthesis thickness can be ascertained.

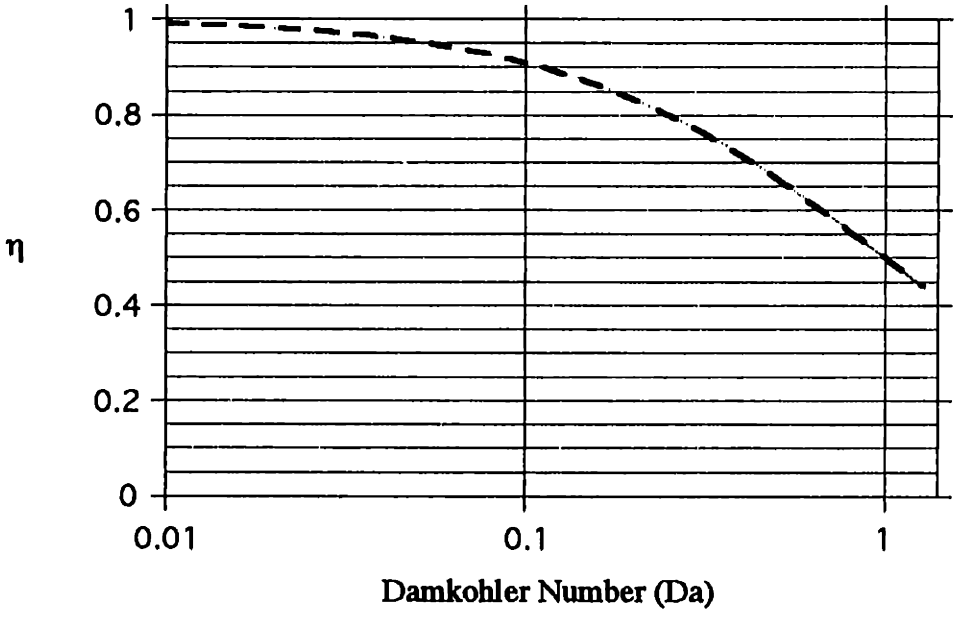

Figure 5.3: Efficiency of Intraphase Limited System

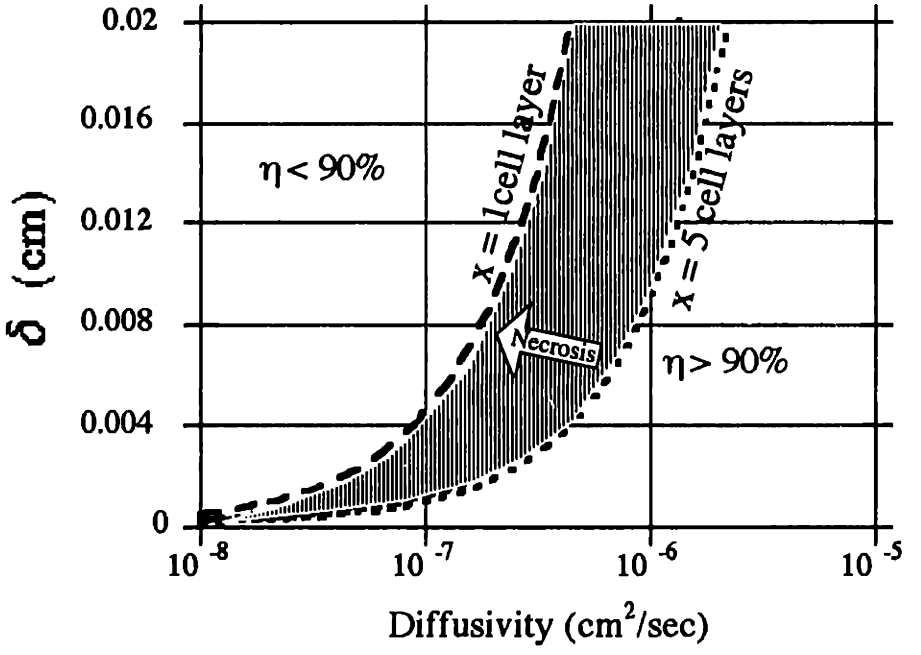

Figure 5.4: Hydrogel Thickness based on Hydrogel Diffusivity

Hydrogel thickness (δ) can now be related to a limitation in apparent nutrient diffusivity (DK_p). In the case of corneal epithelium, the number of cell layers (x) is normally *5*. Published experimental results indicate that the first order glucose metabolism rate constant[23] (k_o) for a single layer of cells is $2.315x10^{-6}\frac{cm}{sec\,celllayer}$. Figure 5.4 displays the hydrogel thickness versus glucose diffusivity within the hydrogel prosthesis. Based on maintaining a 90% effectiveness, two limiting scenarios are shown in Figure 5.4: $x = 1$ cell layer situation and a normal $x = 5$ cell layer situation.

5.3.1 Relevance to Long term Biocompatibility

This theoretical development is derived for a system at steady state after short term healing and multilayered epithelium regeneration. After wound closure, maintenance of a multilayered epithelium ($x > 1$) can be compromised by limited nutrient diffusion. The amount of glucose reaching the outermost epithelial cells may be so small as to cause cell atrophy and death (necrosis). Interestingly, the physiological outer layer cell necrosis has

the potential to improve the metabolism of the overall system. If the number of cell layers decreases, the total metabolic requirements of the system characterized by the rate constant ($k_o x$) will decrease and the overall system will be operating at a lower *Da* (higher effectiveness). It is well documented that the epithelium does thin and erode over the central area of impermeable corneal implants. Using this analysis, it is possible to quantitatively understand this long term tissue thinning over implants and make design criteria based on metabolic requirements.

To evaluate and establish design parameters for composite hydrogel corneal prostheses, a defined thickness of corneal stroma must be set. The diffusion of glucose in corneal stroma[12] has been determined to be $2.47\text{-}3.0 \times 10^{-6}\ cm^2/sec$. As mentioned in Chapter 2, stromal layers can be sectioned in the range from *5-100 μm*. This layer is a "surface" layer and as such can be adequately set at a thickness of *20μm*. The diffusional resistance to steady state glucose flux can be characterized by ($\delta/D \cdot K_p$). For the corneal stromal layer, the value of this diffusional resistance is *667 sec/cm*. Again, taking an estimate of 10% compromise in function to maintain an epithelium of 5 cell layers a limiting thickness of hydrogel portion can be determined.

$$k_o x\left(\sum \frac{\delta}{DK_p}\right) \approx 0.1 \qquad (for\ \eta = 90\%) \tag{5.13}$$

$$\left(\frac{\delta}{DK_p}\right)_{Hydrogel} + \underbrace{\left(\frac{\delta}{DK_p}\right)_{Stroma}}_{667\ sec/cm} \approx 8639 \quad \frac{sec}{cm} \tag{5.14}$$

$$\left(\frac{\delta}{DK_p}\right)_{Hydrogel} = 7972 \quad \frac{sec}{cm} \tag{5.15}$$

From the analysis above, a *20 μm* layer of stroma only results in 7.69% of the defined acceptable diffusional resistance to glucose through a bilayer composite hydrogel prosthesis. The remaining acceptable diffusional resistance establishes the criteria for thicknesses of the synthetic hydrogel portion of the composite. Table 5.1 lists these theoretical maximum hydrogel thicknesses.

Table 5.1: Design Specifications based on Nutrient Homeostasis

Hydrogel Material	**Apparent Diffusivity D·Kp (cm^2/sec)**	**Thickness - δ (microns)**
PEO (2%)	6.7×10^{-6}	*534*
PEO (8%)	6.5×10^{-6}	*518*
HEMA (61.5%)	5.30×10^{-8}	*4.22*
HEMA (21.0%)	1.17×10^{-6}	*93*

Hydrogels that have apparent diffusivities on the order of 1.0×10^{-6} cm^2/sec can theoretically accommodate the necessary glucose homeostasis while remaining thick enough to provide for optical refraction. In particular PEO hydrogels appear to be more than adequate in their ability to accommodate nutrient homeostasis in this physiologic scenario.

Chapter 5 References

[1] Yoichi Minami, Hamime Sugihara, and Shinji Oono. Reconstruction of Cornea in Three-Dimensional Collagen Gel Matrix Culture. In *Investigative Ophthalmology & Visual Science*, 1993; 34: pp 2316-2324

[2] Bernard E. McCarey. Refractive Keratoplasty with Synthetic Lens Implants. In *Refractive and Corneal Surgery*, 1990;6: pp 40-45

[3] H. Nakao et al. Formation of a Hybrid Epithelial and Stromal Tisses and Hierarchically Structured Keratoprosthesis. Investigative Ophthalmology and Visual Science. Vol 34, No. 4, p 1088

[4] S. Nakada et al. Newly Developed Collagen Disk for Substitute Cornea. Investigative Ophthalmology and Visual Science. Vol 34, No. 4, p 1088

[5] H Kobayashi et al. Collagen-Immobililized Hydrogel as a Material for Lamellar Keratoplasty. Journal of Applied Biomaterials. 1991, Vol 2, pp 261-267

[6] R. Sipehia, A Garfinkle, W.B. Jackson, and T.M.S. Chang. Towards an Artificial Cornea: Surface Modifications of Optically Clear, Oxygen Permeable Soft Contact Lens Materials by Ammonia Plasma Modification Technique for the Enhanced Attachment and Growth of Corneal Epithelial Cells. In Biomat., Art., Cells, and Art. Org., 1990, 18(5), pp 643-655

[7] Thomas C. White. Corneal Implant. United States Patent. Pat No. 5,030,230, Jul. 9, 1991

[8] Mitchell A. Watsky, Bernard E. McCarey, and W. Houdjin Beekhius. Predicting Refractive Alterations with Hydrogel Keratophakia. In *Investigative Ophthalmology & Visual Science*, 1985, 26: pp 240-243

[9] George O. Waring III. *Refractive Keratotomy for myopia and astigmatism*, Chapter 4. Mosby-Year Book Inc., 1992

[10] S. J. Simmons, M. M. Jumblatt, and A. H. Neufeld. Corneal Epithelial Wound Closure: an in Vitro Model of Ocular Irritancy. Toxicology and Applied Pharmacology, 1987, Vol. 88, pp 13-23

[11] M. Matsuda, J. L. Ubels, H. F. Edelhauser. Kinetics of Corneal Wound Healing. Chapter 42 in Corneal Surgery - Theory, Tissue, and Technique, F. S. Brightbill (editor) C. V. Mosby Co., 1986. pp 603-612

[12] D. M. Maurice. Chapter 1: The Cornea and Sclera. in The Eye, Vol 1B, Davson H, editor. Florida, 1984, Academic Press, pp 1-158

[13] E. W. Merrill, Kathleen A. Dennison, and Cynthia Sung. Partitioning and Diffusion of Solutes in Hydrogels of Poly(Ethylene Oxide). Biomaterials 1994

[14] C. T. Reinhart and N. A. Peppas. Solute diffusion in swollen membranes. Part II. Influence of crosslinking on diffusive properties. Journal of Membrane Science, 1984, Vol 18, pp 227-239

[15] S. Wisniewski and S. W. Kim. Permeation of Water-soluble Solutes Through Poly(2-Hydroxylethyl Methacrylate) and Poly(2-Hydroxylethyl Methacrylate) Crosslinked with Ethylene Glycol Dimethacrylate. Journal of Membrane Science, 6 (1980) pp 299-308

[16] Y. Sarret et al. Human Keratinocyte Locomotion: The Effect of Selected Cytokines. Journal of Invest. Dermatol. 1992, Vol 98. pp 12-16

[17] B. E. McCarey and F. H. Schmidt. Modeling glucose distribution in the cornea. Current Eye Research. 1990. Vol 9, No. 11, pp 1025-1039

[18] Bernard E. McCarey. Current Status of Refractive Surgery with Synthetic Intracorneal Lenses. Refractive and Corneal Surgery. Jan/Feb 1990, Vol 6, pp. 40-46

[19] Stuart L. Brown and Claes H.Dohlman. A Buried Corneal Implant Serving as a Barrier to Fluid. Archives of Ophthalmology, May 1965, Vol. 75, pp 635-639

[20] William F. Knowles. Effect of Intralamellar Plastic Membranes on Corneal Physiology.

[21] J. J. Carberry. Chemical and Catalytic Reaction Engineering. McGraw-Hill, Inc. Copyright 1976. pp 194-225

[22] Anthony Carruthers. Facilitated Diffusion of Glucose. *Physiological Reviews*, 1990 Vol 70 No 4: pp 1135-1176

[23] Christine A Zurawski, Bernard E. McCarey, and Frederick H. Schmidt. Glucose Consumption in Cultured Corneal Cells. *Current Eye Research*: 1989, Vol 8, No 4, pp 349-355

[24] J.G. Trump and R.W. Cloud. The Production and Characteristics of 3,000 Kilovolt Roentgen Rays. American Journal of Roentgenology and Radium Therapy: 1943 Vol XlIX, No 4, pp 531-535

[25] Hernando Cardona. Keratoprosthesis-Acrylic Optical Cylinder Supporting Intralamellar Plate. Ophthalmology, (1976), pp 284-299

[26] V. TrinkausiRandall, et al. In Vitro Evaluationof Fibroplasia in a Porous Polymer. In *Investigative Ophthalmology & Visual Science*, 1990, 31(7): pp 1321-1326

[27] V. Trinkaus-Randall, J. Capecchi, A. Newton, A. Vadasz, H. Leibowitz, and C. Franzblau. Development of a Biopolymeric Keratoprosthetic Material. In Investigative Ophthalmology and Visual Science. 1985, 29(3), pp 393-400

[28] B. E. McCarey and D. M. Andrews. Refractive Keratoplasty with Intrastromal Hydrogel Lenticular Implants. Investigative Ophthalmology and Visual Science. July 1981, Vol. 21, No. 1, pp. 107-115

Appendix A

Fluorescent Assay for Protein

Materials:

Acetone (100%)

Pure Water (>18 MegaOhm resistance)

Fluorescamine (0.05% in Acetone)
(Sigma Chem. Cat. No. F-9015)

Hydrolyzed Protein Standard (0.1 mg/ml)
(Boehringer Mannheim Cat. No. 238-040)

Oven (Capable of 110°C)10 N HCl
(35.5% wt/vol)

Fluorescent Spectrophotometer
(Perkin Elmer Mod. No. 510M)

Borosilicate glass scintillation vials (22/400 threads)

Autoclavable Caps (22mm)
(Baxter Products Cat. No. B7503-62)

Teflon Liners (.01" thick) 20.5 mm circular discs (No 13 cork borer)

Quartz Cuvette

Hand Bulb Aspirator

Disposable Polystyrene Pipettes-10ml

0.22 µm Bottletop Filter for Media Bottle-500ml

Stock Reagents

- Dissolve Fluorescamine (100mg) into 200 ml of 100% Acetone
  50 mg/100 (0.05%) Final Concentration
  Do not put the acetone over molecular sieve (It contaminates reagent)

- Dissolve 6.183g of H_2BO_3 (Boric Acid) into 500 ml of Pure water. Raise the ph of the solution to ph=10 with 50 % NaOH. Once the solution is at pH = 10.0, add 0.1 grams of Sodium Azide (NaN_3). Filter the solution with a 0.22 µm bottle top filter.

- Protein Solution Hydrolyzed
  Add 3 ml of HCl to 3 ml of .200mg/ml of protein (Albumin) Hydrolyze for hours in a borosilicate glass scintillation vial capped with a teflon lined autoclavable cap.

Directions for Protein Assay

01. Roughly determine how much of your sample corresponds to 24 µg total* .

02. Place this sample amount in a Pristine scintillation vial

03. Using a hand bulb aspirator, aliquot the following volume of 10 N HCl to the sample volume:

---

* Approximately 1 cell corresponds to 1 nanogram of Protein

- if sample is less that 1 ml ===> add 1 ml of HCl

- if sample is between 5 ml and 1 ml ===> add an equal volume of Hcl

- if sample is over 5 ml only use 5 ml of sample volume ===> add 5 ml of HCl

04. Cover the sample with autoclavable caps lined with 2 teflon liners.

05. Incubate at 110°C for at least 7 hours.

06. After incubation, uncover the vials and heat on a hot plate to evaporate the solution to dryness.

(this step should take 10-30 minutes)

07. Add 1ml of Flourescamine reagent in acetone.

08. Add 3 mls of 0.2 M Na_2BO_3 buffer.

09. Make 8 mls of blank by adding 2mls of Fluorescamine reagent to 6 mls of 0.2 M Na_2BO_3 buffer. You should now have the following amounts:
    - Blank (8 mls)
    - Standard (4 mls)
    - Samples (each 4 mls)

The sample should react for at least 15 minutes.

10. Turn on your fluorescent spectrophotometer. The spectrophotometer settings should be: (excitation = 390 nm, emmission = 475 nm)
11nm slit excitation slit, 11nm emission slit

11. Set up calibration standards using the following combinations:

Add this volume of the Blank Solution to===>	This volume of Standard Solution	New Concentration (percentage of standard)
1ml	333µl	25%
1ml	1ml	50%
333µl	1ml	75%
0	1ml	100%

12. Read the sample fluorescence in a quartz cuvette.

RECORD THE HIGHEST READING THAT OCCURS AFTER OPENING THE EXCITATION SLIT. The sample continuously decreases in flourescence due to quenching.

Appendix B

Protocol for Corneal Tissue Acquisition

INSTRUCTIONS

1. If this is a proposal for a teaching exercise, complete sections I, VIII, IX and pages 10-13 of the Supplement.
2. Please type or print clearly in black ink. When possible, use simple terms that will be clear to reviewers without science background.
3. Please do not substitute reprints or attach copies of other printed materials in lieu of explanation in each section.
4. Scan all questions before answering.
5. Answer all questions in Sections I through VIII or indicate "N/A" where not applicable. Complete appropriate details for specific procedures in The Supplement.

I. GENERAL INFORMATION

A. Laboratory Head* (Instructor): Linda G. Cima Dept. Chemical Engineering

B. Contact person for this proposal: Edward Perez

Address: 66-525n Office Ext: 3-6443 Lab Ext: 3-6443 Home Phone: 876-4278

C. Other personnel involved: _____

D. Title of Research (Teaching) Proposal: Composite Hydrogels for Corneal Epithelial Cell Growth

E. Will any aspect of the experimental study (course) or animal husbandry be conducted at another institution? Yes___ No XXX.

If Yes, where? _____

Was the proposal approved by the IACUC of that institution? Yes___ No___. If Yes, please attach the IACUC approval notification.

***This person will be considered Principal Investigator or responsible person at MIT.**

II. FUNDING INFORMATION

A. Funding agency*: Pending Grant No. _____

If verification of approval is required, indicate address of contact person at granting agency:

Name: _____ Address: _____

City: _____ State: _____ Zip: _____

B. Grant Submitted: ___/___/___ Renewal? Yes___ No___

Grant Begins: ___/___/___ Ends: ___/___/___.

C. Institution receiving funding: _____

D. Does the information in this form agree with the animal use section of the grant application (Section F for NIH Grants)? Yes___ No___.

***If funding grant has not been submitted, enter pending.**

III. SUMMARY OF RESEARCH

A. Write a brief description of the purpose and goals (use lay terms).

The purpose of this research is to develop materials that can used to replace diseased corneal tissue. The goals of the work involving this protocol are to: (1) create thin (1-10 micron) surfaces of corneal stroma bound to hydrogel supports, (2) To characterize the nature and extent of the bonding of corneal tissue and hydrogel during synthesis, (3) Use the corneal tissue coated hydrogels as substrate for epithelial cell growth.

B Which of the following best describes the proposed work*: (please check all applicable numbers)

1.[ ] Requires painful or stressful procedure(s)
2.[ ] Requires survival surgery
3.[ ] Requires witholding food/water for training
4.[ ] Requires a method of euthanasia not approved by the Guide
5.[ ] Requires restraint for more than 15 minutes
6.[ ] Requires multiple minor procedures under anesthesia
7.[X] Requires a single, non-survival procedure
8.[ ] Requires species other than primates, dogs, cats domestic or farm animals
9.[ ] Requires procedures which cannot be undertaken in humans or in vitro.

***If you checked one or more of the statements in B1-5 above, make sure you complete the narrative description as requested in Section VIII, page 8.**

C. Research applicability.
This research is applicable to which of the following (please specify which diseases, agents, or scientific basic areas will benefit from this research)

1.[XX] Human disease(s) Corneal scarring, Intractable Corneal Disease
2.[ ] Animal disease(s)
3.[ ] Testing for toxicity or oncogenicity
4.[ ] Basic research without clinical application

D. Research intention:

1.[XX] Provision of new data
2.[ ] Confirmation of existing data (please see Section VII, page 8)

Protocol No._____

SUMMARY OF RESEARCH, continued

E. Have results fulfilling the experimental goals of this research been published? Yes___ No__x__.

1. If "Yes", provide details explaining why the experiment requires repetition:_____

2. If "No, indicate whether you have undertaken sufficient review of published literature and all other available sources of research information tc be certain that the proposed work is not an unnecessary repetition:

I have reviewed the literature through computerized literature searchesand review of the major opthalmologic journals covering the past year.
The computerized MEDLINE data base reviealed no research dealing with synthetic materials used in combination with presearved conneal tissue to construct biocompatible surfaces. No research has been published in IOVS, Current Eey Research. Archives of Ophthalmology, Cornea, or Ophthalmology which detail use of preserved conneal tissue to modify existing synthetic surfaces.
One lecture presentation at the the Boston Connea Conventi n in 1991, illustrated the used of glutaradehyde fixed corneal tissuefor use on a conneal prosthesis, but this work proved to be not efficacious It did not suceed

F. Has this research been subjected to peer review? Yes XX No
If Yes, by what authority/agency? National INst. of General Medical Sciences
If No, please attach Department Head's approval
(If the PI is the Department Head, please provide approval from a knowledgeable person outside the Department.)

Protocol No. [redacted]

IV. RATIONALE FOR SPECIES AND NUMBERS

A. Animal species to be used (indicate strain when appropriate)
New Zealand White
a: Rabbits b:_____ c:_____ d:_____

B. Estimated required number of each species:
First Year a: 20 b:_____ c:_____ d:_____
Second Year a: 20 b:_____ c:_____ d:_____
Third Year a: 20 b:_____ c:_____ d:_____

C. Appropriateness of the species
1. Species selected because the process resembles that in humans?
a: XX b:_____ c:_____ d:_____

2. Species selected because it has been used in prior research.
a: XX b:_____ c:_____ d:_____

3. Species selected because tissues or other substances harvested require quantities necessitating an animal of its size.
a: XX b:_____ c:_____ d:_____

4 Species selected because the anatomy or physiology is best or uniquely suited to the procedures to be performed?
a: XX b:_____ c:_____ d:_____

5. Other:_____

D. Appropriateness of the numbers
1. Statistical significance can only be achieved by the numbers requested. a:_____ b:_____ c:_____ d:_____
NA
2. Amount of material to be obtained requires the numbers requested. a: XX b:_____ c:_____ d:_____

3. Anticipated failure rate requires repetitive attempts to obtain valid data. a:_____ b:_____ c:_____ d:_____
Please explain NA

4. Have statistical analyses been applied to determine the least number of animals required? Yes___ No___ NA XX

5. Has the proposed research been designed to use a larger number of animals as a means of reducing the number of procedures on each animal? Yes___ No___ NA XX

Protocol No._____

V. INVESTIGATOR QUALIFICATIONS

A. Personnel

Last Name	Responsibilities and/or Procedures	Species
1. PEREZ, Edward P	Harvesting Corneal Tissue from Post-Mortem Animal Specimen	NZW Rabbit
2.		
3.		
4.		

B. Personnel Credentials*

Practical Training/Courses Taken	Species & Procedure Experience
1. MEEI Ophthalmic Surgery Research Beth Israel Hospital Ophthalmology	NZW Rabbit - Survival Corneal Surgery
2 Eyer Research INstitute	NZW Rabbit - Survival Corneal Surgery
3.	
4.	

C. Descripton of Anticipated Training*

	Date
1. MIT Training Course on Animal Care	Pending
2.	
3.	
4.	

***Certification of all personnel is required including students, technical staff, and principal investigators. Please call the CAC office for further information. Training or assistance in animal handling and research techniques may be obtained by calling the Division of Comparative Medicine at 253-1757.**

VI. GENERAL PROCEDURES continued

B. Which of these procedures have not been performed in this laboratory before? proceudres
None of these ~~XXXXXXXXXX~~ have been on the MIT Campus

C. Are any of these procedures considered pilot experiments?
Yes___ No XX. If Yes, which ones:_____

D. If restraints are needed, please describe method, frequency and duration of restraint. _____

E. Where will each of these procedures be performed? (Indicate building and room.)
MOst of the post mortem tissue harvest is to take place in animal housing facility in Builing 56-7th Floor

F. Will any animals survive after completion of procedures described in Section VIA? Yes___ No XX

1. If "Yes", which species _____
2. If "Yes", how long will they survive?_____
3. If "No", describe method of euthanasia, drug and dose
IV NaPentabarbital (40gr/animal)

G. If animals survive after completion of any of the procedures, will pain, suffering, and/or development of morbidity result? N/A
Yes___ No___

1. If "Yes", which procedures and what is the nature of the pain, suffering or new morbidity? _____

2. If "Yes" what are the frequency and duration of observations and the criteria for appropriate intervention? _____

3. If "Yes" what analgesic agents and methods including euthanasia are anticipated to prevent or relieve pain or suffering? (specify drug and dosage given)_____

VIII. HAZARDS AFFECTING ANIMALS, PERSONNEL, AND THE ENVIRONMENT

A. Are radionuclides to be used? Yes___ No X.
If Yes, please send Application to Use Hazardous Materials Form to M. Walke, DCM, 45-104.

B. Are biologically hazardous chemical and/or microbial agents to be used? Yes___ No X If Yes, please attach DCM Application to Use Hazardous Materials Form to M. Walke, DCM, 45-104.
Name of Agent(s)_____

C. Recombinant DNA
1. Are transgenic animals used in the experiment? Yes___ No X
If Yes, contact the Biohazard Assessment Office at 3-1740.
2. Does any part of the material being injected into the animal contain recombinant nucleic acid (RNA or DNA)? Yes___ No X
If Yes, contact the Biohazard Assessment Office at 3-1740.

D. If safety of animals and/or personnel may be compromised, is this reflected in your Departmental Safety Plan? Yes___ No___.

Information about safety and health measures such as immunizations and protection against explosion and fire is available through DCM, EMS, the Safety Office, and the Medical Department.

IX. SEE SUPPLEMENT TO COMPLETE DETAILS OF PROCEDURES. SELECT APPROPRIATE SECTIONS FROM THE FOLLOWING AND CIRCLE YOUR SELECTION:

A. Surgical Procedures
B. Immunization and Antibody Harvest
C. Tissue and Fluid Harvest (Non-Immunologic)
D. Chemical, Microbial, Physical Agent Administration
E. Tumor Induction (Other Than Hybridoma)
F. Device Implantation
G. Training and Behavioral Procedures
H. Teaching Proposal
I. Other Experimental Procedures

X. SIGNATURES:

Person preparing this form: Edward Perez Date 8/18/92

Laboratory Head/Instructor: Linda Date 8/18/92

PLEASE NOTE: *A SUBSTANTIAL CHANGE IN PROTOCOL, AN INCREASE IN THE NUMBER OF ANIMALS USED, A CHANGE IN THE ANIMAL SPECIES USED, OR A CHANGE OF PERSONNEL WILL NECESSITATE AN ADDENDUM TO OR RESUBMISSION OF THIS FORM. THE PRINCIPAL INVESTIGATOR MUST INDICATE APPROVAL FOR SUCH CHANGES BEFORE THEY WILL BE REVIEWED BY THE COMMITTEE.*

THE COMMITTEE ON ANIMAL CARE MEETS ON THE FIRST THURSDAY OF EVERY MONTH (EXCEPT AUGUST AND DECEMBER).

PLEASE ALLOW 4 WEEKS FOR ADMINISTRATIVE PROCESSING OF THIS PROTOCOL.

Appendix C

Diffusion Coefficient Determination

Materials:

1 cm diameter MilliCell Cups

Stirrer assembly
(see diagram)

1 cm diameter Trephine or Cork Borer

Silicone Rings
(1 cm OD, 0.7 cm ID, 1mm thickness)

Micro magetic stirring bar
(2x7mm)

Magnetic Stirrer

1ml Blue tips for a pipetteman

Stopwatch or Timer

Silicone vacuum grease

Test Tube 12x75 mm

Stopper Plugs

Pippeteman - 200μl capacity

Forceps

Microthermocouple

Micrometer

Glass coverslips

Procedure:

01. Using the 1cm trephine or cork-borer, cut out a disc of test material.

02. Sparingly coat the one face of each of two silicone rings.

03. Place a ring (coated side face up) into the Millicell cup -- remove any membrane from the bottom of the cup.

04. Place the membrane over the inserted ring and place the other coated ring over the membrane.

The test membrane should be sealed between the two rings.

05. Place 15 mls of a 2 mg/ml solution into the diffusion apparatus system.

06. Turn on the stirrer so that the speed is around 200 rpms.

07. Place 350 μl of solute free solution into the inner Millicell cup.

08. Simultaneously, start the stopwatch and place the Millicell diffusion cell into the diffusion stirrer.

09. At sampling times shown below, remove 200μl of fluid from the inner Millicell well and immediately place 200μl of fresh solute free solution to the inner well.

Sample Number (index)	Sampling Time (min)
n = 0	0
n = 1	5
n = 2	10
n = 3	15
n = 4	20
n = 5	30
n = 6	40
n = •••	•••
n = 14	120

10. To each liquid sample, add 2 ml of Enzymatic Glucose reagent and let sample react at room temperature for 30 minutes.

11. Using a UV/Vis spectrophotometer at 500nm, determine the individual glucose concentrations for all samples

12. Determine the total solute flux Qn (mg) by using the following algorithm:

$$Q_n = (V_t - V_s) \cdot C_n + V_s \cdot \sum_{i=0}^{n} C_i$$

Vt = total volume in center well [=]cc
Vs = volume of a single sample[=] cc
Cn = concentration of sample n [=] mg/cc
Qn = total flux at time point n [=]mg

13. Graph the Flux (Q) versus time.

14. For the linear portion of the curve (late t) draw the best fit line and determine the x-intercept (t_o).

15. Determine the thickness of the hydrogel membrane using calipers. This thickness is l

16. The diffusivity is given by $D=l^2/6t_o$.

Appendix D

Glucose Concentration Determination

Materials:

- 4 liter Erlenmeyer Flask
- 3 - One liter Bottles to store reagent
- Reagents listed below
- MilliQ Water

The reagents mixed together result in a total of 3 liters of reagent.

Reagent Mixture:

	Amount to 3l Final Volume
Dulbeccos Phosphate Buffered Saline (Powder) (GIBCO BRL, Cat No 450-1300EB)	5 g
4 amino antipyrene (Sigma Chemicals, Cat No A-2814)	0.1524 g
Phenol (Mallinkrodt Chemicals, Cat No UN1671)	0.2117 g
Sodium Azide (NaN_3) (Fluka Chemika, Cat No 71290)	0.6 g
Glucose Oxidase (Sigma Chemicals, Cat No G-7141)	50,000 U
Horse Radish Peroxidase (Sigma Chemicals, Cat No P-8000)	5,000 U
Mutaratose (Sigma Chemicals, Cat No M-9776)	10,000 U

Directions for Reagent Synthesis

01. Make Phosphate-Buffered-Saline (PBS) using GIBCO directions in a 4 liter capacity Erlenmeyer flask.

02. Add Sodium Azide (NaN_3) [0.6g], 4 Amino-antipyrene [0.1524g], Phenol [0.2117] (*Be careful with Phenol.....It will cause burns*)

03. Add 2 mls of PBS to each vial of Glucose oxidase, Peroxidase, and Mutaratose.

04. Pipette these 2 ml solutions into the 4 liter Erlenmeyer flask.

05. Wash the vials again with another 2 ml from the stock 3 liters.

06. Divide the solution into three parts each in a 1 liter media bottle.

Directions for Glucose Assay

This assay is meant to determine the glucose concentration in a range from 0 µg/ml to 10 µg/ml of the sample concentration. The sample volumes used in this assay can be adjusted to determine the concentration for other ranges of glucose concentrations.

Methods

01. Aliquot 10 µl of a 1mg/ml Glucose standard into a microcuvette. Add 1 ml of Glucose reagent to this STANDARD.

02. Place (10µl) samples into microcuvettes and aliquot 1ml of Glucose reagent to the sample.

03. Place 1ml of Glucose reagent alone in a microcuvette. This is the BLANK.

04. Cap all microcuvettes with a test-tube cap.

These samples should react at room temperature for 30 minutes.

05. Set up spectrophotometer to read absorbance (ABS) at a wavelength of 500nm.

06. The calibration curve is linear between the BLANK and STANDARD. Use the following equation to calculate your sample glucose concentration.

$$[\text{Glucose}] = \frac{1}{(ABS_{std} - ABS_{blank})} * (ABS_{sample} - ABS_{blank}) \; [=] \; \frac{mg}{ml}$$

Appendix E

Stirrer Assembly for Cell Culture

Stirrer Equipment

A six well tissue culture plate will be used to monitor the diffusion rate of glucose through hydrogels and the epithelial cell growth rate on hydrogels. To ensure that the glucose solution is well mixed small stirring bars are needed in each compartment. These bars move due to the magnetic field created by a magnet which is attached to a toy motor underneath the plate. The following diagrams give actual dimensions of equipment that was built:

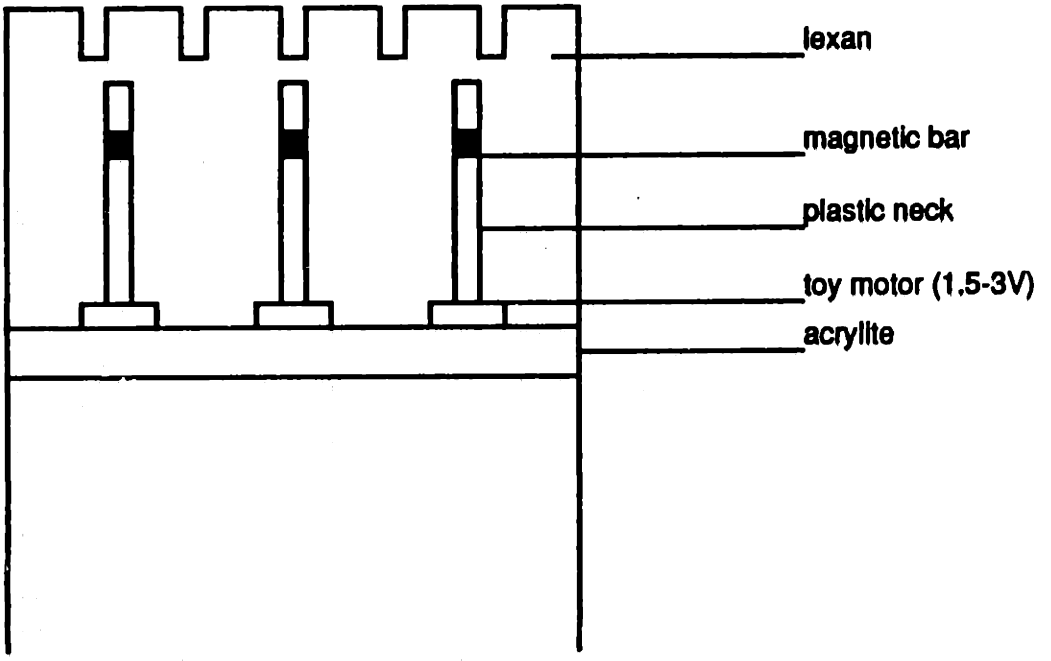

Figure 1. Front View of Stirrer Equipment

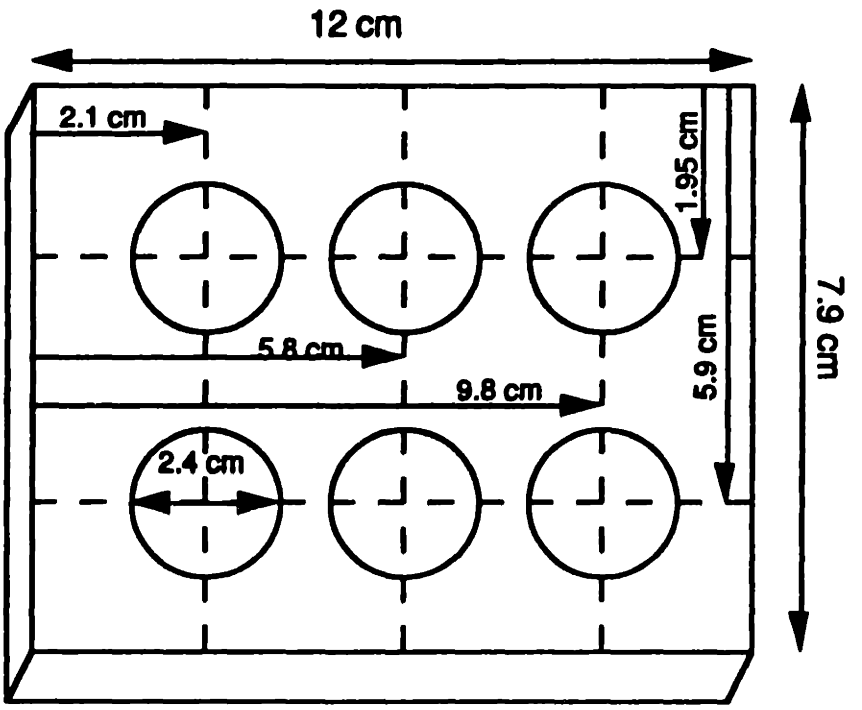

Figure 2. Stirrer arrangement in acrylite base

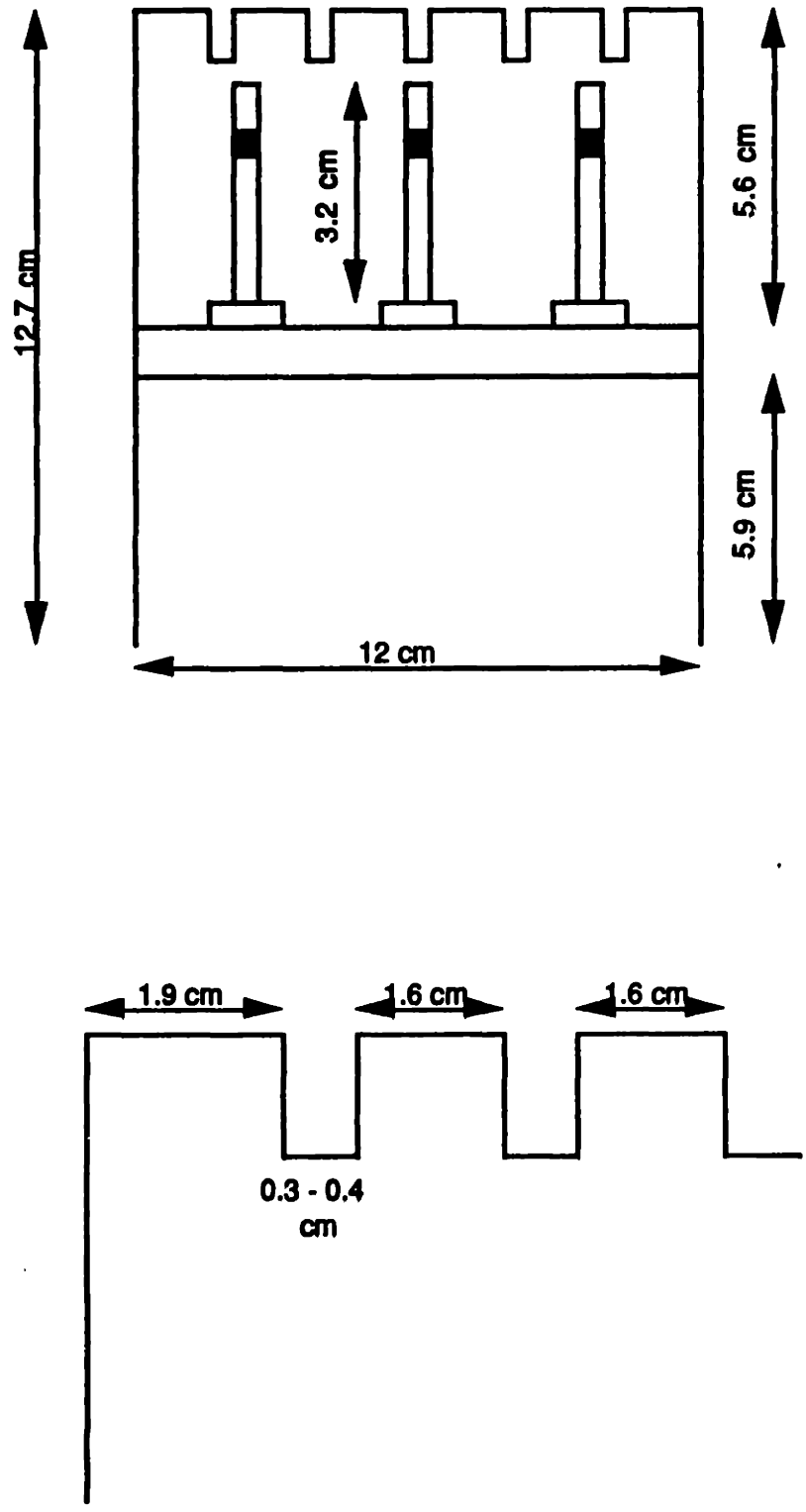

Figure 3. Dimensions of Length side

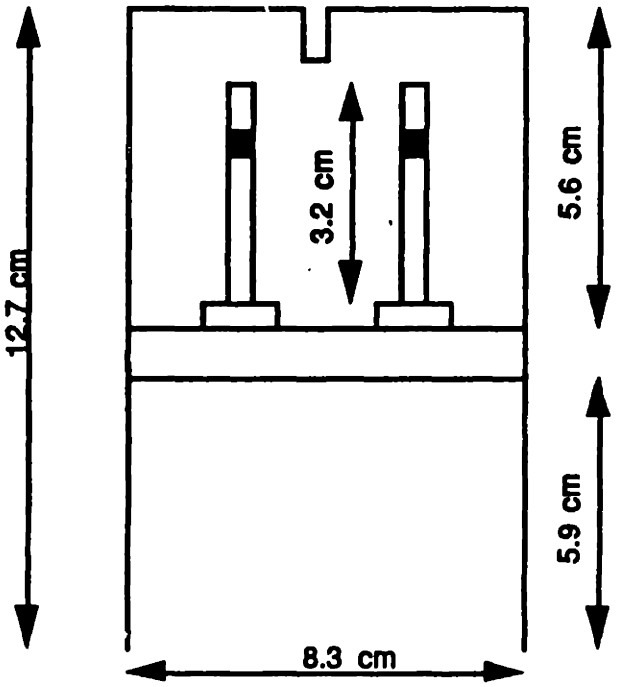

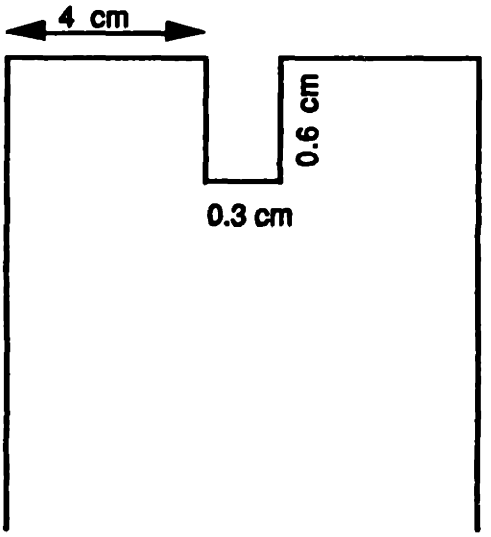

Figure 4. Dimensions of Width side

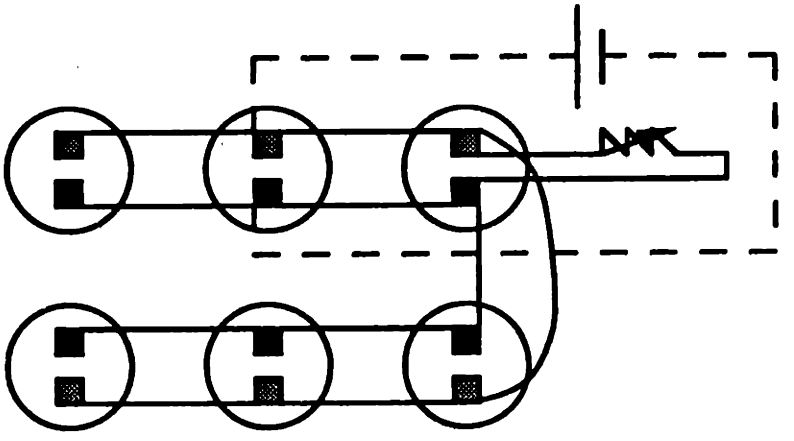

10 K variable resistor

1.5-3 V toy motor

Figure 5. Electrical Arrangement of motors

Testing Diffusion rate of Glucose through PAM gels.

Experimental Procedure

10%, 8%, 6%, 5%, 4% & 2% PAM solutions were made using a 30:1 Acrylmide:bisacrylamide solution. PAM gels were made by adding 8 µL of TEMED and 8µl of 25% Ammonium persulfate to 2ml of PAM solution. The gels were set between rectangular rubber on cover slips. They took approximately 2 minutes to set. They were then stored in NaN_2 water in scintillation vials.

Circular gels of diameter 10 mm and thickness 1mm were cut and placed in Ed's device, sandwiched between two rubber rings. 250 µL of H_2O were put on top of the gel. The device was then placed over the stirrers in the compartments which contained 7 ml of (13 ml H_2O + 2 ml 30mg/ml glucose) solution. At time t = 10, 15, 20, 30, 40 ...120 minutes 200 µL of the top solution was removed and placed in a cuvette. 1 ml of glucose reagent was added to the cuvette which was then placed in a spectrophotometer operated at 500 nm. The blank ws H_2O. 200 µL of H_2O replaced the top solution.

Results

Gels that contained less than 6% PAM were not used in the experiment because they slipped through the circular rings during the experiment. Table 1 shows the results of the experiment.

Table 1. Results of Time Lag diffusion Experiment.

Gel	10%	10%	8%	8%	6%	6%
Time						
10	0.377	0.759	0.216	0.182	0.369	0.198
15	0.866	1.355	0.516	0.426	1.859	0.496
20	1.419	2.141	0.843	0.681	3.116	0.869
30	2.175	2.766	1.496	1.157	4.518	1.513
40	3.144	4.202	2.270	1.745	6.259	2.589
50	4.390	4.642	3.043	2.385	7.719	3.494
60	5.273	5.420	3.800	3.091	9.306	4.631
70	6.285	6.175	4.429	3.850	10.761	5.778
80	7.483	6.482	5.226	4.485	12.139	6.788
90	8.570	7.279	5.962	5.201	13.492	7.464
100	9.586	7.656	6.759	5.933	14.928	8.615
110	10.762	8.384	6.759	6.679	16.026	9.429
120	12.147	9.157	6.759	7.496	17.359	10.554
Q120 (mg)	0.002	0.002	#VALUE!	0.002	0.004	0.002
D cm2/min	9.52E-05		1.11E-04	1.08E-04	1.85E-04	1.11E-04

Figure 6. shows the variation of diffusion with % PAM, where D (cm^2/min) = $l^2$6/to.

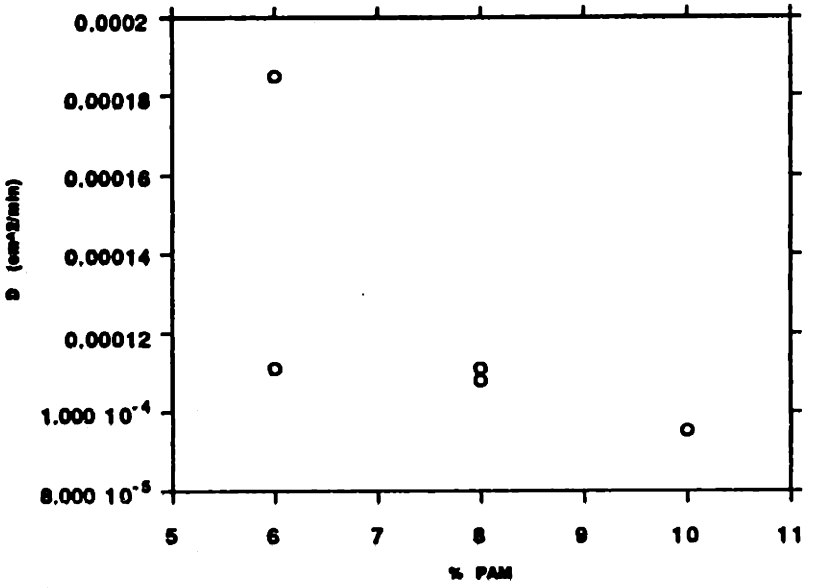

fig . Diffusion as a function of % PAM

Appendix F

Diffusion of Insulin in 2mm Composite Hydrogel

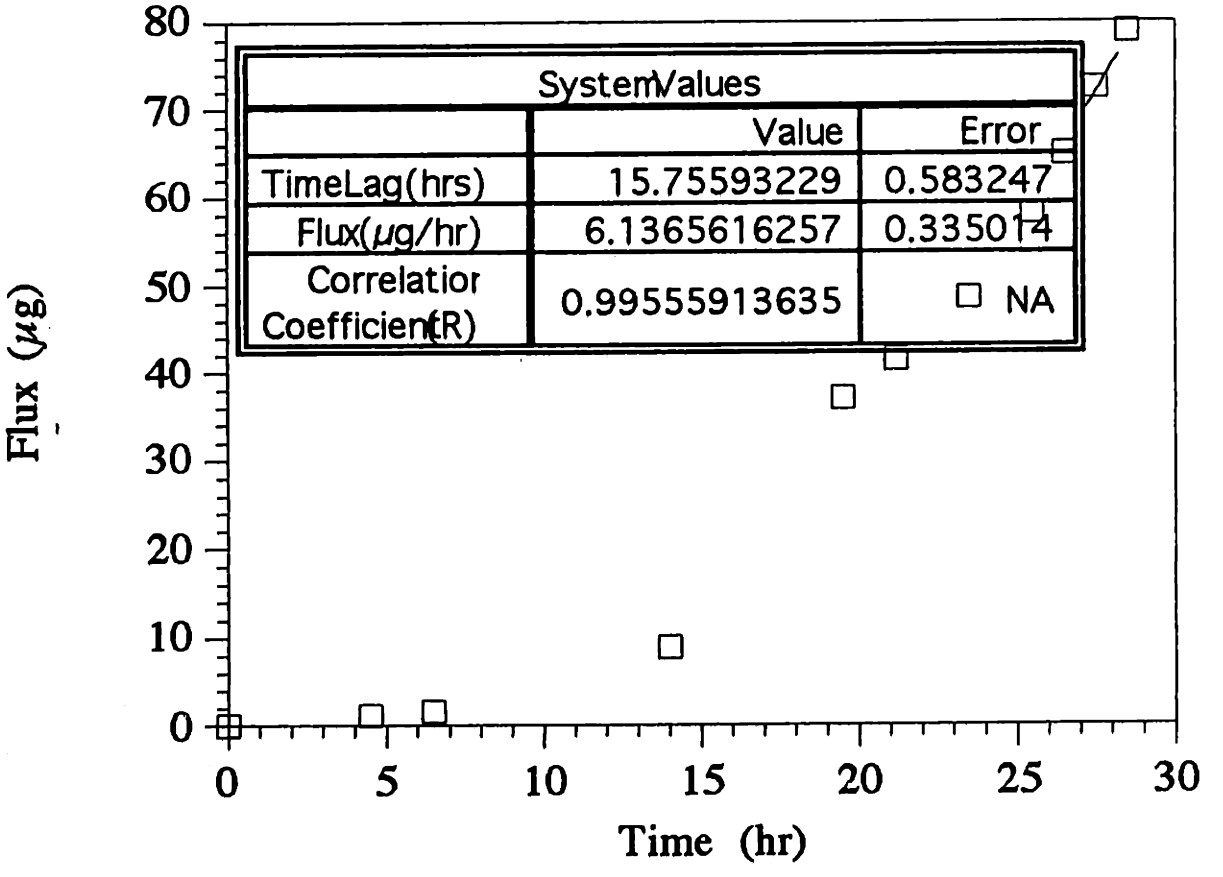

The x-intercept t_o for insulin in these 2 mm composite hydrogels was calculated to be 15.75 hours. Therefore, $6t_o = \frac{l^2}{D} = 6 \cdot 15.75hr = 94.5hr.$